Cocatalysts for Metal-Catalyzed Olefin Polymerization: Activators, Activation Processes, and Structure–Activity Relationships

Eugene You-Xian Chen*

The Dow Chemical Company, Catalysis R&D, Midland, Michigan 48674

Tobin J. Marks*

Department of Chemistry, Northwestern University, Evanston, Illinois 60208-3113

Contents

I. Introduction

One of the most exciting developments in the areas of catalysis, organometallic chemistry, and polymer science in recent years has been the intense exploration and commercialization of new polymerization technologies based on single-site and metallocene coordination olefin polymerization catalysts.[1] The vast number of specifically designed/synthesized transition metal complexes (catalyst precursors) and main-group organometallic compounds (cocatalysts) allows unprecedented control over polymer microstructure, the generation of new polymer architectures, and the development of new polymerization reactions. Commercialization of new generations of single-site and metallocene catalyst-based technologies has provided the multibillion pound per year polyolefins industry with the ability to deliver a wide range of new and innovative olefin-based polymers having improved properties.[2−4] The intense industrial activity in the field and the challenges to our basic understanding that have come to light have in turn

Eugene You-Xian Chen is a Research Specialist in Corporate R&D of the Dow Chemical Co., Midland, MI. He received his M.S. degree in Chemistry from Nankai University in China and then came to the University of Massachusetts, where he earned his Ph.D. degree in the area of organometallic and polymer chemistry in 1995 under the direction of Professors J. C. W. Chien and M. D. Rausch. After two years of postdoctoral study with Professor T. J. Marks at Northwestern University, he joined Dow Chemical in late 1997. His current research interests include polyolefin synthesis and structure–activity/reactivity relationships in Ziegler–Natta and single-site homogeneous polymerization. He wishes to dedicate this review to Professor Chien on the occasion of his 70th birthday.

Tobin J. Marks is Vladimir N. Ipatieff and Charles E. & Emma H. Morrison Professor of Chemistry and Professor of Materials Science and Engineering at Northwestern University, Evanston, IL. He received his B.S. degree in Chemistry from the University of Maryland in 1966 and his Ph.D. degree in Inorganic Chemistry from M.I.T. in 1970 under the direction of Professor F. A. Cotton. He moved to Northwestern University as an assistant professor in 1970. His research interests include synthetic and mechanistic f- and d-element organometallic chemistry, particularly with applications in olefin polymerization catalysis, as well as the design, synthesis, and physicochemical properties of unususal molecules and molecule-derived materials.

stimulated a burst of fundamental academic research. The keen competition in the marketplace, the desire to design and develop new and useful polymeric materials, and the combined resources of industry and government have also strengthened collaboration between research groups in industry and academic institutions.[4] In return, research activities in universities have been of value to industry and have brought much basic knowledge to the field.

Cocatalysts, often in the form of main-group organometallic compounds in traditional two-component Ziegler–Natta catalytic systems, have also played a very important role in the single-site polymerization

revolution. Historically, discoveries of new and more effective cocatalysts have contributed significantly to fundamental understanding as well as to technology developments in this field. As this review will present, these discoveries have rejuvenated classical Ziegler–Natta catalysis and enabled the rapid development of metallocene and single-site catalysis. From an economic point of view, the cost of the cocatalyst is frequently more than that of the precatalyst, especially for group 4 metal-catalyzed olefin polymerization systems. Thus, the potential value of developing a new catalyst system or rendering a current system more efficient by discovering high-performance and low-cost cocatalysts and understanding their role in the polymerization processes is compelling. Furthermore, it is likely that, in solution, slurry, or gas phase polymerizations, some processes may have to rely on cocatalyst screening and anion engineering to afford better control of catalyst solubility and stability and the polymerization kinetic profile, as well as morphological behavior of the resulting polymers.

The importance of the cocatalyst in metal-catalyzed polymerization processes can be appreciated as follows. First, to form active catalysts, catalyst precursors must be transformed into active catalysts by an effective and appropriate activating species. Second, a successful activation process requires many special cocatalyst features for constant catalyst precursor and kinetic/thermodynamic considerations of the reaction. Finally, the cocatalyst, which becomes an anion after the activation process, is the vital part of a catalytically active cation–anion ion pair and may significantly influence polymerization characteristics and polymer properties. Scheme 1 depicts the aforementioned relationships between catalyst and cocatalyst in metal-catalyzed olefin polymerization systems.

Scheme 1
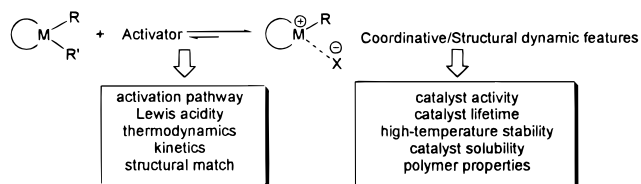
The emergence of numerous studies suggesting a significant influence of the cocatalyst on catalytic activity, stability, polymerization kinetic profile, and polymer molecular weight and stereoregularity in cationic transition metal-catalyzed olefin polymerization processes has gradually changed our view of the functions of activators in single-site olefin polymerization. This article reviews three principal topics in cocatalytic chemistry: types and intrinsic structural features of commonly used activators; activation processes embodied in the various chemical reactions between the precatalyst and cocatalyst; catalyst–cocatalyst structure–activity relationships as revealed by the nature of cation–anion interactions in both the solid state and in solution; thermodynamics of catalyst activation; kinetics of ion pair dissociation/reorganization processes as well as how these interactions are intimately connected with

polymerization activity and stereospecificity. Common deactivation processes and the forces stabilizing highly electrophilic cationic metal complexes in solution are also discussed.

II. Activators

A. Aluminum Alkyls

Aluminum alkyls, including trialkylaluminums and alkylaluminum chlorides, are important components in classical heterogeneous Ziegler−Natta coordination polymerization catalysis.[5,6] A wide variety of homogeneous Ziegler−Natta catalysts based on aluminum alkyls as cocatalysts were also reported in the early literature for the polymerization of olefins. As an example, vanadium-based catalysts in combination with aluminum alkyls were found to promote the syndiospecific polymerization of propylene at temperatures below −60 °C.[7,8] These catalysts were also used for polymerization of higher α-olefins as well as the copolymerization of ethylene with higher α-olefins.[9,10] Although as the temperature of the polymerization increases, the polymerization becomes nonstereospecific in these systems, they can be used to prepare a variety of homo, block, random, and alternating polyolefins. Cr[11]- and Ni[12]-based homogeneous catalysts, when activated by aluminum alkyls, are also known as diene polymerization and ethylene oligomerization catalysts, respectively.

Breslow and Newburg at the Hercules Research Center first discovered the homogeneous catalytic system consisting of Cp_2TiCl_2 in the presence of diethylaluminum chloride (Et_2AlCl) for ethylene polymerization under mild conditions.[13] Subsequent studies by Natta and Pino[14] and detailed spectroscopic, kinetic, and isotope labeling studies carried out at Hercules Laboratories by Breslow, Newburg, and by Long,[15] Chien,[16] and others[17] have contributed significantly to our understanding of olefin polymerization using homogeneous Ziegler−Natta systems in terms of cocatalyst function, generation of active species, and olefin insertion mechanisms. Sinn, Kaminsky, and co-workers[18] subsequently investigated zirconocene complexes activated with alkylaluminum species for ethylene polymerization.

The studies at Hercules[15,16] demonstrated that ligand exchange between Cp_2TiCl_2 and the R_2AlCl cocatalyst forms the alkyl titanocene complex $Cp_2Ti(R)Cl$, that $Cp_2Ti^{\delta+}(R)-Cl\cdots Al^{\delta-}R_2Cl$ adduct formation polarizes the Ti−Cl bond, and that ethylene undergoes insertion into the $Ti^{\delta+}-R$ bond of the alkylaluminum halide activated complex. These early studies based on an alkylaluminum activated titanocene system contributed to the ideas put forth by Cossee[19] with regard to insertion mechanisms in heterogeneous Ziegler−Natta catalysis.

Shilov et al.[20b] suggested the possibility of the participation of the cationic species Cp_2TiMe^+ in these polymerization systems as early as 1961. On the basis of electrochemical results, Dyachkovskii et al.[20a] proposed that ethylene insertion takes place at a true cationic Cp_2Ti^+-R center, generated by Cl^- abstraction in reaction of $Cp_2Ti(R)Cl + AlRCl_2$ (eq 1).
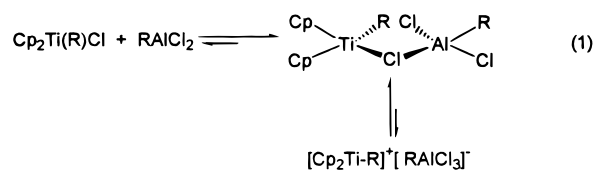
Eisch and co-workers[21] later intercepted and determined the crystal structure of the initial insertion product formed from the $Cp_2TiCl_2/AlMeCl_2$ system in the presence of the silylacetylene $Me_3SiC\equiv CPh$. This finding argued strongly that the active component of the $Cp_2TiCl_2 + AlMeCl_2$ reaction is the cationic species Cp_2TiMe^+ ion-paired with the anion $AlCl_4^-$, after Ti−Cl/Al−Me ligand exchange and subsequent Cl^- abstraction by the Lewis acidic Al center (eq 2).
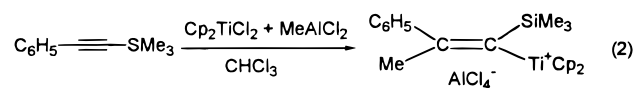
These Ti- or Zr-based metallocene/alkylaluminum catalysts usually exhibit low-to-medium activities for ethylene polymerization and only ethylene, narrow product molecular weight distributions, and rapid catalyst deactivation leading to formation of an inactive species, presumably due to side reactions such as alkyl exchange and H-exchange, as well as reduction to lower Ti oxidation states.[18,22] Extensive kinetic and reactivity studies as well as multinuclear NMR investigations by Fink[23] and by Eisch[24] have demonstrated that dynamic equilibria exist in the $Cp_2Ti(R)Cl/AlCl_3$ catalyst system between $Cp_2TiR\cdots Cl\cdots AlCl_3$ contact ion pairs and solvent-separated $Cp_2TiR^+||AlCl_4^-$ ion pairs and that the solvent-separated ion pairs are the most catalytically active sites. Contact ion pairs, which appear to dominate in these equilibria, can then be considered as "dormant" sites. Increasingly polar media and higher dilution have been shown to favor the solvent-separated ion pair over the contact ion pairs, thus to enhance the polymerization activity.[25] Chelating effects using rigid, chelating Lewis acids of the type $1,2\text{-}(AlRR')_2C_6H_4$ (R, R′ = alkyl, aryl, halo) also assist the generation of solvent-separated cation−anion ion pairs, thus enhancing ethylene polymerization activity.[26]

Overall, the inability of metallocenes activated by alkylaluminum halides to polymerize propylene and higher α-olefins has limited their utility in this field. A number of attempts were made to improve the performance of these catalyst systems. Among these efforts, Reichert and Meyer[27] first discovered a surprising rate enhancement in ethylene polymerization activity upon addition of water to the $Cp_2TiEtCl/AlEtCl_2$ catalyst system. Subsequent studies by Long and Breslow[28] on the effects of water in the otherwise inactive $Cp_2TiCl_2/AlMe_2Cl$ system led to the suggestion that the formation of a dimeric aluminoxane, e.g., $ClMeAl-O-AlClMe$, which is presumably a stronger Lewis acid than Me_2AlCl and therefore a more efficient activator, is responsible for enhanced ethylene polymerization activity.

By addition of water to the halogen-free, polymerization-inactive $Cp_2ZrMe_2/AlMe_3$ system, Sinn and

Kaminsky[29] observed a surprisingly high activity for ethylene polymerization, which led to the discovery of a highly efficient activator, an oligomeric methyl aluminoxane (MAO).[18,30] This discovery, a result of research efforts seeking more effective cocatalysts, rejuvenated Ziegler−Natta catalysis and, along with major advances achieved in controlling polymer stereochemistry and architecture, began the metallocene and single-site polymerization catalysis era.[31−34]

B. MAO

1. General Structural Features of MAO

Alkylaluminoxanes, oligomeric compounds consisting of −Al(R)−O− subunits, have been known to be active for the polymerization of monomers such as oxiranes since the early 1960s.[35] Methylaluminoxane [−Al(Me)−O−]$_n$ (MAO), prepared by controlled hydrolysis of AlMe$_3$ and typically having $n \approx 5-20$, affords highly active catalysts for polymerizing ethylene, propylene, and higher α-olefins when combined with group 4 metallocenes.[31c] Since these discoveries, MAO has become a very important cocatalyst for metal-catalyzed olefin polymerization. Although very extensive research has been carried out in both academia and industry, the exact composition and structure of MAO are still not entirely clear or well-understood.[36,37] The proposed structures for MAO include one-dimensional linear chains (**1**) or cyclic rings (**2**) which contain three-coordinate Al centers, two-dimensional structures (e.g, **3**), and three-dimensional clusters (e.g., **4**) (Scheme 2). The three-

Scheme 2

1   **2**   **3**

4   **5**
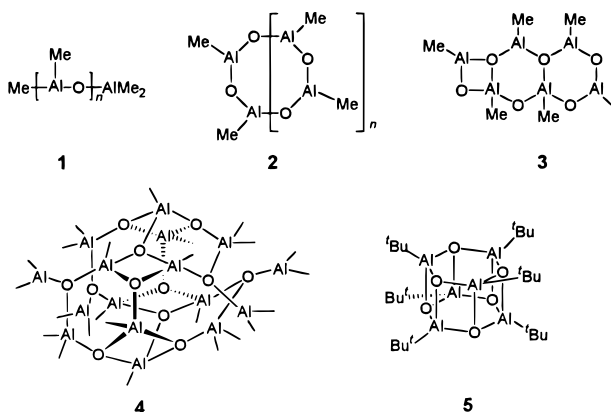
dimensional structure **4** recently proposed by Sinn[38] is based on structural similarities with *tert*-butylaluminoxanes, which form isolable and X-ray crystallographically characterizable cage stuctures (e.g., **5**).[39] Structure **4** has the basic formula [Al$_4$O$_3$(CH$_3$)$_6$]$_4$ with a CH$_3$:Al ratio of ~1.5, which is in agreement with the general formula [AlO$_{0.8-0.75}$(CH$_3$)$_{1.4-1.5}$]$_n$, recently reported by Albemarle researchers from ^{1}H NMR measurements.[40] Sinn et al.[38b] recently presented additional evidence for hexamethyl-tetraaluminoxane, [Al$_4$O$_3$(CH$_3$)$_6$]$_4$, as a major component of MAO, and have proposed an alternative structural model (similar to **4** but having a more rigid structure with four-, six-, and eight-membered rings) for this tetramer. Multinuclear NMR investigations of MAO

also indicate a possible cage structure under ambient conditions.[41] Most aluminum centers in structure **4**, except for the peripheral ones, are tetracoordinated. Characterization of MAO by ^{27}Al NMR spectroscopy has shown that four-coordinate Al centers predominate in MAO solutions,[42] although three-coordinate Al sites are also present.[43] Chemical evidence that MAO contains three-coordinated aluminum was also demonstrated by Siedle et al.,[44] who showed that MAO undergoes facile ($\Delta G^{\ddagger} = 13.9$ kcal/mol at 22 °C in dichloromethane) reversible methyl exchange with Cp$_2$Zr(^{13}CH$_3$)$_2$ as also do Me$_6$Al$_2$ and MeAl(BHT)$_2$.

Despite its unique effectiveness as a cocatalyst, MAO still remains a "black box".[36] Depending on the nature of the hydrated salt (the H$_2$O source) used for the MAO synthesis and the exact MAO synthetic reaction conditions, MAO-activated metallocenes may exhibit widely differing activities in olefin polymerization. The MAO structure can hardly be elucidated directly because of the multiple equilibria present in MAO solutions, and residual trimethylaluminum in MAO solutions appears to participate in equilibria that interconvert various MAO oligomers.[45−47] There are two types of TMA present in typical MAO solutions: "free" TMA and "associated" TMA (eq 3).

$$\left[Al(Me)O\right]_n \cdot x\, AlMe_3 \rightleftharpoons \left[Al(Me)O\right]_n \cdot (x-y)\, AlMe_3 + y\, AlMe_3 \quad (3)$$
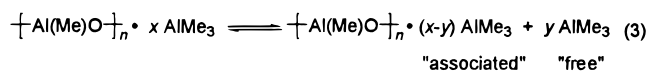
"associated"   "free"

It is difficult to reduce the CH$_3$:Al ratio to less than 1.5 by evaporation of volatile components because vacuum-drying removes only the free TMA, while the associated TMA can only be removed chemically. Tritto et al.[48] found that cryoscopic MAO molecular weights decrease after AlMe$_3$ addition according to a linear relationship, which is caused by disproportionation reactions. However, recent in-situ FTIR spectroscopy investigations do not indicate any obvious reaction between TMA and MAO.[49] Nevertheless, in light of its complicated, unresolved structural features, MAO is usually represented for the sake of simplicity as having linear chain or cyclic ring structures [−Al(Me)−O−]$_n$, containing three-coordinate aluminum centers.

2. Modified MAOs

Conventional MAO has very low solubility in aliphatic solvents as well as poor storage stability in solution, which considerably limits its utility. Other more soluble and commonly used aluminoxanes are ethylaluminoxane and isobutylaluminoxane, which are synthesized by the partial hydrolysis of triethylaluminum (TEA) and triisobutylaluminum (TIBA), respectively. However, these alkylaluminoxanes do not perform as well as MAO in metallocene-mediated olefin polymerization.[50] It was reported, however, that tetrakis(isooctyl) alumoxane [(*i*-octyl)$_2$−O−Al-(*i*-octyl)$_2$], prepared by reaction of Al(*i*-octyl)$_3$ with 0.5 equiv of water,[51] exhibits remarkable cocatalytic activity, comparable to or even greater than that obtained with MAO, for ethylene polymerization catalyzed by racemic *ansa*-bis(indenyl)-type zirconocene dichlorides.[52] Furthermore, commercial modified methylaluminoxanes (MMAO) available from

Akzo-Nobel, and prepared by controlled hydrolysis of a mixture of trimethylaluminum and triisobutylaluminum, exhibit improved solution storage stability and improved solubility in aliphatic solvents and can be produced at lower cost while providing good polymerization efficiency.

A well-known problem in the preparation of MAO is the inevitable presence of trimethylaluminum in the MAO product or trialkylaluminum species in the MMAO product.[36–37,45–46] The quantity of residual R_3-Al has major effects on the catalytic activity of MAO.[37] Very low activities have been reported in the literature when TMA is used alone as the cocatalyst for Cp_2ZrR_2-catalyzed ethylene polymerization.[45] The effect of free TMA on polymerization activity and polymer molecular weight has been studied by altering [TMA]/[MAO] ratios in zirconocene-catalyzed ethylene polymerization.[47,53–54] as well as by replacing TMA with TEA or TIBA in combination with the catalyst Cp_2ZrCl_2 or $CpTiCl_3$.[55–57] It is generally found that, with increasing addition of free TMA to MAO, both catalyst activity and polymer molecular weight decrease. The kinetic profile also changes from a decay type (the maximum rate of polymerization, R_p, is reached within minutes followed by decay of R_p to approximately half of the maximum rate) to a buildup type curve (there is a period of R_p buildup and then plateau to a constant value) for ethylene polymerization.[54]
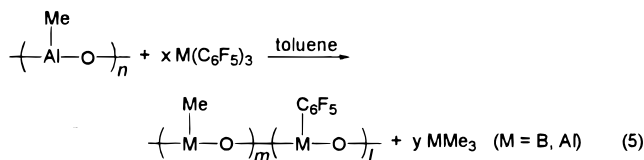
To solve this residual TMA problem in the synthesis of MAO, a new process has been developed for preparing MAO substantially free of trimethylaluminum ("PMAO-IP" from Akzo-Nobel), using nonhydrolytic means (e.g., by thermal and/or catalytic means).[58] PMAO-IP is prepared in two steps. The first is the initial reaction between an oxygen-containing reagent and TMA to form a PMAO-IP precursor species, and the second step is thermal conversion of the precursor species to pure methylaluminoxane (eq 4). The product PMAO−IP contains less free TMA and is claimed to exhibit higher catalytic activity in ethylene polymerization mediated by *rac*-ethylenebis(indenyl)zirconium dichloride at a 2000:1 Al:Zr ratio, compared to conventional MAOs.

$$Me_3Al + 0.8\ Me_3COH \longrightarrow Me_{2.2}Al(OCMe_3)_{0.8} + 0.8\ MeH \quad (4)$$

$$\xrightarrow[\text{metathesis}]{\text{Al-C/Al-O}} Me_{1.4}AlO_{0.8} + \text{hydrocarbons}$$
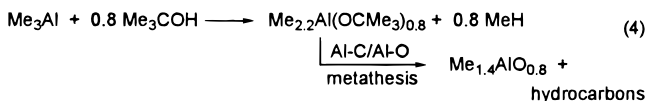
Treating MAO with a small quantity of *p*-hydroquinone results in formation of another modified MAO which is insoluble in toluene.[59] This modified MAO, however, cannot activate metallocenes alone, and additional TIBA is required to render the system active for olefin polymerization.

3. Pentafluorophenyl-Substituted MAO

When $B(C_6F_5)_3$[60] or $Al(C_6F_5)_3$[61] is mixed with dried, solid MAO and heated in toluene at 60−65 °C, B/Al or Al/Al ligand exchange occurrs and some of the C_6F_5 groups are believed to transfer to the MAO backbone, forming partially pentafluorophenylated MAO[62,63] (eq 5). Some decomposition products often result from extended heating or at higher reaction temperatures.

$$\text{Me—Al—O}_n + x\ M(C_6F_5)_3 \xrightarrow{\text{toluene}}$$

$$\text{Me—M—O}_m\text{—}\text{C}_6\text{F}_5\text{—M—O}_l + y\ MMe_3 \quad (M = B, Al) \quad (5)$$

The catalytic activity of this partially C_6F_5-substituted MAO is enhanced by 3.7- to 7-fold for ethylene polymerization catalyzed by Cp_2ZrCl_2 at Al:Zr = 1600:1 and [MeAlO]:$M(C_6F_5)_3$ (M = B, Al) = 200:1, compared to cocatalytic results with untreated MAO under identical reaction conditions.[62] However, it is also reported that heavier C_6F_5 substitution (increasing amounts of $M(C_6F_5)_3$ vs MAO) reduces the favorable effects of the C_6F_5 substitution.

In hydrocarbon solution, the residual aluminum alkyls present in MAO and MMAO (up to 40%) undergo facile ligand exchange with $B(C_6F_5)_3$ to form mixtures of aluminum-containing Lewis acids, corresponding to the formula [(−AlR−O−)(−Al(C_6F_5)−O)]-[(C_6F_5)$_x$Al$_2$R$_{6-x}$], where R = Me and ^{i}Bu.[63] This mixture has been found to be a very efficient cocatalyst in mixed alkanes for ethylene + 1-octene copolymerization at 130 °C in the presence of [(tetramethylcyclopentadienyl)dimethylsilyl-*N*-*tert*-butylamido]titanium−1,3-pentadiene. This activator composition utilizes the facile alkyl/aryl redistribution between R_3Al and $B(C_6F_5)_3$ to both chemically remove the R_3Al residue from MMAO and to further modify the MAO architecture for achieving a more reactive form.

Despite the success of MAO in promoting high-activity metallocene-mediated olefin polymerization, it also exhibits disadvantageous features. High MAO: catalyst precursor ratios (10^2 to 10^4:1) are generally required for obtaining acceptable polymerization activity and relatively stable kinetic profiles, which raises issues of the high cost of this cocatalyst and the high ash content (Al_2O_3) of the product polymer. Poor control over polymer morphology may be another matter of concern when polymerizations are carried out other than in the solution phase. Finally, the intrinsically complicated structural features of MAO as well as the superstoichiometric quantities of MAO required in the activation process prevent full characterization of the catalytically active species. The overall activation process and the nature of the resulting active species are therefore not well-understood. Consequently, there is a great need to develop new cocatalyst systems which can provide equivalent or even greater catalytic activity and, at the same time, allow isolation and characterization of the active species for a better fundamental understanding of cationic transition metal-mediated coordination polymerization.

C. Perfluoroaryl Boranes

The synthesis of tris(pentafluorophenyl)borane, $B(C_6F_5)_3$ (FAB), was first reported in 1964 by Massey and Park.[60,64] However, there were only ca. 25 citations of the early Massey and Park papers in the 25 years after their initial publication.[65,66] Beginning in early 1990s when Marks[67] and Ewen[68] independently
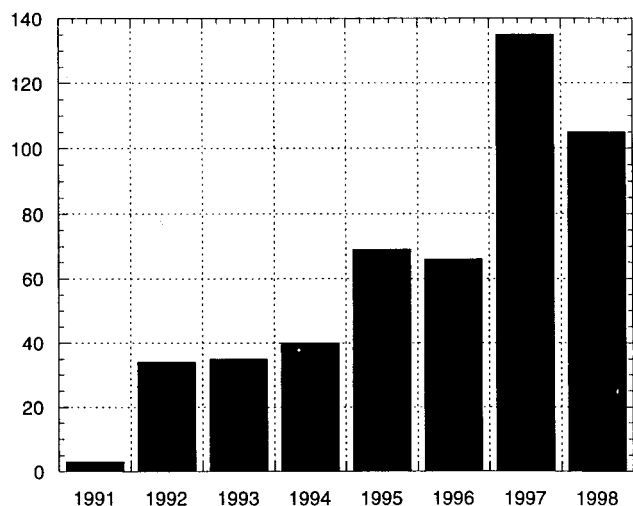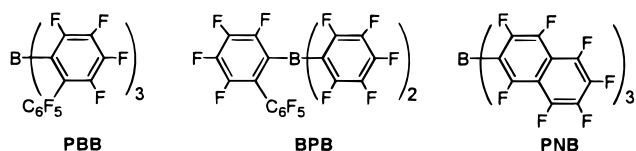
Figure 1. Citations to the 1991 and 1994 *J. Am. Chem. Soc.* publications of Yang and Marks describing cationic zirconocene catalysts based on B(C$_6$F$_5$)$_3$. The vertical scale is the number of citations in the indicated year.

discovered that, in combination with group 4 metal-locene alkyls, strongly Lewis acidic FAB promotes highly efficient olefin polymerizations and allows isolation of crystallographically characterizable cationic metallocene complexes,[67] research activity involving this reagent in both academia and industry has exploded. In 1998 alone, citations to using FAB exceeded 121, and citations of the 1991 and 1994 *J. Am. Chem. Soc.* publications describing FAB activation of zirconocene alkyls and utility in olefin polymerization catalysis have grown rapidly (Figure 1). The Lewis acid properties of FAB other than in abstracting alkide anions from metallocene alkyls have also been extensively investigated.[69−71]

Over the past few years, the research groups of Marks and Piers have developed a number of new and effective perfluoroarylborane activators as well as bifunctional boranes. Bis(pentafluorophenyl)borane [HB(C$_6$F$_5$)$_2$]$_2$ was synthesized by Piers et al.[72] by reduction of monomeric chloroborane with Me$_2$-Si(Cl)H (which also serves as the solvent for the reaction) in a quantitative yield. This white, crystalline material exists in a dimeric form in the solid state and in suspension in toluene or benzene promotes rapid hydroboration of a range of simple alkenes and alkynes. The details of the hydroboration chemistry as well as the reaction of the products with zirconocene dialkyls have been the subject of a recent review article.[66]

The sterically encumbered perfluoroarylboranes tris(2,2′,2″-perfluorobiphenyl)borane (PBB),[73] bis(pen-

tafluorophenyl)(2-perfluorobiphenyl)borane (BPB),[74] and tris(β-perfluoronaphthyl)borane (PNB),[75] have been recently synthesized by the Marks group. The synthesis of PBB involves basically a two-step pro-

cess. The first is the preparation of 2-bromononafluorobiphenyl[76] from bromopentafluorobenzene in 91% yield. The second is lithiation and followed by the reaction with BCl$_3$ in a diethyl ether and pentane mixture to afford the crystalline solid in 91% yield after sublimation[73,77] (Scheme 3).

Scheme 3
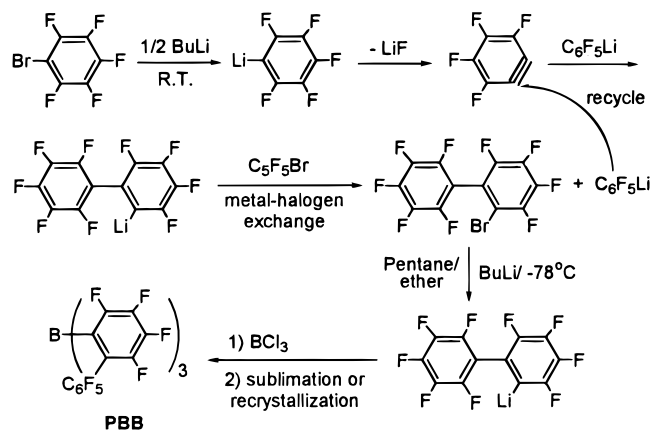
The synthesis of BPB is essentially identical to that of PBB, except that in the final step the reagent (C$_6$F$_5$)$_2$BCl is used, instead of BCl$_3$. The solid-state structure of this new organo-Lewis acid has been determined by X-ray diffraction. (Figure 2).[74]
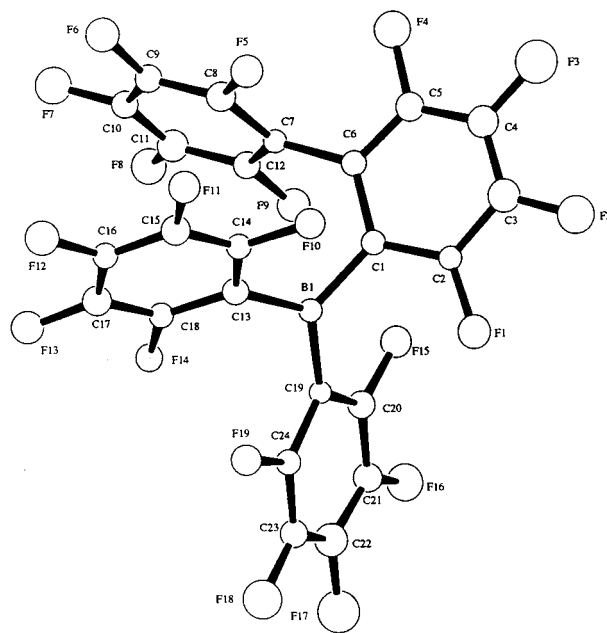
Figure 2. ORTEP drawing of the molecular structure of the borane (C$_{12}$F$_9$)B(C$_6$F$_5$)$_2$ (BPB). From ref 74.

The PNB synthesis is based on β-bromoheptafluoronaphthalene, prepared from β-perfluoronaphthylhydrazine. Low-temperature lithium−halogen exchange using ^{n}BuLi produces the corresponding lithium salt, which is then reacted with BCl$_3$ at low temperature to afford, after workup and purification by sublimation, yellow PNB (Scheme 4).[75]

Recently, several bifunctional perfluoroarylboranes, *para*-phenylenediborane **6**,[78] *ortho*-phenylenediborane **7**,[79] and octafluoro-9,10-bis(pentafluoro-

Scheme 4
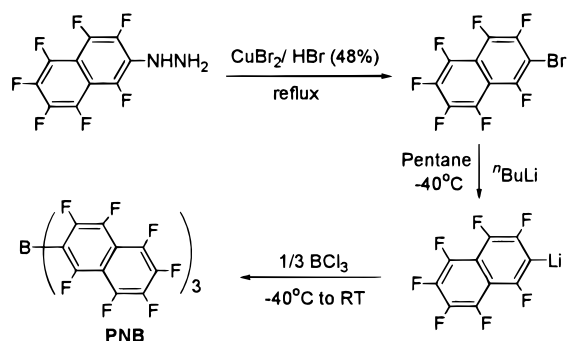
phenyl)-9,10-diboraanthracene (**8**),[80] have also been reported from the Marks and Piers research groups.
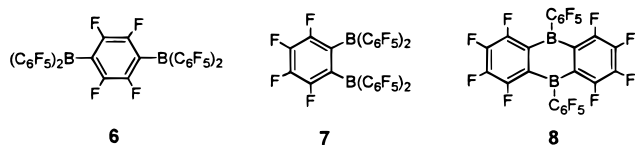
The synthesis of *para*-diborane **6** utilizes an Sn/B ligand metathesis reaction between *para*-(Me₃Sn)₂C₆F₄ and (C₆F₅)₂BCl (eq 6). Although the exchange reaction in toluene solution is very slow at 120 °C, heating the two reagents in the neat state at 120 °C affords the desired product in good yield.
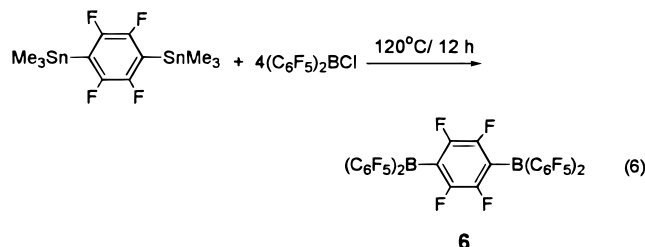
The *ortho*-diborane **7** was recently reported by Piers et al.[79] and was prepared via the mercury trimer [(C₆F₄)Hg]₃. This reagent undergoes reaction with BBr₃ to produce 1,2-bis(dibromoboryl)tetrafluorobenzene, which then further reacts with Zn(C₆F₅)₂ to afford the final product.

When *ortho*-(Me₃Sn)₂C₆F₄ undergoes reaction with excess BCl₃ at high temperatures in a sealed pressure vessel, the main product is octafluoro-9,10-dichloro-9,10-diboraanthracene. Further reaction with Me₂-Sn(C₆F₅)₂ then produces diboraanthracene **8** (Scheme 5).[80]

Scheme 5
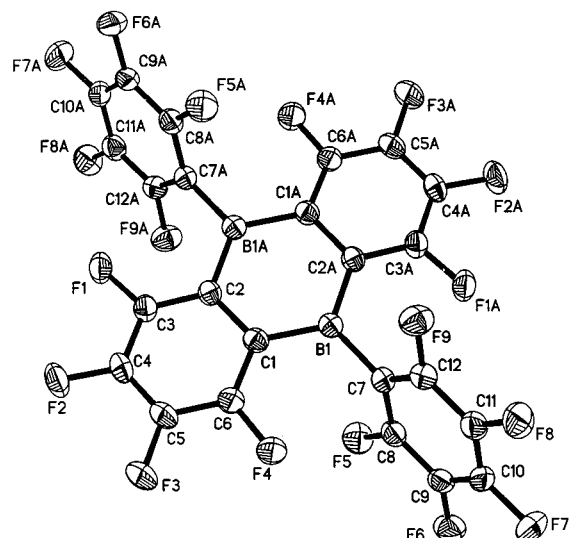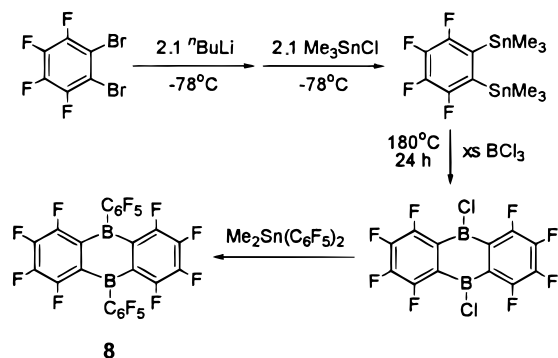
Figure 3. ORTEP drawing of the molecular structure of 1,2-[C₆F₄B(C₆F₅)]₂ (**8**). From ref 80.

This diborane is expected to exhibit very high Lewis acidity because the nearly perpendicular conformation of the two C₆F₅ rings prevents significant π electron density transfer to the B centers, both of which exhibit a strong electron-withdrawing effect. This indeed can be seen from both the observation in the ¹⁹F chemical shifts in solution and the solid-state structure (Figure 3). For two C₆F₅ moieties in **8**, the *ortho*-, *meta*-, and *para*-F chemical shifts in the ¹⁹F NMR are −134, −152, and −162 ppm at 25 °C in C₆D₆, respectively, as compared to −129, −142, and −160 ppm for FAB. In the solid state, two groups are twisted out of the diboron plane by 76°. Indeed, when combined with group 4 metallocene and other single-site precatalysts, cationic active species based on **8** have generally significantly higher olefin polymerization efficiency (up to 20 times) than those based on FAB.

D. Fluoroarylalanes

Although ether[81] or THF[82] coordinated Al(C₆F₅)₃ has been reported previously, attempts to remove the ether molecule from the complex by heating at elevated temperatures are reported to result in a violent explosion of the reaction mixture.[81] Recently, Biagini et al.[61] developed a new process to synthesize Al(C₆F₅)₃, a very strong Lewis acid. By stirring equimolar mixtures of B(C₆F₅)₃ and trialkylaluminum (TMA and TEA preferred) in a hydrocarbon solvent, B/Al ligand exchange affords the desired product in 70−90% isolated yield. When an aromatic solvent is used, the final product is solvated Al(C₆F₅)₃, after working up and drying at room temperature. Although the patent claims that the molecule of aromatic solvent can be easily removed if the drying step is carried out under vacuum at 80 °C, extra caution should be exercised when handling this material due to the extreme thermal and shock sensitivity. When the exchange reaction is carried out in an aliphatic solvent such as hexane, the nonsolvated Al(C₆F₅)₃ can be precipitated out from the reaction mixture and isolated as the clean product (eq 7). The crystal structure of the Al(C₆F₅)₃·toluene

$$B(C_6F_5)_3 + AlMe_3 \xrightarrow{\substack{\text{toleuene} \\ \text{hexane}}} \begin{array}{l} Al(C_6F_5)_3 \cdot \text{toluene} \\ \\ Al(C_6F_5)_3 \end{array} + BMe_{3\ (g)} \qquad (7)$$
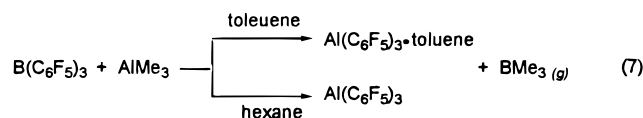
adduct has been recently determined[83] and features η^1-coordination of the arene to Al in the solid state. Such interactions are believed to persist in solution as well.

E. Trityl and Ammonium Borate and Aluminate Salts

The trityl cation Ph_3C^+ is a powerful alkide and hydride-abstracting (and oxidizing) reagent, and ammonium cations of the formula $HNRR'_2^+$ can readily cleave M−R bonds via facile protonolysis. In combination with $M(C_6F_5)_4^-$ (M = B, Al) noncoordinating/weakly coordinating anions, borate and aluminate activators, $[Ph_3C]^+[B(C_6F_5)_4]^-$,[84,85] $[HNRR'_2]^+[B(C_6F_5)_4]^-$,[86,87] and $[Ph_3C]^+[Al(C_6F_5)_4]^-$,[88] have been developed as effective cocatalysts for activating metallocene and related metal alkyls, thereby yielding highly efficient olefin polymerization catalysts. Since these initial discoveries, a number of other new borate- and aluminate-based highly efficient activators have been developed. They can be classified into three different categories based on features of anions: protected/bulky/bidentate borates (9−11), diborates (12−16), and sterically encumbered fluorarylaluminates (17) and (perfluorophenoxy)aluminates (18; vide infra).

Although $[B(C_6F_5)_4]^-$-based activators have proven to be highly effective for olefin polymerization, they suffer from poor solubility in hydrocarbons and especially poor thermal stability and crystallizability of the cationic complexes derived therefrom, which results in very short catalytic lifetimes and limits the useful tools to characterize these species.[89] For this reason, functionalized fluoroarylborate salts (9) have been synthesized according to the synthetic Scheme 6.[89] These activators offer several advantageous

Scheme 6
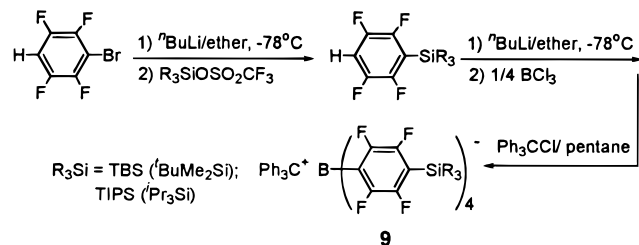
properties, including improved solubility, thermal stability, isolability, and characterizability of the resulting cationic complexes, as well as high catalytic efficiency—comparable to the analogous $[B(C_6F_5)_4]^-$-based catalysts.[90] The solid-state structure of the TBS anion is depicted in Figure 4. In attempts to generate the corresponding anionic tetrakis derivative of PBB, many other byproducts are formed. Nevertheless, a trityl salt of a pefluoroarylborate anion with one perfluorobiphenyl ligand (10) can be readily synthesized according to eq 8.[91] When combined with (1,2-$Me_2Cp)_2ZrMe_2$, the catalyst activated by 10 produces high molecular weight polyethylene ($M_w = 7.1 \times 10^5$,
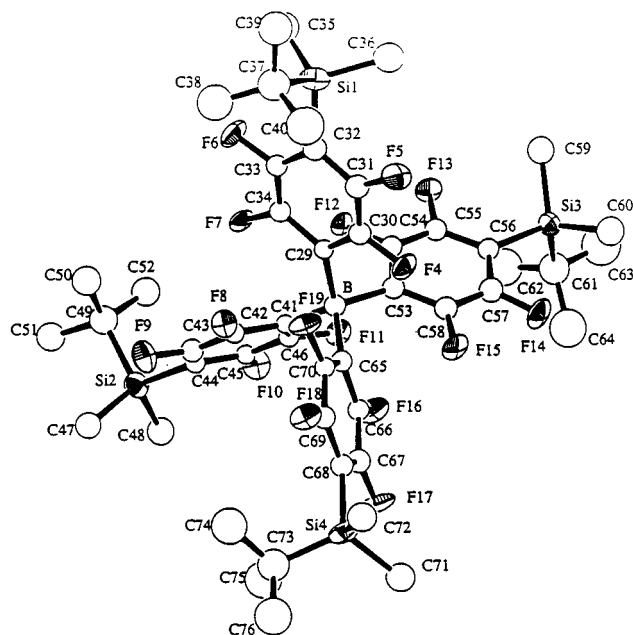
Figure 4. ORTEP drawing of the structure of the anion $B[(C_6F_4Si(^tBuMe_2)]_4^-$. From ref 90.

$M_w/M_n = 3.02$) with a 2.0×10^7 g of PE/(mol of Zr·atm·h) efficiency.
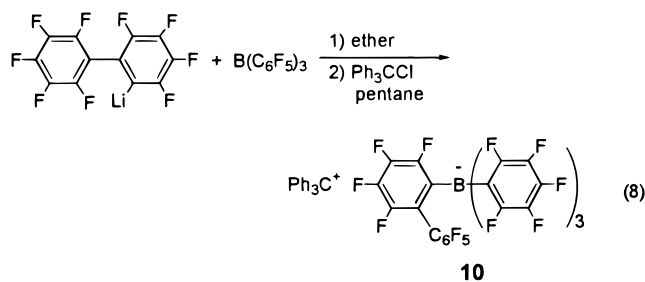
A bidentate fluoroarylborate-based activator (11)[92] has been conveniently synthesized from the reaction of BCl_3 and the corresponding dilithium salt according to eq 9. This activator has proven to be even more
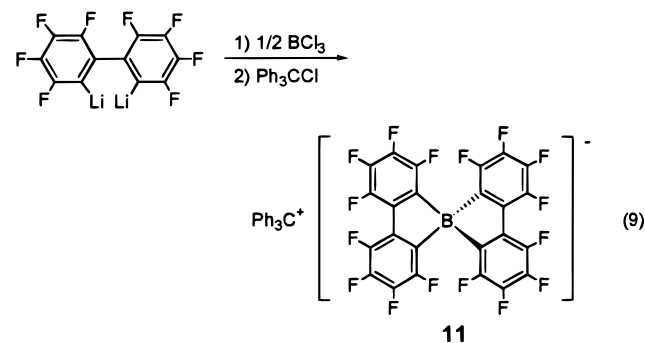
effective for ethylene polymerization when combined with zirconocene dimethyls than $[B(C_6F_5)_4]^-$-based and functionalized borate-based activators (9). Figure 5 shows the structure of the anionic portion of 11.

The synthesis of the chelating binuclear fluoroarylborate-based activator 12[93] is outlined in Scheme 7. Reaction of 12 with Cp'_2ThMe_2 (Cp' = C_5Me_5) yields the corresponding cationic complex, which is
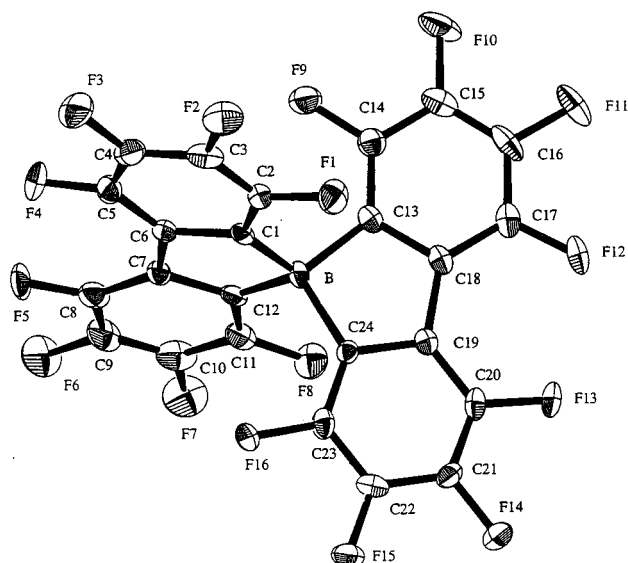
Figure 5. ORTEP drawing of the structure of $[B(2,2'-C_{12}F_8)_2]^-$, the anionic of portion of **11**. From ref 92.

Scheme 7
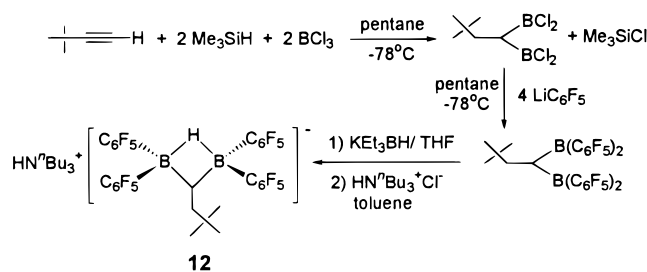
a highly active catalyst for ethylene polymerization and 1-hexene hydrogenation. Figure 6 shows the structure of the anionic component of **12**, as the product of the reaction of **12** with Cp'_2ThMe_2 followed by a THF quench.
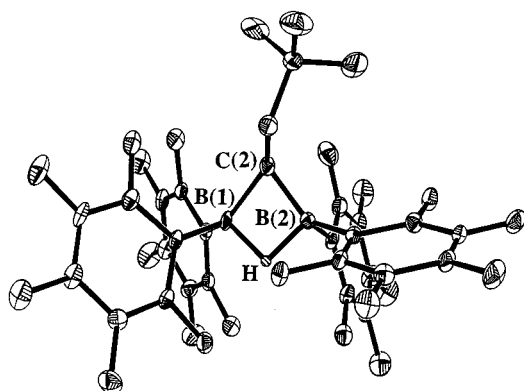
Figure 6. ORTEP drawing of the structure of the anionic component of **12**. From ref 93.

The neutral diborane intermediate undergoes slow alkyl/aryl redistribution to produce FAB and other unidentified boranes. More recently, Piers et al.[94] reported that similar neutral diboranes RCH= C[B(C_6F_5)_2]_2 have been synthesized by regioselective hydroboration of the corresponding 1-boraalkynes using $HB(C_6F_5)_2$. These neutral diboranes have been isolated, characterized, and utilized to activate group 4 metallocene diakyls for ethylene polymerization.

An interesting bifunctional borane/borate activator (**13**)[78a] has been synthesized from the corresponding neutral diborane **6** according to eq 10. Bis(borate)
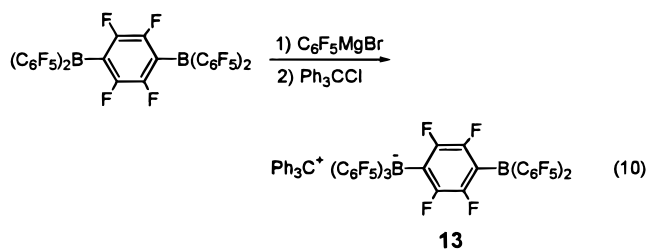
dianion-based activator (**14**)[78a] has also been synthesized via reaction of octafluoro-9,10-dichloro-9,10-diboraanthracene with multiple equivalents of LiC_6F_5 according to eq 11.
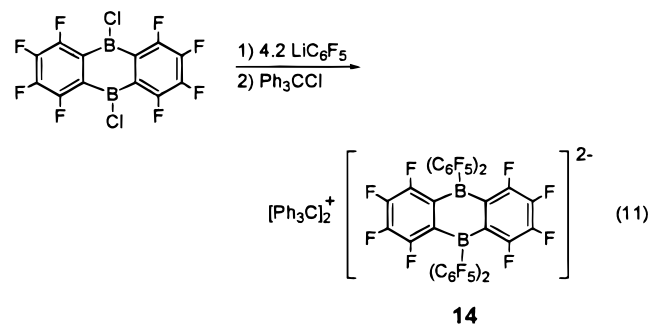
Bochmann et al.[95] have recently reported the synthesis of trityl salts of borate anions (**15**, **16**) having multiequivalences of FAB in one-pot reactions (eqs 12 and 13) which generate highly active zirconoce-

$$2\ B(C_6F_5)_3\ +\ KCN\ \xrightarrow[\substack{2)\ Ph_3CCl \\ CH_2Cl_2}]{1)\ Et_2O}\ [Ph_3C]^+[(C_6F_5)_3B\text{-}CN\text{-}B(C_6F_5)_3]^- \quad (12)$$
$$\mathbf{15}$$

$$4\ B(C_6F_5)_3\ +\ K_2[Ni(CN)_4]\ \xrightarrow[\substack{2)\ Ph_3CCl \\ CH_2Cl_2}]{1)\ Et_2O}\ [Ph_3C]_2^+\{[(C_6F_5)_3BNC]_4Ni\}^{2-} \quad (13)$$
$$\mathbf{16}$$
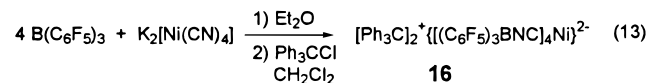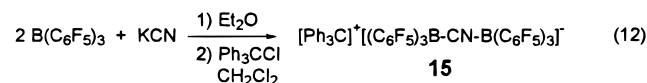
nium catalysts for ethylene polymerization. LaPointe[96] earlier synthesized **15** and other extended anions having two $M(C_6F_5)_3$ (M = B, Al) moieties linked by conjugated anionic bridges such as immidazolide, e.g., $((C_6F_5)_3M)_2C_3H_3N_2^-$.

Under a variety of conditions, reaction of (2-nonafluorobiphenyl)lithium with $AlCl_3$ leads to a salt having the composition $Li^+(C_{12}F_9)_3AlF^-$, which presumably results from aryl fluoride activation by strongly Lewis acidic, transient "tris(perfluorobiphenyl)aluminum" (Scheme 8). Ion exchange metathesis with Ph_3CCl yields the corresponding trityl (perfluorobiphenyl)fluoroaluminate, $Ph_3C^+PBA^-$ (**17**).[97] The crystal structure of **17** features an unassociated trityl cation and sterically congested chiral C_3-symmetric (fluoroaryl)fluoroaluminate anion (Figure 7). In the solid state, fluoroaryl rings are substantially twisted out of coplanarity (86°(av), ranging from 53 to 104°). In solution, however, free rotation of the fluoroaryl rings averages pairs of instantaneously nonequivalent *ortho-* and *meta*-arylfluorine atoms, and the PBA^- anion exhibits only seven ^{19}F NMR resonances
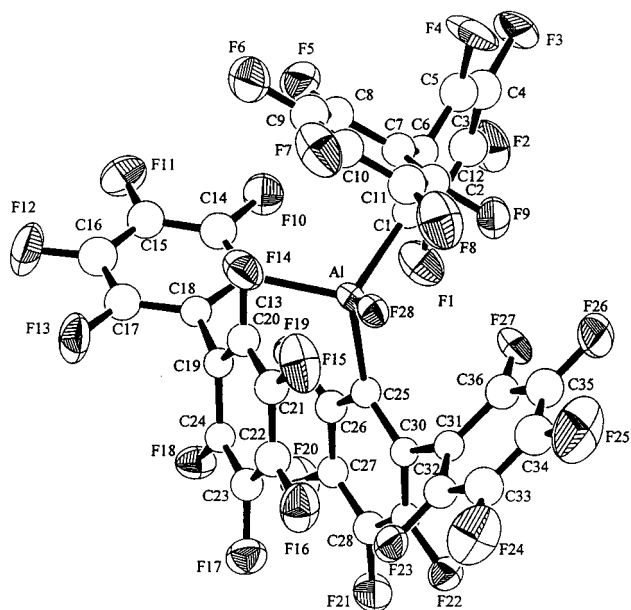
Figure 7. ORTEP drawing of the structure of the anionic component of **17** (PBA⁻). From ref 97.

(plus one broad Al−F signal) at room temperature. Interestingly, when this anion is coordinated to an electrophilic metal center, aryl ring rotation is restricted in solution.[77]

Scheme 8

17
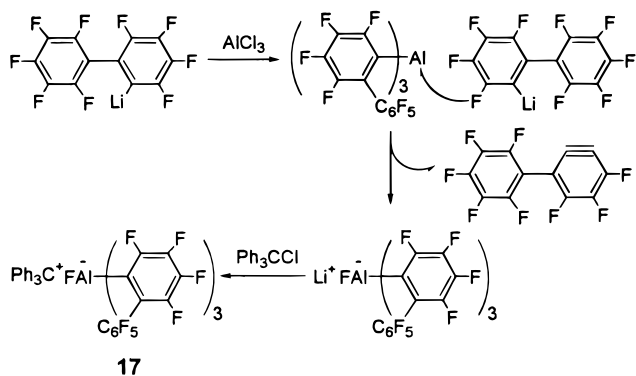
The aforementioned C−F bond activation by very Lewis acidic Al species operative in the preparation of **17** can be conveniently inhibited by replacing C_6F_5 groups with OC_6F_5 groups. Thus, reaction of $LiAlH_4$ with HOC_6F_5 affords $Li^+[Al(OC_6F_5)_4]^-$,[98] and subsequent metathesis with Ph_3CCl yields the corresponding trityl aluminate $[Ph_3C]^+[Al(OC_6F_5)_4]^-$ (**18**; eq 14).[99] Ethylene polymerization activities achieved by in-situ activating Cp'_2ZrMe_2 at room temperature with **18** are comparable to those of the same precatalyst activated with $Ph_3C^+B(C_6F_5)_4^-$.

(14)

18
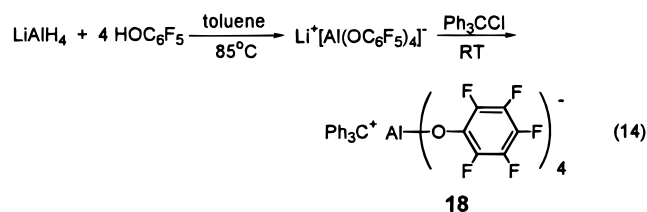
F. Cocatalysts Containing Non-Group 13 Elements

As can be seen from the preceding discussion, the vast majority of cocatalysts for metallocene and related single-site catalyst-mediated olefin polymerization are based on group 13 elements. In light of this situation, development of other families of cocatalysts containing non-group 13 elements would be of great interest. One family that is particularly interesting is based on six-coordinate octahedral Ta- or Nb-based perfluoroaryl and perfluoroaryloxide anions (**19**, **20**). Early efforts[100] to synthesize $M(C_6F_5)_6^-$
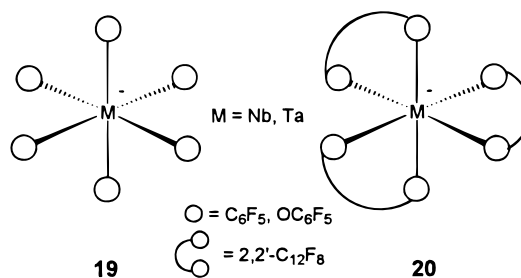
(M = Ta, Nb) anions as well as chelated $M(2,2'-C_{12}F_8)_3^-$ anions from reaction of various C_6F_5-based organometallic reagents with MX_5 reagents (X = Cl, Br, alkoxy) resulted in the formation of the desired product in very low yields, and the reaction is often accompanied by numerous byproducts such as those resulting from reductive elimination—perfluorobiphenyl and lower valent metal species. However, when $C_6F_5^-$ is replaced by $C_6F_5O^-$, the reactions have proven very successful.[99] Thus, reaction of the metal pentachlorides with 6 equiv of pentafluorophenoxy lithium at 25 °C in diethyl ether solution affords complexes having the composition $[Li(OEt_2)_n]^+\{Li\text{-}[M(OC_6F_5)_4(\mu_2\text{-}OC_6F_5)_2]_2\}^-$ (**21**). X-ray diffraction studies reveal the quasi-octahedral nature of the group 5 centers and square-planar Li^+ coordination (Figure 8).
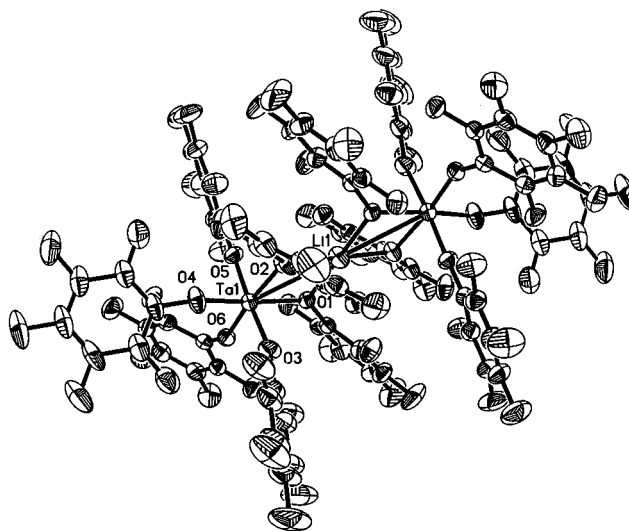
Figure 8. ORTEP drawing of the structure of the salt $[Li(OEt_2)_3]^+\{Li[Ta(OC_6F_5)_4(\mu_2\text{-}OC_6F_5)_2]_2\}^-$ (**21**). From ref 99.

Subsequent ion exchange metathesis of these lithium salts with trityl chloride affords the desired
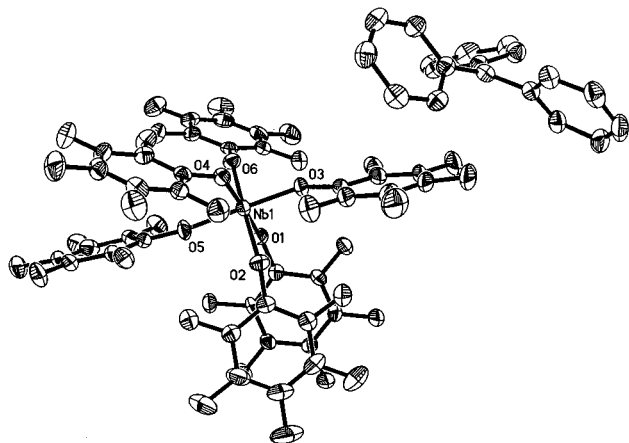
Figure 9. ORTEP drawing of the structure of the salt $[Ph_3C]^+[Nb(OC_6F_5)_6]^-$ (**22**). From ref 99.

$Ph_3C^+M(OC_6F_5)_6^-$ (M = Nb (**22**), Ta (**23**)) salts as orange crystals, which are stable in solution. The solid-state structures feature discrete trityl cations and anionic six-coordinate metal centers with pronounced nonlinearity of the M$-$O$-$C$_6$F$_5$ linkages (Figure 9). Preliminary ethylene polymerization results at room temperature mediated by in-situ activated bulky metallocene dimethyls such as Cp$'_2$ZrMe$_2$ indicate that the activities are approximately the same as the analogous B(C$_6$F$_5$)$_4^-$ -based catalysts, although in situ NMR studies reveal that activation is accompanied by eventual decomposition via C$_6$F$_5$O$^-$ transfer to Zr.[99]

G. Supported Organometallic Activators

A large proportion of commercial polyolefin production is currently achieved by large scale slurry- and gas-phase polymerization processes, which require the polymerization catalysts to be anchored on solid supports. Although supported catalysts are generally less active than homogeneous catalysts,[101] they often offer advantages in producing polymeric products with good morphology and high bulk density. Supported catalysts also enable the use of highly active polymerization systems with less reactor fouling than in conventional homogeneous processes. The focus of this section is on supported activators only, while the broader scope of supported polyolefin catalysts has been the subject of several recent reviews.[101−107]

1. Supported MAO

The most commonly used supports for anchoring MAO have been porous inorganic oxides such as alumina, MgCl$_2$, especially silica, using methodologies developed by Chien,[108] Collins,[109] Soga,[110] Kaminsky,[111] and co-workers. Most preparations using silica/alumina supports involve a thermal or chemical pretreatment, to remove residual water or hydroxyl groups which can deactivate the metallocene active sites. This approach usually involves initial absorption of MAO on the support with subsequent addition of the metallocene catalyst precursor in a second step, followed by extensive washing with hydrocarbon solvents to ensure removal of nonchemisorbed catalyst molecules. The washed catalysts are then used in the polymerization, with additional MAO or other

common aluminum alkyls introduced if necessary for achieving good activity (Scheme 9).

Scheme 9
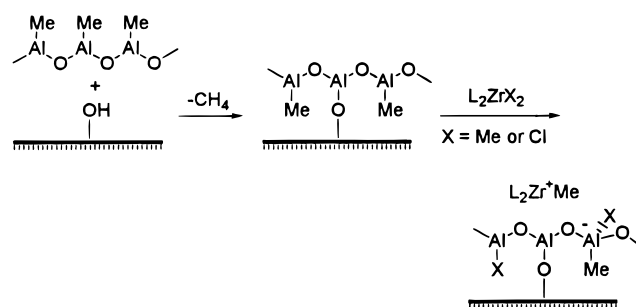
Although catalysts supported by the above approach usually behave similarly to those from homogeneous systems and yield polymers with essentially the same properties, the equivalents of MAO vs the catalyst precursor can be reduced significantly—down to 100−500 equiv, compared to ~10^3−10^4 equiv in a homogeneous systems. This behavior has been rationalized with the hypothesis that because the silica surface is essentially coated with MAO molecules, the weak ion pairs may be able to "float" over the surface much like in solution, thus resulting in a similarity between this type of system and the catalyst in solution.[112] The difference in MAO equivalents required, however, may be attributed to the fact that immobilization of the zirconocenium species may partially or completely inhibit bimolecular deactivation processes.[108] The supported MAO activator can also be prepared by in situ hydrolysis of AlMe$_3$ with hydrated silicas (10−50 wt % absorbed water).[113,114]

Other supports such as zeolites have also been reported to immobilize MAO.[115] An NaY zeolite when pretreated with MAO apparently traps Cp$_2$ZrCl$_2$ in its supercage (~12 Å diameter) to generate an active catalyst for olefin polymerization. However, the pore size of NaY limits impregnation of larger metallocene complexes such as *rac*-ethylenebis(indenyl)zirconium dichloride [Et(Ind)$_2$ZrCl$_2$]. Nevertheless, larger pore size zeolites allow difffusion of this particular complex into their internal pores. For example, a new heterogeneous alumoxane derivative generated by in situ hydrolysis of TMA in the mesopores of the siliceous molecular sieve MCM-41 (40 Å),[116] in which the MAO phase produced is chemically linked to the pore walls of the support, can activate [Et(Ind)$_2$ZrCl$_2$] for cooligomerization of ethylene and propylene.[117]

A new type of support has also been developed by reaction of predried silica with MAO and simultaneous cross-linking with aromatic diols.[118] The carrier material is a supported MAO network, which can be used as a cocatalyst for activating *ansa*-metallocene dichlorides. Additional aluminum alkyls are necessary to activate the supported catalyst and to control the polymerization profile as well as other polymer properties.

2. Silica-Bound ≡Si–O–B(C$_6$F$_5$)$_3^-$ Anions

It was reported that the surface silanols of amorphous silica react with strong, hydrolytically stable Lewis acid FAB in the presence of tertiary amines

to yield discrete, weakly coordinating anionic sites on the silica surface, each with an associated ammonium counterion (eq 15).[119] The ammonium salts

$$R_3N + B(C_6F_5)_3 + \quad \overset{OH}{\underset{}{Si}} \longrightarrow R_3NH^+ \quad \overset{O-\bar{B}(C_6F_5)_3}{\underset{}{Si}} \quad (15)$$
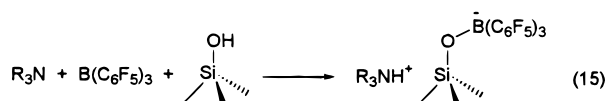
of these "silica-bound anions" are reported to behave much like $[PhNMe_2H]^+[B(C_6F_5)_4]^-$ in olefin polymerization. Thus, they also react with a variety of metallocene alkyls such as Cp_2ZrMe_2 to produce cationic species weakly coordinated to the anionic silica surface. In the absence of tertiary amines in the preparation, however, the attachment of $B(C_6F_5)_3$ to surface hydroxyl groups appears to be reversible under the same conditions, which results in the preferential formation of the toluene-soluble species $Cp_2ZrMe^+MeB(C_6F_5)_3^-$, which is subject to leaching by washing with toluene during the synthesis. This results in significant polymerization activity loss.[120] Model reactions for supported $XB(C_6F_5)_3^-$ anions were demonstrated by Siedle et al., using the reaction of FAB with water, alcohols, thiols, and polyols for preparation of adducts $(C_6F_5)_3B\cdot(REH)$ (E = O, S).[121]

Trityl salts of the silica-bound anion $\equiv Si-O-B(C_6F_5)_3^-$ were also prepared by reacting partially dehydroxylated silica with BuLi followed by reaction with FAB and metathesis with Ph_3CCl.[122]

3. Supported $PhNMe_2H^+B(C_6F_5)_4^-$ and Borate Anions

Hlatky and Upton[123] reported that by reacting the activator $[PhNMe_2H]^+[B(C_6F_5)_4]^-$ with TEA pretreated Davison 952 silica in CH_2Cl_2 or warm toluene, the activator can be evenly dispersed on the silica surface. The precatalyst Cp_2HfMe_2 can then be activated by this supported reagent by slurring in pentane.

To adapt to heterogeneous polymerization processes, Frechet and co-workers[124] have designed a route to support the activator $[PhNMe_2H]^+[B(C_6F_5)_4]^-$ onto noninteracting, lightly cross-linked polystyrene (PS) resin beads, which allows a nominally heterogeneous polymerization to proceed in a microscopically homogeneous "solution-like" environment. Thus, reaction of chloromethylated polystyrene-*co*-divinylbenzene beads with a secondary amine yields the basic tertiary amine functionalized polymer shown in Scheme 10. Reaction of the polymer-bound amine with $PhNMe_2H^+B(C_6F_5)_4^-$ affords the resin-bound ammonium tetrakis(perfluoroaryl)borate anion. The $PhNMe_2$ coproduct can be readily washed out with organic solvents, and the final active catalyst is generated by treating the borate beads with a toluene solution bis(tetramethylcyclopentadienyl)dimethylhafnium (Scheme 10). The supported catalysts display excellent activity for the slurry-phase copolymerization of ethylene and 1-hexene to afford discrete spherical polyolefin beads of millimeter dimension, according to the paper. Importantly, the presence of the Lewis basic polymer-bound amine and the higher polarity of the PS matrix relative to the polymerization medium (hexane) and monomer (hexene) liquid phase are thought to prevent leaching of the catalyst cation—anion pairs from the matrix, and thus the

Scheme 10
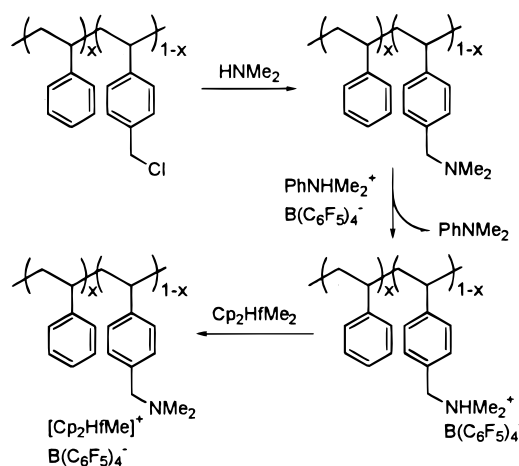
metallocene cations are believed to be homogeneously distributed throughout the particle. Therefore, the polymerization occurs within the PS particle rather than on a thin surface layer, as is the case for traditional supported catalysts. This method should in principle allow the rapid screening of different metallocene dialkyls via a combinatorial approach.

In contrast to the above strategy, methods have also been developed to prepare supported borate activators by tethering borate anions to a support. Typically, the preparation involves reacting partially dehydroxylated silica with $HNMe_2Ph^+(C_6F_5)_3B(C_6F_4-RCl)^-$ (RCl = $SiCl_3$, $SiMe_2Cl$, et al.),[125] or contacting alkylaluminum-treated silicas with $R_3NH^+(C_6F_5)_3B-Ar-OH^-$,[126] to form covalently bound activators. Polymer-bound borate-containing activators were also prepared by the AlBN-initiated copolymerization of the tris(pentafluorophenyl)-4-vinylphenylborate salt $R_3NH^+4-CH_2=CH_2C_6H_4B(C_6F_5)_3^-$ with styrene.[127]

4. Superacidic Solid Brønsted Acids

Chemisorption of metallocenes on conventional Brønsted acid surfaces often results in formation of catalytically inert μ-oxo species via M−CH₃ protonolysis.[1m,128] Recently, "superacidic" solid Brønsted acids, i.e., having weak conjugate base sites such as sulfated zirconia, have been utilized to activate metallocene precatalysts via metal−carbon bond protonolysis to generate highly electrophilic supported cationic metallocene hydrogenation and polymerization catalysts.[129] Characterization via ^{13}C CPMAS NMR spectroscopy, along with FT-IR and olefin/arene hydrogenation and ethylene polymerization results, argues that sulfated zirconia Brønsted acid sites generate cationic adsorbate species via metal−carbon bond protonolysis. The resulting conjugate base anionic sites are believed to be extensively charge-delocalized and weakly coordinating (eq 16), hence substantially different from the inert μ-oxo species, formed on typical alumina, silica, and other hydroxylated oxide surfaces.[128]

$$Cp_2Zr(^{13}CH_3)_2 \quad \xrightarrow{-\ ^{13}CH_4} \quad Cp_2Zr-^{13}CH_3 \quad (16)$$
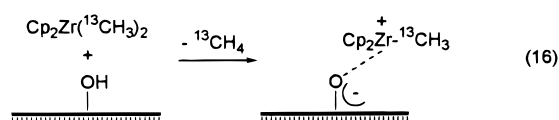
III. Activation Processes

There are five major activation processes involved in activating metal complexes for single-site olefin polymerization. These are oxidative and abstractive cleavage of M−R bonds by charged reagents, protonolysis of M−R bonds, alkyl/hydride abstraction by neutral strong Lewis acids, ligand exchange and subsequent alkyl/halide abstraction for activating metal halide complexes, and one-electron oxidation/reduction.

A. Oxidative and Abstractive Cleavage of M–R Bonds by Charged Reagents

Jordan et al.[130−132] reported that the reaction of neutral Cp_2ZrR_2 complexes with one-electron oxidants such as $(C_5H_4R)_2Fe^+$ or Ag^+ in the presence of the donor ligands (L) forms Lewis base-stabilized cationic $Cp_2ZrR(L)^+$ complexes (eq 17). The key to the

$$Cp_2Zr(CH_3)_2 + Ag^+BPh_4^- \xrightarrow{CH_3CN}$$

$$Cp_2Zr(CH_3)(CH_3CN)_2^+BPh_4^- + 1/2\ CH_3CH_3 + Ag^0 \quad (17)$$
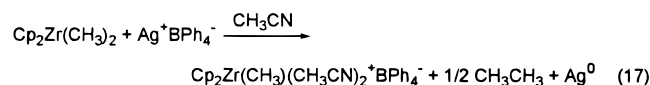
isolation of stable salts is the use of relatively noncoordinating, nonreactive (at that time) counterions such as $B(C_6H_5)_4^-$. However, even with large and weakly coordinating anions such as $B(C_6H_5)_4^-$ and $C_2B_9H_{12}^-$, fairly strong interactions/coordination patterns have been observed with base-free cationic metallocene species.[133−136] Cationic Cp_2ZrMe^+ complexes ion-paired with $B(C_6H_5)_4^-$ and $C_2B_9H_{12}^-$ or other carborane anions therefore mediate the polymerization of propylene at modest rates, if at all.

Achieving high catalytic activity of cationic catalysts by minimizing the cation−anion interactions/coordination was accomplished with the introduction of noncoordinating tetrakis(pentafluorophenyl)borate anion $B(C_6F_5)_4^-$ by Hlatky and Turner,[86] Marks,[87] Chien and Rausch,[84] and Ewen.[85] Thus, highly active cationic complexes are readily formed from the reaction of the neutral zirconocene dialkyl with $Ph_3C^+B(C_6F_5)_4^-$ (e.g., eq 18).[84]

$$Et(Ind)_2ZrMe_2 + Ph_3C^+B(C_6F_5)_4^- \xrightarrow{toluene}$$

$$Et(Ind)_2ZrMe^+B(C_6F_5)_4^- + Ph_3C\text{-}Me \quad (18)$$

(or as a dimeric form)
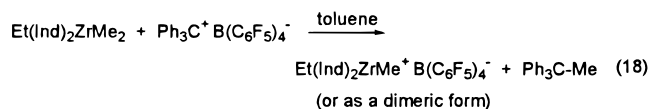
An in situ NMR investigation of the above reaction by Bochmann et al.[137] revealed that a dimeric μ-Me species $[Cp_2ZrMe(\mu\text{-}Me)MeZrCp_2]^+B(C_6F_5)_4^-$ is initially formed and probably subsequently converted to the monomeric cation species, the spectrum of which cannot be assigned by NMR with complete certainty. The quantitative formation of such dinuclear species, however, can be observed by NMR in reactions with a 2:1 ratio of $Cp_2ZrMe_2/Ph_3C^+B(C_6F_5)_4$. A similar dimeric thorium complex $[Cp'_2\text{-}ThMe(\mu\text{-}Me)MeThCp'_2]^+B(C_6F_5)_4^-$ was identified earlier.[87] A cationic dinuclear Al complex[138] with a amidinate ligand (**24**) can also be generated by the reaction of $Ph_3C^+B(C_6F_5)_4^-$ with the corresponding dimethyl Al compound (eq 19).
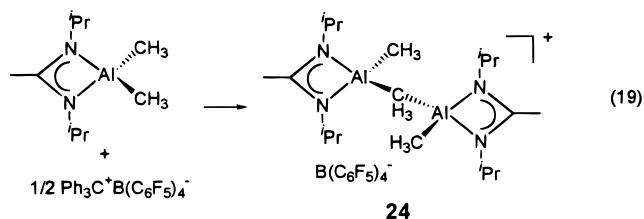
Even at −60 °C, activation of $CGCM(CH_2Ph)_2$ (M = Ti, Zr) complexes, the dibenzyl derivatives of the well-known "constrained geometry" catalysts[1e,139−141] ($CGC = Me_2Si(Me_4Cp)^tBuN$[142]), with $Ph_3C^+B(C_6F_5)_4^-$ readily produces the corresponding separated ion pair (**25**) in which the benzyl group of the cation component is bound to the Zr in an η^2-fashion (eq 20).[143]
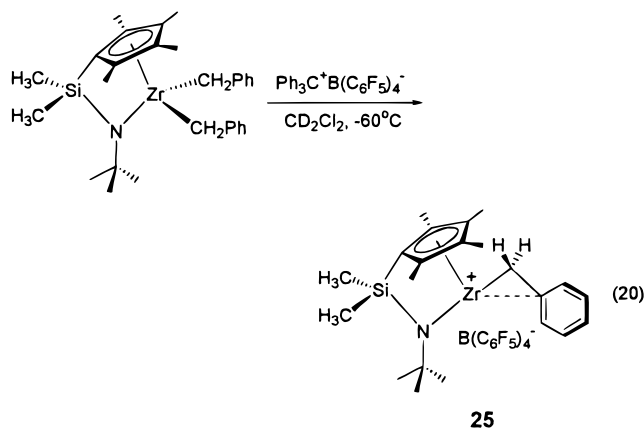
Similarly, reaction of metallocene dibenzyls with $Ph_3C^+B(C_6F_5)_4^-$ affords η^2-bound cationic benzyl complexes, which are typically thermally more stable than the corresponding methyl complexes.[144] In contrast, if a dimethyl precursor is used instead, reaction of $CGCZrMe_2$ with $Ph_3C^+B(C_6F_5)_4^-$ (solvent = toluene) yields an arene complex (**26**), reflecting the weakly coordinating characteristics of $B(C_6F_5)_4^-$.[90]
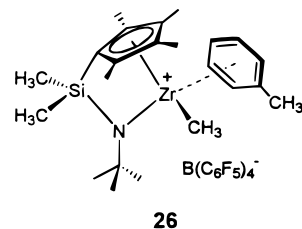
To significantly modify the electronic requirements for CGC catalyst polymerization activity and to tune the Cp-appended heteroatom functionality, a phenolated CGC-like dibenzyl catalyst was prepared. In situ activation with $Ph_3C^+B(C_6F_5)_4^-$ yielded **27**, which is very active for ethylene, propylene, and styrene polymerization.[145]
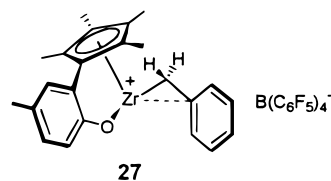
Despite high effectiveness for in-situ activation to yield some of the highest reported catalytic activities for single-site olefin polymerization,[84] efforts to isolate $Ph_3C^+B(C_6F_5)_4^-$-derived cationic complexes often result in complicated oily mixtures of unstable, unidentified species that have proven difficult to characterize in the pure state.[90,144] On the other hand, trialkylsilyl-functionalized borate trityl salts Ph_3C^+B-$(C_6F_4SiR_3)_4^-$ (**9**) offer advantages in affording the ability to cleanly isolate a variety of cationic metallocene complexes and to characterize them in the pure state. These pure, isolated metallocenium cations $Cp^x_2MCH_3^+$ (Cp^x represents a variety of substituted Cp ligands; M = Zr, Th) and "constrained geometry" catalysts $CGCZrCH_3^+$ in general have overall activities similar to those of the corresponding $Ph_3C^+B(C_6F_5)_4^-$-derived cationic complexes generated in situ. The relative coordinative ability of a series of fluoroarylborates with respect to metallocene cations has been evaluated on the basis of dynamic and equilibration NMR investigations as well as reactivity data and follows the approximate order $MeB(C_6F_5)_3^- > B(C_6F_4SiR_3)_4^- > B(C_6F_5)_4^-$. In cases of weakly coordinating anions, the neutral metallocenes compete with the anions for the cationic metallocenes, forming dimeric μ-Me complexes (eq 21).[73,90,137]

$$L_2MMe^+X^- + L_2MMe_2 \rightleftharpoons L_2M(\mu\text{-Me})ML_2^+X^- \quad (21)$$
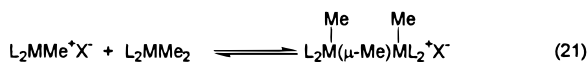
Reaction of the sterically encumbered fluoroarylaluminate-based trityl salt $Ph_3C^+PBA^-$ (**17**) with a variety of group 4 metallocene dialkyls having various symmetries (C_{2v}, C_2, and C_s) and CGC dimethyls in toluene cleanly generates the corresponding cationic complexes with NMR and X-ray diffraction data revealing coordination of the PBA^- anion via M- - -F–Al bridges (e.g., **28**).[77,97] The majority of these

28
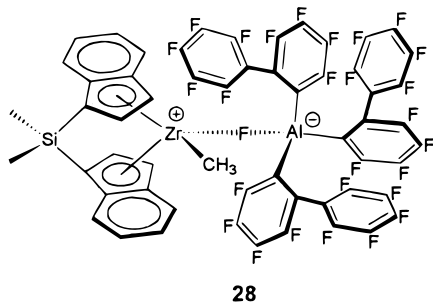
cationic complexes can be isolated cleanly and have been characterized by standard $^1H/^{13}C/^{19}F$ NMR and elemental analytical techniques and by X-ray diffraction for several representative complexes. In the case of those having very bulky ancillary ligation such as $Cp'_2ZrMe^+PBA^-$, the increased cation–anion separation results in formation of an oil on attempted isolation from toluene. There are two very interesting features of the ion pairs generated from $Ph_3C^+PBA^-$: (a) the bridging ^{19}F–Al NMR chemical shifts are extremely sensitive to the group 4 metal ancillary ligand steric bulk, reflecting varying degrees of M^+- - -F–Al$^-$ interaction which is supported by X-ray diffraction data; (b) the strong ion pairing interplay between the PBA^- chirality and the cation intrinsic

symmetry. These unique aspects of chemistry and their impact on rates and stereochemistry of olefin polymerization will be the subject of discussion in section IV.E.

B. Protonolysis of M–R Bonds

In 1986, Bochmann and co-workers[146] reported the synthesis of $Cp_2TiMe(NH_3)^+X^-$ (X = PF_6^-, ClO_4^-) complexes by reaction of Cp_2TiMe_2 with $NH_4^+X^-$ in THF at ambient temperature. Marks et al.[147] reported in 1987 that trialkylammonium tetraphenylborate reagents effect quantitative protonolysis of actinide alkyls in *noncoordinating* solvents (toluene) to yield cationic metallocenium tetraphenylborate complexes, e.g., $Cp'_2ThMe^+BPh_4^-$. Hlatky and Turner[133] reported in 1989 that the reaction of Cp'_2ZrMe_2 with $HN^nBu_3^+BPh_4^-$ in toluene yields the zwitterionic complex $Cp'_2Zr^+C_6H_4BPh_3^-$ via initial Zr–Me bond protonolysis, followed by subsequent BPh_4^- aryl C–H bond activation. The acidic carborane $C_2B_9H_{13}$ was also utilized to protonate a Zr–CH_3 bond, forming the corresponding zirconocene cation with the C_2B_9-H_{12}^- anion coordinating via a B–H–Zr bridge.[133,148] Cations paired with carboranyl and related anions can also be introduced by ammonium protonolysis[148,149] or Ag$^+$ oxidative cleavage.[150] To avoid C–H activation and strong ion-pairing of the BPh_4^- anion with the resulting metallocene cation, the dimethylanilinium or tri-n-butylammonium salt of the noncoordinating and chemically more robust perfluorophenylborate anion $B(C_6F_5)_4^-$ has been developed to produce highly active forms of the metallocenium catalysts (eqs 22 and 23).[86,87]

$$Cp_2ZrMe_2 + NHMe_2Ph^+ B(C_6F_5)_4^-$$
$$\longrightarrow Cp_2ZrMe^+ B(C_6F_5)_4^- + CH_4 + NMe_2Ph \quad (22)$$

$$Cp'_2ThR_2 + NH^nBu_3^+ B(C_6F_5)_4^- \longrightarrow$$
$$Cp'_2ThR^+ B(C_6F_5)_4^- + RH + N^nBu_3 \quad (23)$$
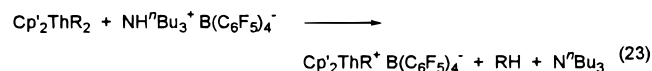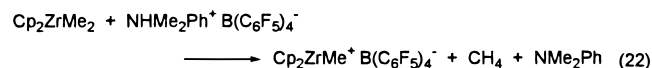
The crystal structure of the thorium complex $Cp'_2ThMe^+B(C_6F_5)_4^-$ (**29**)[87] reveals that the only close contacts between cation and anion are two fluorine atoms (F18, F19), with contacts to the metal cation of 2.757(4) and 2.675(5) Å, respectively (Figure 10).
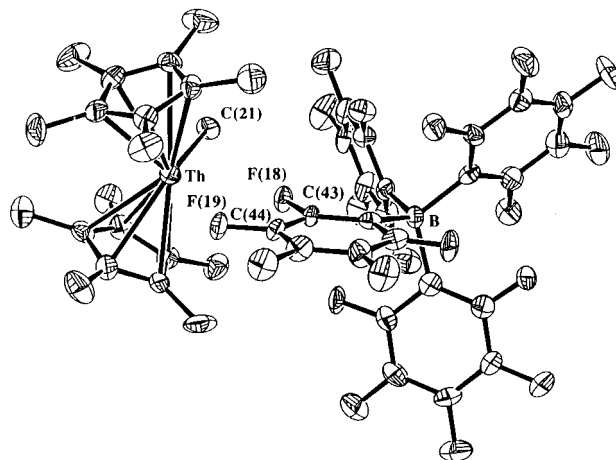
Figure 10. ORTEP drawing of the structure of the complex $Cp'_2ThMe^+B(C_6F_5)_4^-$ (**29**). From ref 87.

These Th- - -F distances in **29** are considerably longer than the sums of relevant Th^{4+} and F^- ionic radii. Additionally, the observed shortening of the Th^+-Me and Th^+-C_{ring}(av) contacts doubtlessly reflects increased electron deficiency and coordinative unsaturation at the metal center. As a result, complex **29** is about 3300 times more reactive for ethylene polymerization, and $\sim$ 4100 more reactive for 1-hexene hydrogenation, than the BPh_4^- analogue.[87] On the other hand, the tight ion-pairing via Th$-$H$-$B bonding in $Cp'_2ThMe^+X^-$ [bisdicarbollide $X^- = M[(B_9C_2H_{11})^-]_2$, M = Co, Fe] results in virtual chemical inertness.[149]

The highly electron-deficient, formally 12-electron, d^0 cationic constrained geometry catalysts (**30**)[151] can be readily prepared with ammonium salts of $B(C_6F_5)_4^-$ (eq 24). Furthermore, Campbell[152] has disclosed that mono-Cp titanium trialkyls can be activated with $HNR_3^+B(C_6F_5)_4^-$ salts for the efficient syndiospecific polymerization of styrene.

30
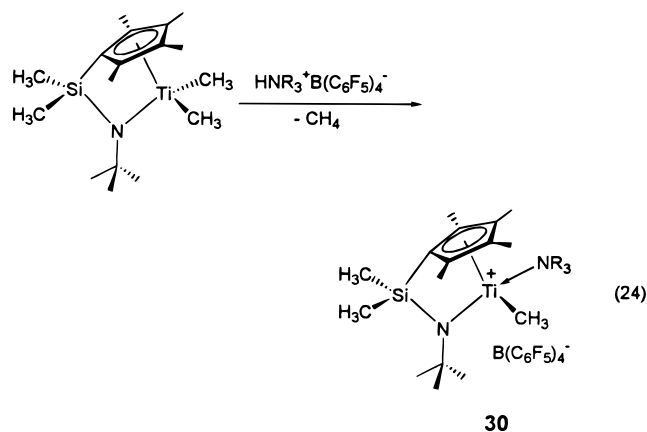
Neutral amine coodination to the cationic metal center is often observed in the activated form when $HNMe_2Ph^+B(C_6F_5)_4^-$ is employed in the protonolytic activation process. Complexes **31** and **32** are examples for non-Cp zirconium complexes derived from activation of the corresponding dialkyl precursors as reported by Horton et al.[153]

31   **32**
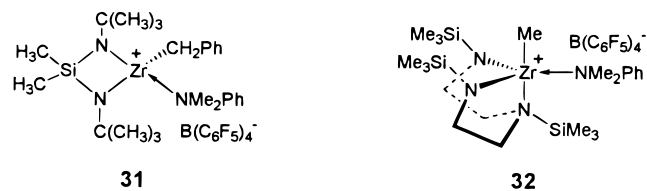
In contrast, there are also cases where the neutral amine coproduct is not coordinated to the isolated electrophilic metal center. In two zirconium complexes incorporating 8-quinolinato ligands and having similar steric environments, it appears that increased electrophilicity of the metal induced by electron-withdrawing group substitution on the ligand backbone governs the strength of amine coordination.[154] Amine coordination apparently affects polymerization activity. A study by Ishihara et al.[155] showed that for syndiospecific styrene polymerization catalyzed by $Cp'TiMe_3/TIBA/[ammonium]^+B(C_6F_5)_4^-$, the activity increases sharply with decreasing pK_a of the

ammonium salt. However, there are contrasting reports[156,157] that the presence of amine has no detectable effect on polymerization activity, suggesting that, at dilute catalyst concentrations, the catalyst is dissociated and the amine coordination is not a limiting factor for the catalytic activity in ethylene polymerization catalyzed by $(C_5H_4SiMe_3)_2$-$ZrMe_2/PhNHEt_2^+B(C_6F_5)_4^-$ [156] and in propylene polymerization catalyzed by $Et(Ind)_2ZrMe_2/PhNHMl_2^+B$-$(C_6F_5)_4^-$.[157]

Brookhart et al. reported that protonolysis of bulky diimine Pd(II) and Ni(II) dimethyl precursors with the activator $H(OEt_2)_2^+B[3,5-(CF_3)_2C_6H_3]_4^-$ [158,159] results in loss of methane and formation of cationic diethyl ether adducts (**33**, eq 25), which are effective

M = Ni, Pd; R = ^{i}Pr
R' = H, Me, or R',R' = 1,8-naphthdiyl

33
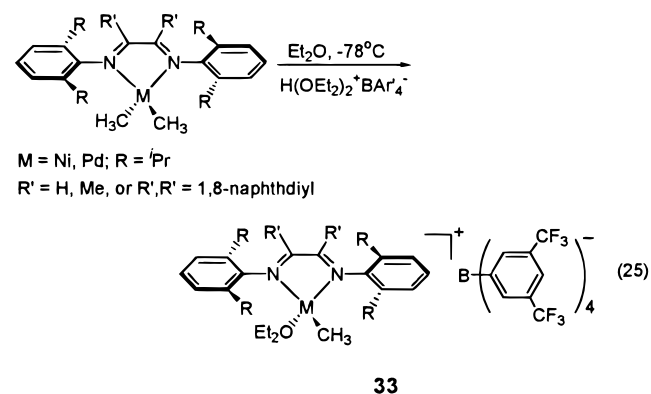
ethylene and α-olefin polymerization catalysts for the production of branched polymers.[160] The sodium salt $Na^+B(3,5-(CF_3)_2C_6H_3)_4^-$ is often used with the Pd precatalysts [N^N]Pd(Me)Cl to generate the cationic Pd(II) catalysts for copolymerization of ethylene or propylene with functionalized vinyl monomers.[161]

C. Alkyl/Hydride Abstraction by Neutral Strong Lewis Acids

In 1985, Marks et al.[162,163] reported compelling evidence for CH_3^- transfer from $Cp_2M(CH_3)_2$ complexes to coordinatively unsaturated surface sites on dehydroxylated alumina (DA) or other solid Lewis acids to yield surface-bound $Cp_2M(CH_3)_2$/DA (or $MgCl_2$) (M = actinide, Zr) complexes. Evidence was from solid-state CP-MAS ^{13}C NMR spectroscopy and chemical reactions, as well as catalytic hydrogenation and olefin polymerization studies.[162-166] The rigorously anhydrous Lewis acidic sites effectively abstract CH_3^- groups, and the resulting very reactive cationic complexes $Cp'_2M(CH_3)^+$ interact with the surface via electrostatic forces or weak μ-Cl, μ-O, or μ-CH_3 bridges (Scheme 11). The fraction of active

Scheme 11
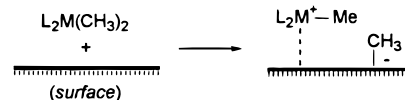
sites after the abstraction varies from $\sim$50% for $MgCl_2$ to $\sim$4% for DA. These active sites promote extremely rapid olefin hydrogenation as well as polymerization of ethylene. This work constitutes the

first example of alkyl group abstraction to yield the corresponding cationic metallocene species on a surface. Moreover, it served as a model for abstractive activation metallocene alkyls in solution, thus drawing direct connections between heterogeneous and homogeneous metallocene catalysis.

1. Bis-Cp Type Group 4 Metallocene Activation

The reaction of tris(pentafluorophenyl)borane, $B(C_6F_5)_3$, with a variety of zirconocene dimethyl complexes proceeds rapidly and quantitatively at room temperature in noncoordinating solvents to yield cationic alkylzirconocene methyltriarylborate complexes (**34**; eq 26).[67] Reaction with excess of

(26)

34
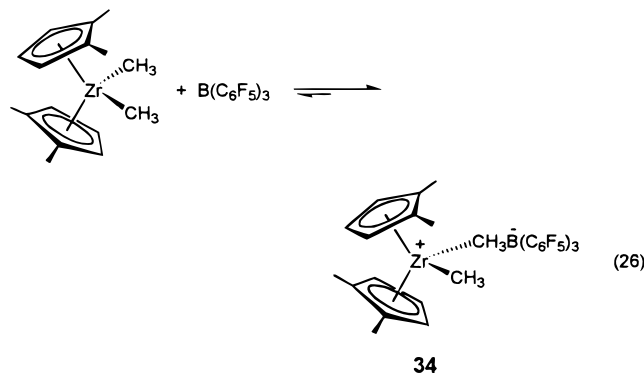
$B(C_6F_5)_3$ does not effect the removal of the second metallocene methyl group, even after extended periods of reaction.[67a] However, Green et al.[167] recently reported NMR spectroscopic evidence that a second 1 equiv of FAB abstracts a second CH_3^- group from the bis(benzyl-substituted Cp)zirconocene (p-MeC$_6$H$_4$-CMe$_2$Cp)$_2$ZrMe$_2$ at −60 °C in CD$_2$Cl$_2$. Arene coordination of the Cp benzyl group to Zr is attributed to the stabilization of the resulting dication-like structure. However, this species reverts to the monocationic species and neutral FAB above −40 °C in solution.

As noted above, the methyltris(pentafluorophenylborate) anion, $MeB(C_6F_5)_3^-$, is a somewhat more coordinating anion with respect to metallocenium cations than the tetrakis borate anion, $B(C_6F_5)_4^-$, and thus the relatively stronger cation−anion ion pairing stabilizes highly electron-deficient metal centers. This interaction improves hydrocarbon solubility, catalyst stability, and catalyst lifetime significantly. However, this coordination appears to be sufficiently weak and labile to allow an α-olefin to displace the anion from its coordination site for rapid enchainment. Unlike cations paired with $B(C_6F_5)_4^-$, cationic complexes of the type $Cp^x_2Zr(CH_3)^+$- - -$H_3CB(C_6F_5)_3^-$ are usually isolable and X-ray crystallographically characterizable. Because of these features, the versatility of FAB activation is advantageous. Thus, the catalyst precursor can be preactivated to yield an activated catalyst solution, can be activated in situ, and/or can be activated inside the reactor (in-reactor activation).

The crystal structure of complex **34** (Figure 11) consists of a "bent-sandwich" $(1,2\text{-}Me_2Cp)ZrCH_3^+$ cation weakly coordinated to the $CH_3B(C_6F_5)_3^-$ anion via a nonlinear (161.8(2)°), highly unsymmetrical
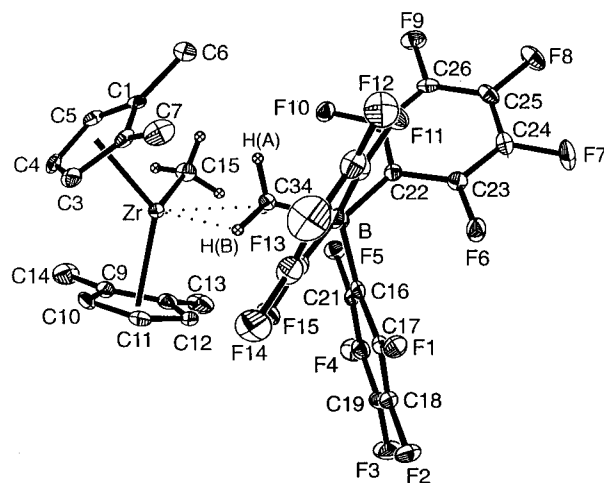
Figure 11. ORTEP drawing of the structure of the complex $(1,2\text{-}Me_2Cp)_2ZrMe^+MeB(C_6F_5)_3^-$ (**34**). From ref 67.

Zr- - -(μ-CH$_3$)−B bridge. While the B−CH$_3$ distance appears to be normal, the Zr−C34(bridge) distance is elongated by ∼0.3 Å with respect to the shortened Zr−C15(terminal) distance (2.252(4) Å). Because of the cationic character, increased electron deficiency, and coordinative unsaturation at the Zr center, this and other related cationic complexes derived from $B(C_6F_5)_3$ are highly active in olefin polymerization.

The metallocene cations undergo rapid, stepwise hydrogenolysis to yield mono- and dihydrido complexes (e.g., **35**), respectively (Scheme 12).[168] Alter-

Scheme 12

35
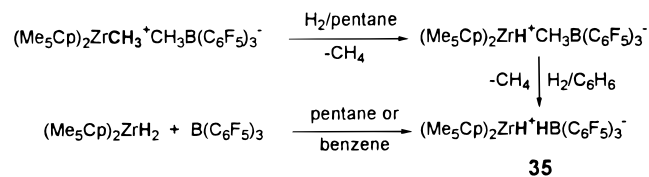
natively, the dihydrido complex can be prepared by hydride abstraction from the dihydride precursor $(Me_5Cp)_2ZrH_2$.

Activation of group 4 metallocene dibenzyls with FAB also cleanly affords η^2-bound cationic benzyl complexes (e.g., **36**),[169] and the resulting anion is well-separated from the Zr cation based on spectroscopic evidence.

36
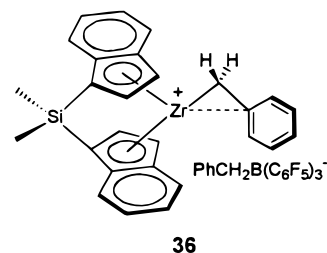
Horton[170] observed direct β-Me elimination in activating zirconocene methyl neopentyl complexes with FAB. Depending on the cyclopentadienyl ligand steric bulk, instantaneous isobutylene elimination is observed at −75 °C for bis-Cp′ ligation; however for a bis-Cp ligation environment, the cationic species formed is stable at 0 °C yet undergoes clean, revers-

Scheme 13
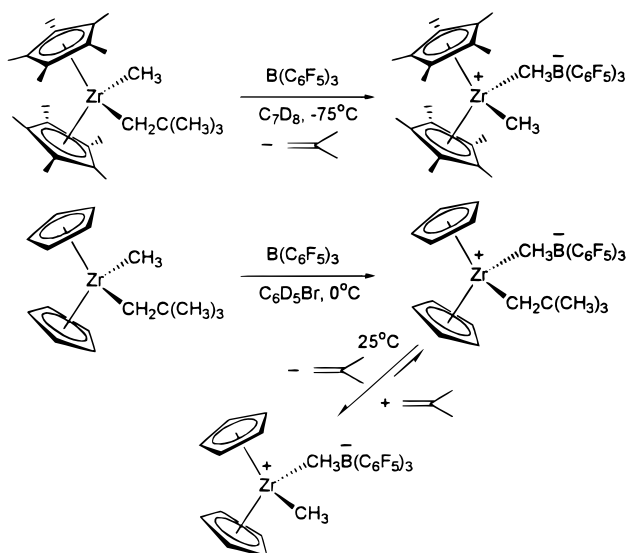
Scheme 14

ible β-Me elimination at 25 °C (Scheme 13). This finding is consistent with β-Me elimination as the major chain transfer pathway in propylene oligomerization using the sterically encumbered metallocene catalyst Cp′$_2$ZrMe$_2$/MAO.[171]

Activation of η^1,η^5-Cp′ "tuck-in" zirconocene complexes[172−174] results in formation of zwitterionic[175] single-component olefin polymerization catalysts. Reaction of "tuck-in" zirconocene **37** with 1 equiv of FAB in hexane initially forms a yellow kinetic product which under mild conditions subsequently undergoes conversion to an orange thermodynamic product **38**, in which the Zr center is stabilized by interactions with the methylene carbon and the *ortho*-hydrogen of the phenyl group.[172] Hydrogenolysis of **38** affords the corresponding hydride derivative **39**, an active single-component ethylene polymerization catalyst (eq 27). All of these active species have been isolated and crystallographically characterized.
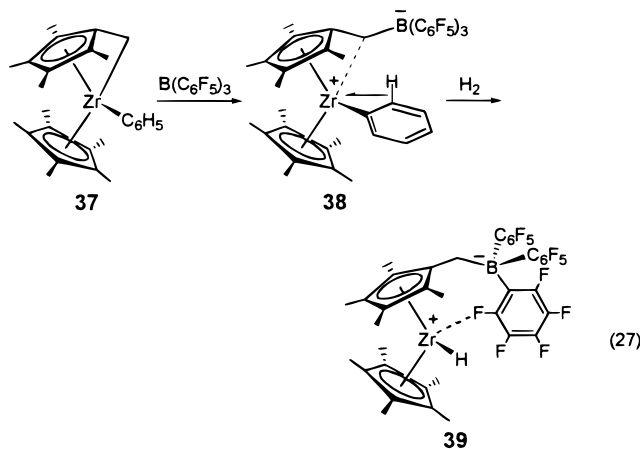
Erker et al.[176] have shown that FAB adds to zirconocene (butadiene) complexes in toluene to yield zirconocene−(μ-C$_4$H$_6$)−borate−betaine complexes (**40**, Scheme 14). A characteristic feature of the structure of **40** is the weak coordination of an *ortho*-fluoro substituent to the zirconium center to give a stable metallacyclic complex. This is a common structural
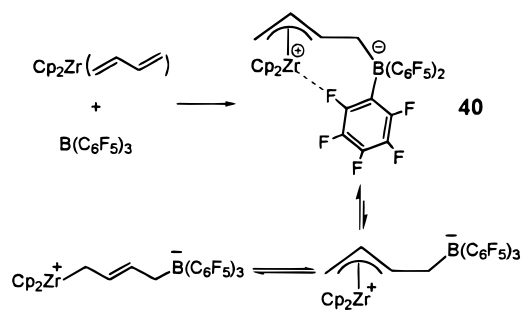
motif in metallocene-based zwitterions and is based on a weak donor interaction. Such compounds readily dissociate in solution, as evidenced by the dynamic behavior often observed in their ^{19}F NMR spectra, with an NMR-derived Zr- - -F bond dissociation energy of ∼8.5 kcal/mol.[177] Thus, compound **40** equilibrates in solution with coordinatively unsaturated isomers, presumably enabling **40** to serve as an effective olefin polymerization catalyst.

Piers et al.[178] reported that the reaction of HB-(C$_6$F$_5$)$_2$ and dialkylzirconocenes Cp$_2$ZrR$_2$ (R = CH$_3$, CH$_2$TMS, CH$_2$Ph) proceeds via initial alkyl/hydride exchange to yield "Cp$_2$Zr(H)R" complexes and RB-(C$_6$F$_5$)$_2$. In the presence of excess HB(C$_6$F$_5$)$_2$ in benzene or toluene, further reaction results in a single major product, the bis(dihydrido)borate complex Cp$_2$Zr[(μ-H)$_2$B(C$_6$F$_5$)$_2$]$_2$ (**41**), as well as 2 equiv of MeB(C$_6$F$_5$)$_2$ (eq 28).
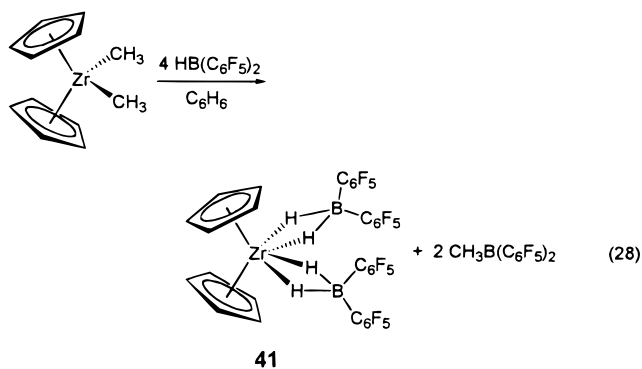
A competing reaction pathway involved in the reaction of HB(C$_6$F$_5$)$_2$ and Cp$_2$ZrMe$_2$ in hexane is the initial loss of CH$_4$ and the formation of a transient "Zr=CH$_2$" species which is then complexed by two HB(C$_6$F$_5$)$_2$ fragments to produce a borane-stabilized alkylidene derivative (**42**, eq 29).[179] Complex **42** is inactive as an ethylene polymerization catalyst under ambient conditions.
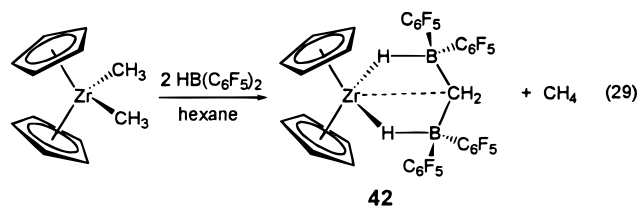
The electronic features and steric environment inherent in perfluoroarylborane abstractors strongly affect the structures of the resulting cationic metal

complexes. For instance, the reaction of the sterically encumbered borane PBB with group 4 metallocene and CGC dialkyls having a variety of symmetries (C_{2v}, C_2, or C_s) affords cationic, μ-Me dinuclear complexes (e.g., **43**; eq 30),[73,180] except for Cp$'_2$ThMe$_2$,

(30)

43
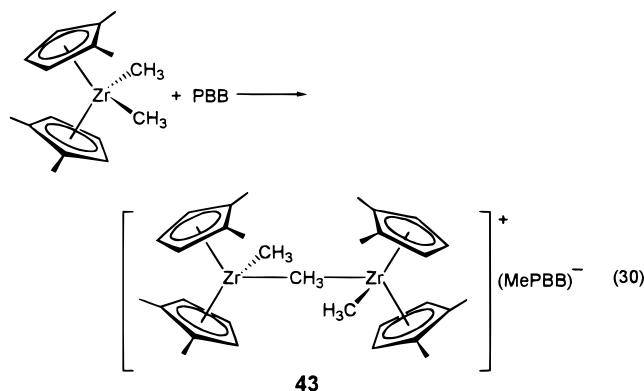
CGCZrMe$_2$, and Cp$'$MMe$_3$ which form the corresponding monomeric cationic complexes.[77] The remarkably enhanced stability of μ-Me bonding here likely reflects reduced coordinative tendencies of bulky MePBB$^-$ vs CH$_3$B(C$_6$F$_5$)$_3^-$ and the neutral LL$'$MMe$_2$ precursors, the latter of which exhibit a greater affinity for the LL$'$MMe$^+$ cation than does MePBB$^-$. The solid-state structure of **43** features a discrete separated, dinuclear cation and a MePBB$^-$ anion (Figure 12). For those metallocene and related systems forming diastereomers in the dimeric form, the ratio of diastereomers formed depends on the ancillary ligation. For example, CGCTiMe$_2$ remarkably yields only one of the two possible diastereomers on reaction with PBB,[143] while other complexes form diastereomers in much closer ratios.[77]

The isolated and well-characterized cationic, bimetallic zirconium μ-Me complexes are effective initiators for polymerization of methyl methacrylate (MMA).[77] Depending on symmetry of the dimethylzirconocene precursor, either moderately syndiotactic P(MMA) (rr ~ 65%) from C_{2v}-symmetric precursors, or highly isotactic P(MMA) (mm ~ 93%) from C_2-symmetric precursors can be obtained. Interestingly, cationic dimers from C_s-symmetric precursors having CGC and Me$_2$C(Flu)Cp ligations do not initiate MMA polymerization, presumably due to the openness of the coordination sphere of such Lewis acidic metal centers and thus stronger binding of the basic MMA monomer. Similar findings have been reported by Soga et al.,[181] who reported that monomeric dimethylzirconocenes in combination with stoichimetric amounts of activators such FAB and Ph$_3$C$^+$B(C$_6$F$_5$)$_4^-$, in the presence of a large excess of dialkylzinc, initiate syndiospecific (using bis-Cp type zirconocene) or highly isospecific (using rac-Et-(Ind)$_2$ZrMe$_2$ or rac-Me$_2$Si(Ind)$_2$ZrMe$_2$) polymerization of MMA. However, no polymerization activity is observed with Me$_2$C(Flu)CpZrMe$_2$.[182] Collins et al.[183] reported earlier that the cationic zirconocene complex Cp$_2$ZrMe(THF)$^+$BPh$_4^-$ promotes syndiospecific polymerization of MMA in the presence of excess neutral zirconocene dimethyl. The polymerization mechanism is different from that observed in olefin
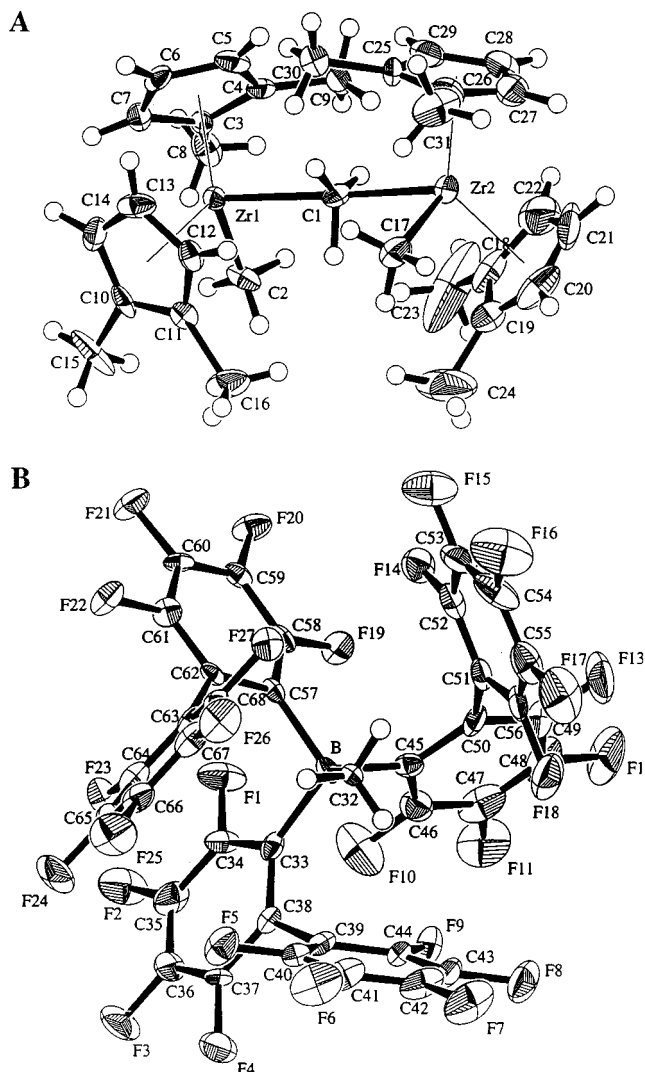
Figure 12. ORTEP drawing of the structure of the complex [(1,2-Me$_2$Cp)$_2$ZrMe]$_2$(μ-Me)$^+$(MePBB)$^-$ (**43**): (A) cation; (B) anion. From ref 77.

polymerization. Slow initiation of this polymerization involves Me transfer from Cp$_2$ZrMe$_2$ to a Cp$_2$ZrMe$^+$·MMA adduct to form a neutral enolate, Cp$_2$ZrMe(O$-$C$-$CH$_3$=C(CH$_3$)(CH$_2$CH$_3$), which then participates in the propagation process via intermolecular Michael addition to an activated monomer in the cationic adduct Cp$_2$ZrMe$^+$·MMA to ultimately produce PMMA.[77,183]

Interestingly, the alkyl abstraction chemistry of tris(β-perfluoronaphthyl)borane (PNB) lies somewhere between B(C$_6$F$_5$)$_3$ and PBB, affording either monomeric cationic complexes or dimeric cationic species, depending on the ratio of PNB to the metallocene or CGC precatalyst.[75] These activated species generally exhibit higher α-olefin polymerization activity than the FAB-derived analogues but lower acivity than the PBB-derived analogues, presumably reflecting the relative degree of cation$-$anion interaction and the anion$-$metallocenium cation coordinative tendency.

Bifunctional bis(borane) **6** reacts with 1 or 2 equiv of Cp$_2$ZrMe$_2$ to produce a mixed borane/borate complex or bis(borate) complex (**44**), respectively.[78a] The
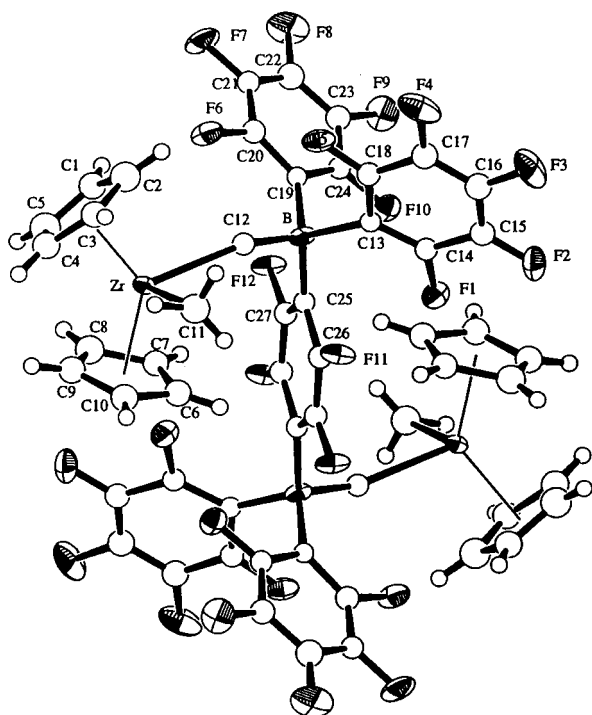
Figure 13. ORTEP drawing of the structure of the complex $Cp_2ZrMe^+MeB^-(C_6F_5)_2(1,4-C_6F_4)(C_6F_5)_2B^-Me\ Me^+$-$ZrCp_2$ (**44**). From ref 78a.

solid-state structure of the latter has also been determined (Figure 13).
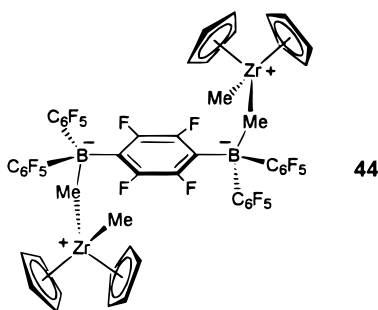
In sharp contrast to $B(C_6F_5)_3$, and despite that fact that $Al(C_6F_5)_3$ is expected to be a stronger Lewis acid, effecting facile alkyl group abstraction from group 4 dimethyl or diene complexes to form cationic zirconocene (μ-Me)Al[184] or zwitterionic complexes,[185] respectively, the unstable μ-Me complexes rapidly decompose via C_6F_5 transfer. Thus, at temperatures above 0°C, $Cp_2Zr(Me)(\mu$-Me)Al$(C_6F_5)_3$ decomposes to form $Cp_2ZrMe(C_6F_5)$ (eq 31),[184] resulting in very poor olefin polymerization efficiency.
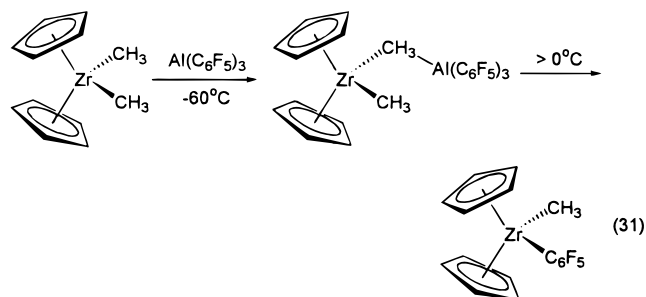
2. Mono-Cp Group 4 Complexes

The reaction of FAB with group 4 $Cp'MMe_3$ complexes produces either η^6-arene complexes, $Cp'M$-$(CH_3)_2(\eta^6$-toluene$)^+CH_3B(C_6F_5)_3^-$ (**45**, M = Zr, Hf),[186−188] or $Cp'Ti(CH_3)_2^+(\mu$-$CH_3)B(C_6F_5)_3^-$ (**46**; Scheme 15).[186]

Scheme 15
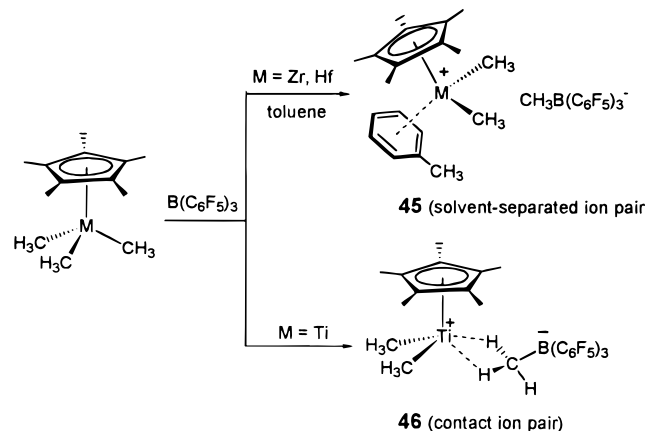
The π-arene complexes of Zr and Hf can be isolated and characterized in the pure state; however, the Ti complexes of this single ring ligand are usually too thermally unstable to isolate analytically pure. However, they can be readily characterized spectroscopically at low temperatures.[189] Complex **45** can be viewed as consisting of solvent-separated ion pairs, and **46**, as consisting of contact ion pairs, the most accurate description of which may be a function of solvent. As expected, further reaction of **46** with another 1 equiv of $Cp'TiMe_3$ produces cationic dinuclear species of the type $[Cp'Ti(CH_3)_2]_2(\mu$-$CH_3)^+$-$CH_3B(C_6F_5)_3^-$. These types of structures can also be formed by activating with $Ph_3C^+B(C_6F_5)_4^-$ directly.[190]

When methyl groups are replaced with benzyls in the one-ring precursors, similar activation processes afford interesting structures for the resulting ion pairs. Thus, Pellecchia et al.[191] found that the reaction of $CpZr(CH_2Ph)_3$ with 1 equiv of FAB gives a contact ion pair (**47**) with a benzylborate anion
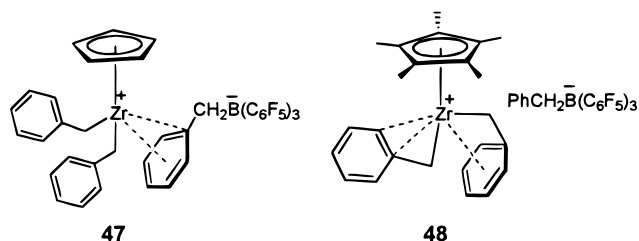
associated via η^n-coordination (best described as η^5-arene coordination; vide infra) as revealed by both the solid-state structure and solution spectroscopic investigatons. In contrast, the pentamethyl-Cp analogue affords separated ion pairs in which the cation is stabilized by multihapto-benzyl coordination (**48**).[192]

Further variations in R groups in half-sandwich Cp^xMR_3 complexes (Zr, Hf) by Bochmann et al. have revealed several interesting new reactions with FAB.

For example, allyl complexes of the type $Cp^xM(diene)$-(η^3-allyl) are attacked by FAB exclusively at the less substituted terminal carbon atom of the diene ligand to give zwitterionic complexes (e.g., **49**), which readily

49 **50**

51
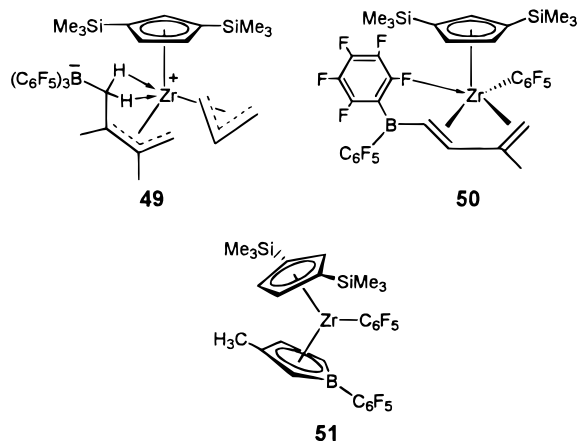
polymerize ethylene to high molecular weight polymers.[193] On the other hand, the reaction of FAB with the related benzyl complexes $Cp^xM(diene)(CH_2Ph)$ is more complex as a result of FAB attack on both the diene and the benzyl ligand.[194] Further elimination of toluene via C–H activation and concomitant migration of a C_6F_5 group from boron to zirconium generates complex **50**. Structure **50**, which was also obtained from thermal decomposition of **49**, was reported to undergo self-activation to form a new complex, **51**, with a dianionic pentafluorophenyl-substituted borole ligand.[195]

The highly electron-deficient, base free, formally 12-electron, d^0 cationic CGC catalysts (**52**) can also be readily prepared with this powerful Lewis acid (eq 32).[196] Computational investigations[197,198] and syn-

$$(32)$$

52
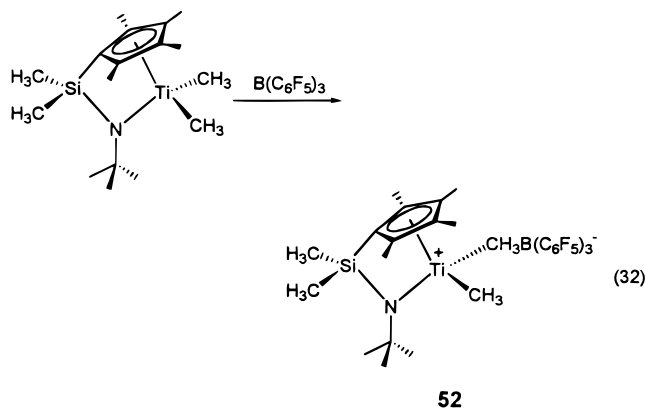
thetic, structural, and polymerization studies[77,143,145,199] on the isolated complexes $CGCMCH_3^+CH_3B(C_6F_5)_3^-$ (M = Ti, Zr) have provided much insight into this highly efficient catalytic system, especially for ethylene and α-olefin copolymerizations.

On the other hand, activating $CGCTiMe_2$ with the sterically the encumbered PBB borane results in formation of a cationic dinuclear complex (**53**) even when a 1:1 ratio of reactants is employed. Remarkably, only one of the two possible diasteromers is selectively formed and isolated in pure state.[77]

53
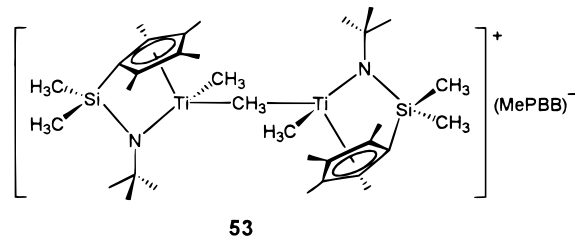
By activating with FAB in C_6D_5Br, Teuben et al.[200] studied the ancillary ligand dependence of cation–anion interactions in cationic bridged Cp-amido zirconium benzyl complexes (eq 31). The ratios of two ion pair structures generated via in situ activation, i.e., contact ion pair **54** via η^6-anion coordination and solvent-separated ion pair **55** via η^2-benzyl stabilization of the cation, are highly dependent on the nature of the $C_5H_4(CH_2)_nNR^{2-}$ ligand structure. From low-temperature ^{19}F NMR studies, it is found that, for the $n = 2$ bridge length, changing the substituent R from ^iPr to ^tBu shifts the equilibrium (eq 33) from a

54

$$(33)$$

55
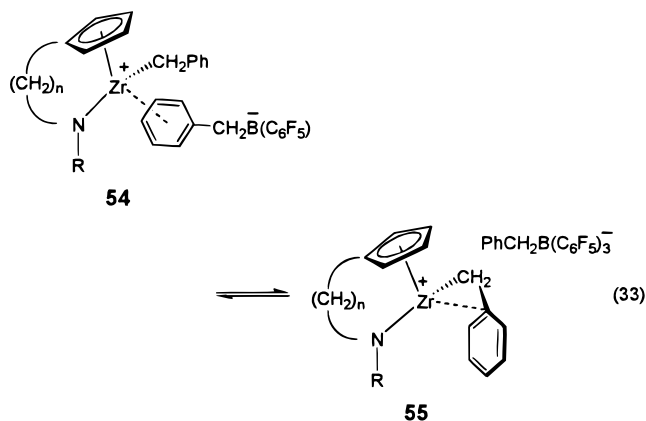
predominantly bound to a predominantly free anion structure (i.e., to the right). There is a comparable change induced by increasing the bridge length from $n = 2$ to 3 for a given R. For a comparative example, the $Me_2Si(Me_4Cp)^tBuN$ (CGC)Zr analogue exists predominantly as structure **55**. This observation further illustrates the subtle interplay of ligand steric bulk and cation–anion separation.

Activation of the tridentate-linked amido-Cp titanium dialkyls $Me_2Si(Me_4C_5)[N(CH_2)_2X]MR_2$, X = OMe and NMe_2, using protonolysis or oxidative cleavage methods failed to generate detectable or isolable cationic species.[201] However, when the zirconium dimethyl and titanium dibenzyl complexes were treated with 1 equiv of FAB in bromobenzene, the formation of the corresponding methylzirconium cation (**56**) and benzyltitanium cation (**57**), respectively, is observed. At room temperature in solution these structures exhibit mobile coordination of the side chain; however, the diastereotopic methyl substituents of the NMe_2 group are well-resolved at -25 °C, indicating slowing dissociation/recoordination of the additional donor functionality. For structure **57**, it was suggested that the solvent-separated ion pair **57** is favored over the contact ion pair **58**.[201]

X = OMe, NMe₂, **56**

L = C₆D₅Br, **57**

58
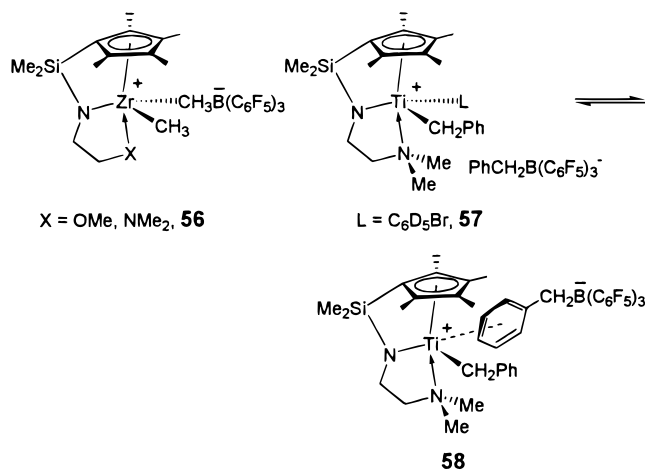
3. Non-Cp Group 4 Metal Complexes

Tetrabenzylzirconium activated with FAB in toluene forms an active catalyst for both ethylene and propylene polymerization.[202] Reaction of these two reagents in toluene at room temperature yields, after addition of heptane, an orange-red crystalline solid, identified spectroscopically as the cationic complex $Zr(CH_2Ph)_3^+PhCH_2B(C_6F_5)_3^-$ (**59**). Both variable tem-

59
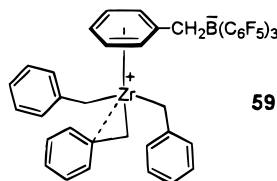
perature NMR studies and the solid-state structure reveal association of the cation and anion via η^6-coordination of the *B*-benzyl group. Toluene solvent molecules (1 per Zr atom) are also present in the unit cell.

Chelating diamide titanium complexes of the type $[RN(CH_2)_3NR]TiMe_2$ (R = 2,6-^{i}Pr₂C₆H₃, 2,6-Me₂C₆H₃) have been found to catalyze the living aspecific polymerization of α-olefins at ambient temperature, when activated with FAB, thereby producing narrow polydispersity polymers ($M_w/M_n = 1.05-1.09$).[203] To explain the fact that activities are suppressed when the polymerizations are performed in the presence of toluene, a cationic alkyl arene complex has been proposed, although no spectroscopic evidence or isolation has been provided in the paper.

Horton et al.[153] studied the FAB activation chemistry of a sterically open, Me₂Si-bridged bis(diamido)-zirconium dibenzyl as well as tridentate diamide zirconium dibenzyl and dimethyl complexes. NMR investigations revealed η^6-anion coordination to Zr for the former (**60**) and η^2-benzyl stabilization for the latter (**61**).

60

61
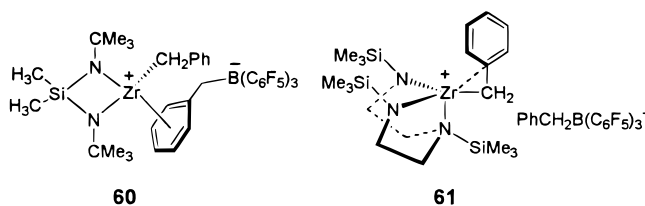
In contrast, activation of a nonbridged, sterically encumbered (diamido)zirconium dibenzyl complex with FAB affords cyclometalated product **62** after benzyl abstraction and elimination of toluene (eq 34).[204] Strong anion coordination to Zr in complex

(34)

62
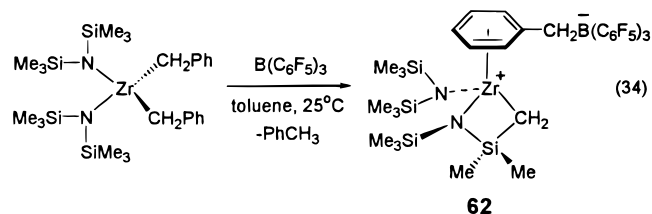
product **62** suppresses alkene polymerization. The solution structure of **62** has been studied by Landis et al.[205] using a conformer population analysis method with quantitative analysis of the ^{1}H NOESY data. It is concluded that the dominant conformers in solution are rapidly exchanging benzyl borate rotamers, closely bound to the asymmetric zirconium center.

Green et al.[206] reported recently that treatment of $M\{N(SiMe_3)_2\}_3Me$ complexes (M = Zr, Hf) with 1 equiv of FAB in pentane yields $M\{N(SiMe_3)_2\}_3^+MeB(C_6F_5)_3^-$ products (**63**) as white solids which can be recystallized from toluene (eq 35). The crystal struc-

M = Zr, Hf

(35)

63
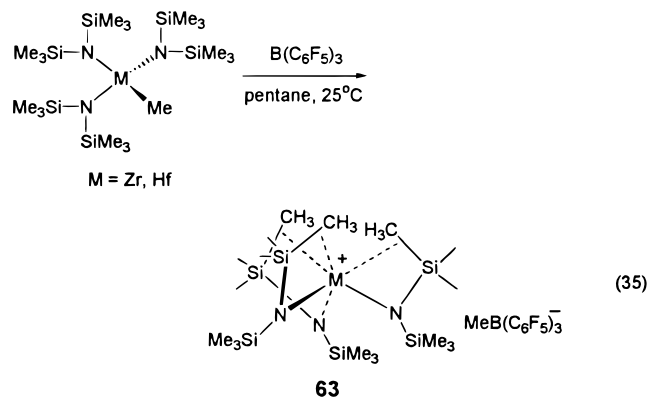
tures reveal completely separated cations and anions and that the cation is pyramidally coordinated by three amide ligands (NSi−CH₃ moieties) in which each amide ligand has one of six Si−CH₃ units located in close proximity to the metal atom. These multicenter M−Si−C interactions observed in the solid-state structures may also be present in solution at low temperatures; however, the Si−CH₃ groups are magnetically equivalent at room temperatures.

Sterically hindered Zr and Ti chelated phenoxide complexes represent a new class of homogeneous olefin oligomerization/polymerization catalysts when combined with cocatalysts such as MAO and FAB (eq 36).[207] Spectroscopic investigations of the reaction between the Zr dibenzyl complex with FAB in toluene reveals the formation of the corresponding cationic complex associated with a benzylborate anion via η^6-Ph coordination (**64**; eq 36). Similar findings were obtained from bis(*o*-arylphenoxide)M(CH₂Ph)₂ complexes (M = Zr, Ti),[208] while the corresponding dimethyl complexes yield unstable species after FAB activation. The products mediate the polymerization of ethylene and propylene.

(36)

64
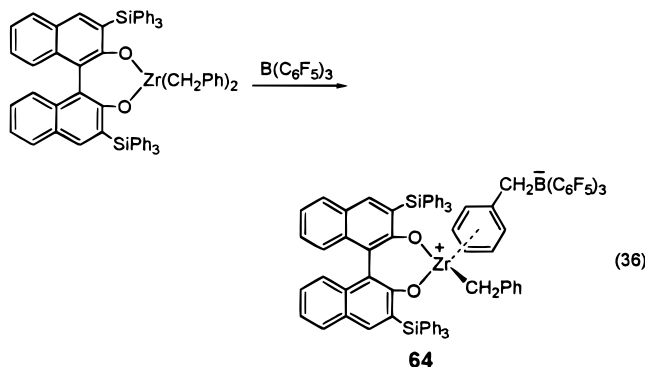
Schrock et al.[209] have developed tridentate diamido/donor ligand [(ᵗBu-d_6-N-o-C$_6$H$_4$)$_2$O]$^{2-}$ ([NON]$^{2-}$) and prepared the corresponding Zr complex for ethylene and living 1-hexene polymerizations. Upon activation, FAB abstracts the "apical" methyl group of [NON]ZrMe$_2$ to form a cationic species (**65**) analogous

65   **66**
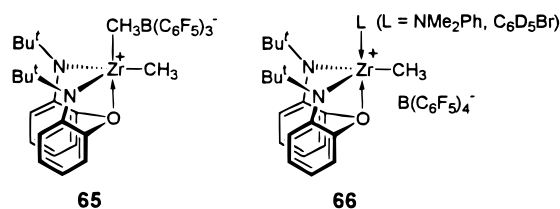
to structurally characterized compounds obtained by reacting FAB with group 4 metallocene dimethyls. The solid-state structure of **65** exhibits a trigonal bipyramidal coordination geometry with elongated Zr–Me (bridge) bond of 2.487(12) Å with respect to Zr–Me (terminal) of 2.200(13) Å, as well as a single Zr–O donor bond (2.2568(8) Å). An amine or bromobenzene separated ion pair (**66**) can be spectroscopically observed by reacting [NON]ZrMe$_2$ with HNMe$_2$Ph$^+$B(C$_6$F$_5$)$_4^-$ or Ph$_3$C$^+$B(C$_6$F$_5$)$_4^-$, respectively.[209,210] Both **65** and **66** are active catalysts for ethylene polymerization, but **66** also catalyzes 1-hexene polymerization in a living fashion.

4. Other Metal Complexes

Strong Lewis acidic boranes such as FAB can abstract alkyl groups from metal complexes other than group 4. Puddephatt et al.[211] showed that platinum-(II) cations (**67**) can be generated via a methide abstraction from the complex (dbbipy)Pt(CH$_3$)$_2$ (eq 37).

(37)

67
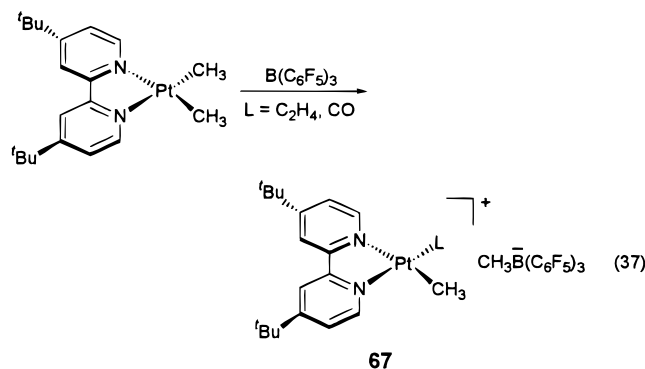
Strong Lewis acids such as FAB can also be used for generating active neutral Ni(II) ethylene polymerization catalysts. Grubbs et al.[212] reported that

68
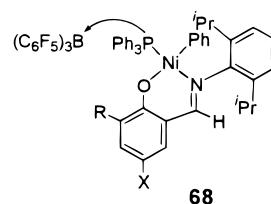
neutral salicylaldiminato Ni(II) complexes (**68**) are highly active catalysts for the polymerization of ethylene under mild conditions in the presence of a phosphine scavenger such as FAB or Ni(COD)$_2$. The phosphine scavengers bind PPh$_3$ more strongly than the Ni(II) catalyst for efficient activation.

The cationic yttrium complexes Cp$_2$*Y(μ-Me)B-(C$_6$F$_5$)$_3$ (**69**, Cp^x = Cp, TMS-Cp) have been obtained and isolated from the reaction of [Cp^{x}Y(Me)]$_2$ with FAB by Bochmann et al. (eq 38).[213] The solid-state

(38)

69
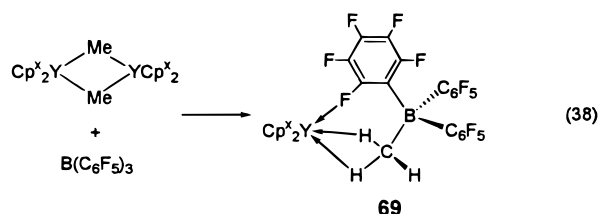
structure of the TMS-Cp derivative indicates that the anion is coordinated to Y via one *ortho*-fluorine atom and agostic interactions with two methyl hydrogen atoms. These complexes are stereochemically dynamic in solution and act as initiators for the carbocationic polymerization of isobutylene.

Piers et al.[214] have reported that dibenzylscandium complexes having β-diketiminato ligands can be activated rapidly and cleanly with FAB to form an ion pair (**70**) in which the anion is associated with the cation via strong η^6-bonding (eq 39).

(39)

Ar = 2,6-ᶦPr$_2$C$_6$H$_3$ **70**
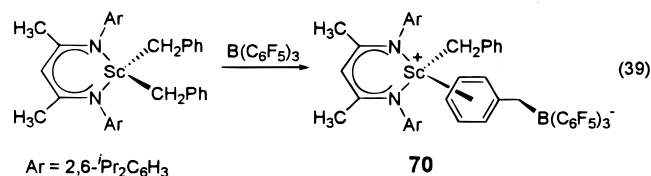
Green et al.[215] found that simple methide abstraction does not occur between Cp(CO)FeCH$_3$ and FAB. In a much more complicated reaction sequence, formation of the final observed product (**71**) is proposed to occur via a multistep process, involving Lewis acid-assisted CO migratory insertion, followed by rearrangement of this intial intermediate, and formal insertion of a C$_6$F$_4$ group into the Fe acyl carbon bond, accompanied by loss of fluoroboranes BF$_n$(C$_6$F$_5$)$_{3-n}$ (n = 1−3). The following equation illustrates only the overall reaction:

(40)

71

Bochmann et al.[216] have shown that the methide abstraction by FAB occurs not only from a transition metal complex but from an aluminum cyclopentadienyl complex, Cp_2AlCH_3, to produce the aluminocenium cation ion pair $Cp_2Al^+MeB(C_6F_5)_3^-$ (**72**; eq 41), which is an effective cationic initiator for the polymerization of isobutylene.

$$(41)$$

72

Jordan et al.[138,217] have reported that the reaction of FAB with monoamidinate Al complexes produces either cationic dinuclear Al μ-Me complex (**24**) or a monomeric complex (**73**), depending on steric bulk of the ligand (eq 42).

$$(42)$$

73

D. Ligand Exchange and Subsequent Alkyl/Halide Abstraction for Activating Metal Halide Complexes

When toluene solutions of Cp_2ZrCl_2 are treated with MAO, a rapid, initial ligand exchange reaction generates primarily the monomethyl complex $Cp_2Zr(Me)Cl$;[50,218] excess MAO leads to Cp_2ZrMe_2.[50] These systems become catalytically active when the concentration of excess MAO is raised to Al:Zr ratios of a few hundreds to thousands:1 or higher, typically in solution-phase polymerizations. It is generally assumed that some of the Al centers in MAO have an exceptionally high propensity to abstract a Cl^- from $Cp_2ZrMeCl$ or a CH_3^- from in-situ formed Cp_2ZrMe_2 and to form ion-paired structures such as $Cp_2ZrMe^+Cl[-Al(Me)O-]_n^-$ or $Cp_2ZrMe^+Me[-Al(Me)O-]_n^-$ based on solid-state XPS[219] and ^{13}C NMR[220] studies, as well as ^{91}Zr and ^{13}C NMR investigations of Cp_2ZrMe_2/MAO solutions (eq 43).[221,222]

$$Cp_2Zr(CH_3)_2 + [Al(CH_3)O]_n \rightleftharpoons Cp_2Zr(CH_3)^+ Me[Al(CH_3)O]_n^-$$

$$(43)$$

In the overall MAO mechanism for activating metal dichloride precursors, it is now generally accepted that Cp_2ZrCl_2 is monoalkylated by the TMA contained in MAO or directly by MAO to give $Cp_2Zr(CH_3)Cl$ and that the Cl ligand of the resulting $Cp_2Zr(CH_3)Cl$ is abstracted by MAO to form a catalytically active species.[218] The overall activation scenario for a zirconocene dichloride with MAO can be represented as in Scheme 16.[223,224]

An alternative hypothesis[45] that the "free" TMA, not MAO, might be the actual cocatalyst in the metallocene–MAO-based system has been challenged. Tritto et al. showed by comparative NMR studies of reactions between $Cp_2Ti(CH_3)Cl + Al(CH_3)_3$

Scheme 16

and $Cp_2Ti(CH_3)Cl$ + MAO that MAO is a superior alkylating agent and has a greater capacity to produce and stabilize cation-like complexes.[222] Unlike MAO activation, the equilibrium involved with TMA lies far to the left (eq 44).[44] MAO is a significantly stronger Lewis acid, and the resulting counterion is far less coordinating than that of TMA. Therefore, "free" TMA is not the actual cocatalyst in metallocene–MAO-based catalytic systems.

$$Cp_2ZrMe_2 + Me_3Al \rightleftharpoons Cp_2ZrMe^+AlMe_4^-$$

$$(44)$$

^{13}C NMR spectroscopic studies of the in-situ polymerization of ^{13}C-enriched ethylene in the presence of $Cp_2Zr(^{13}CH_3)_2$ and MAO by Tritto et al. have obtained direct evidence of the formation in solution of monomeric $Cp_2ZrMe^+MeMAO^-$ and dinuclear $(Cp_2ZrMe)_2(\mu\text{-Me})^+MeMAO^-$ species, as well as the heterodinuclear $Cp_2Zr(\mu\text{-Me})_2AlMe_2^+MeMAO^-$ cationic species.[56,225] The last two dinuclear complexes are possible dormant states for the active sites in olefin polymerization.

The Lewis acidity of aluminoxanes can arise from functionality other than three-coordinate Al centers. Barron et al.[226] found that, in the case of aluminoxane clusters such as **5**, three-coordinate aluminum is not a prerequiste for ethylene polymerization activity when combined with zirconocene dimethyl. Coordinatively saturated aluminoxane **5** reacts exothermically with Cp_2ZrMe_2 at room temperature to produce, according to the ^1H NMR spectrum, an ethylene polymerization-active tightly ion paired species, $Cp_2ZrMe\cdots(^tBu)_6Al_6(\mu_3\text{-O})_6Me$ (**74**). The driving force for

74

the formation of four-coordinate Al centers in these aluminoxane clusters by abstraction of CH_3^- is proposed to be the "latent Lewis acidity"—a consequence of the ring strain present in the cluster (opening of the structure occurs during the metallocene activation process).

MAO or MMAO also effectively activates late-transition metal halide α-olefin polymerization precatalysts such as 2,6-^iPr-substituted aryl bulky diimine Ni(II) dibromides for branched polymers[160] and block copolymers by living polymerization at low temperatures,[227] *para*- and unsubstituted aryl diimine Ni(II) dibromides for production of linear

α-olefins,[228] and tridentate pyridine diimine Fe(II) and Co(II) dihalides for linear, high-density polyethylene[229,230] and moderately isotactic polypropylene via a 2,1-insertion mechanism.[231,232]

A ternary system that consists of a zirconocene dichloride, a trialkyl aluminum, and $Ph_3C^+B(C_6F_5)_4^-$ has been developed by Chien et al.[233] for ethylene and propylene polymerizations with superb activity. The use of excess of R_3Al serves both to alkylate the dichloride precursor as well as to scavenge O_2, H_2O, and other protic impurities in the system.[234] The entire activation process can be perceived as the initial in-situ alkylation of the zirconocene dichloride by the alkylaluminum, followed by subsequent oxidative cleavage of a Zr−R bond by Ph_3C^+ (eq 45). This

$$Me_2Si(Ind)_2ZrCl_2 \xrightarrow[\text{2) } Ph_3C^+ B(C_6F_5)_4^-]{\text{1) } R_3Al \text{ (xs.)}}$$

$$Me_2Si(Ind)_2ZrR^+ B(C_6F_5)_4^- + Ph_3C\text{-}R \quad (45)$$
$$\text{or as a dimeric form}$$

convenient approach avoids using zirconocene dialkyls as catalyst precursors; however, caution must be taken regarding the quantity of trialkylaluminum needed to optimize the catalytic efficiency. Although an excess of such species can serve as a scavenger, it could also deactivate the system and thus lower the efficiency. For example, TMA has been found to react with $Ph_3C^+B(C_6F_5)_4^-$ to form a series of exchange products[184] as well as to "intercept" metallocenium cations to form heterodinuclear complexes.[137] Unlike MAO-activated catalytic systems, the optimum activity of this system is very sensitive to the polymerization temperature.[233−236] Typically, the highest activity obtained from $L_2ZrR^+B(C_6F_5)_4^-$ species generated in situ is when the polymerization is carried out from 0 to −20 °C. The noncoordinating features of the anion and the low olefin insertion barrier for this system allows high efficiencies to be achieved at low polymerization temperatures—as low as −60 °C. On the other hand, there is an activity loss in high-temperature polymerizations. Choice of aluminum alkyls also sometimes affects the stereospecificity of propylene polymerization[237] and chain transfer reactions.[238] It was reported that propylene polymerization catalyzed by a $[ArN(CH_2)_3NAr]TiCl_2$ (Ar = 2,6-$^iPr_2C_6H_3$) complex, when activated with TMA (or TEA)/$Ph_3C^+B(C_6F_5)_4^-$, produces atactic polypropylene. However, when TIBA/ $Ph_3C^+B(C_6F_5)_4^-$ is employed as the activator, propylene polymerization affords a mixture of atactic and isotactic polypropylene.[237] The isotactic index (II; defined as weight fraction of isotactic polymer in refluxing heptane; hexane was used to fractionate the crude polymer in this example) depended strongly on the polymerization temperature, and the highest isotacticity (II = 78.9%, T_m = 129.2 °C) was achieved at a polymerization temperature of ∼40 °C.

E. One-Electron Oxidation and Reduction

One-electron oxidation of the stable Ti(III) complex $(C_5Me_5)_2Ti(CH_3)$ by $Ag^+[BPh_4]^-$ in THF yields $(C_5Me_5)_2$-$Ti(CH_3)(THF)^+$.[239] Similar oxidation of $[Cp_2ZrCl]_2$ by Ag^+ was used earlier to prepare $Cp_2ZrCl(L)^+X^-$ (X−

= BF_4^-, ClO_4^-) salts.[240] Furthermore, (CGC)Ti(III) catalyst precursors can be activated with ferrocenium tetrakis(pentafluorophenyl)borate and oxidized to cationic Ti(IV) species **75**, which is a very active olefin polymerization catalyst (eq 46).[241] Another disclosure

$$(46)$$

75

by the Dow group suggests that active catalysts can alternatively be prepared by electrochemical oxidation of Ti(III) and Ti(IV) catalyst precursors, obviating the need for chemical oxidizing agents such as ferrocenium salts.[242]

Mono-Cp (single-ring)-type titanium complexes Cp^xTiX_3 (X = Cl, CH_3, CH_2Ph, BuO) when activated with MAO, $B(C_6F_5)_3$, or $Ph_3C^+B(C_6F_5)_4^-$ catalyze rapid syndiospecific styrene polymerization to produce highly syndiotactic polystyrene.[243−248] The activation mechanism and the true active species responsible for the syndiospecific enchainment of styrene have been subjects of considerable debate. A popular hypothesis is that the true active species is actually a $Ti(III)^+$ complex, formed by reduction of the initial Ti(IV) species by MAO, AlR_3, or by some other mechanism.[249−251] Reduction is probably caused by the free trimethylaluminum contained in MAO, since aluminum alkyls are more effective reducing agents than alumoxanes (Scheme 17).[243] Although

Scheme 17

$$CpTiX_3 + Al(CH_3)_3 \longrightarrow CpTiX_2 + Al(CH_3)_2X + \text{"}CH_3\text{•"}$$

$$\Big\Updownarrow MAO \qquad\qquad\qquad \downarrow$$

$$\qquad\qquad\qquad\qquad\qquad C_2H_6$$

$$CpTi(X)CH_3 + MAO\text{-}X$$

$$\Big\Updownarrow MAO$$

$$CpTiCH_3^+ MAO\text{-}X^-$$

ESR studies have confirmed the formation of such $Ti(III)^+$ species, present in significant amounts (the exact percentage varies with ligands and catalyst aging time) in the activated solution mixture, the activation mechanism and the function of other species formed are yet to be determined. Other experiments appear to support this hypothesis, since isolated and characterized $Cp'M(IV)Me_2^+$ (M = Zr, Hf) complexes catalyze only aspecific styrene polymerization to yield actactic polystyrene.[73] However, the isolable Ti(III) complex $Cp'Ti(OMe)_2$ produces highly syndiotactic polystyrene after activation with either MAO or TIBA/$PhMe_2NH^+B(C_6F_5)_4^-$ and even exhibits greater catalytic activity than $Cp'Ti(OMe)_3$/MAO.[252]
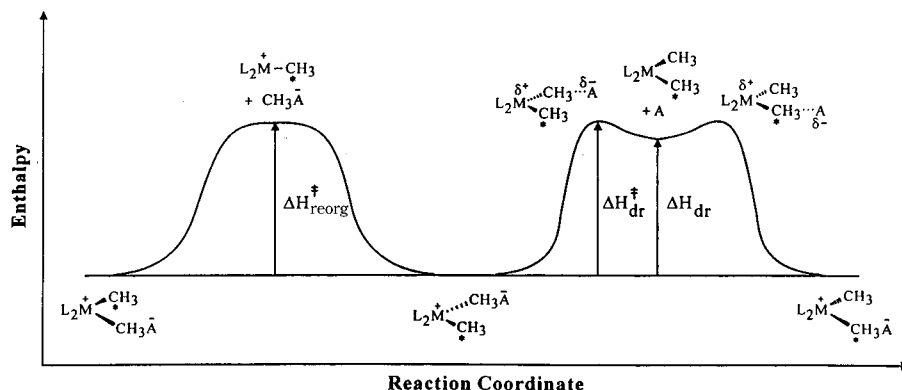
Figure 14. Schematic enthalpic reaction coordinates for metallocenium ion pair reorganization processes. Left: ion pair separation/reorganization (reorg). Right: Lewis acid methide dissociation/formation (dr/form).

The reduction of initially formed Ti(IV)$^+$ borate species Cp′TiR$_2$(μ-R)B(C$_6$F$_5$)$_3^-$ to what is believed to be the true active species, Cp′TiR$^+$, is not well-understood. This is often described as a reductive decomposition, which can be monitored by ESR. Althought this decomposition mechanism is not yet well-defined (homolytic cleavage, reductive dimerization, hydride formation, or other mechanisms), it is practically meaningful. Styrene polymerization by Cp′TiMe$_3$/FAB carried out in the low-temperature regime (below the decomposition temperature) produces only atactic polystyrene, possibly via a carbocationic polyaddition. However, at higher polymerization temperatures (above the decomposition temperature), highly syndiotactic polystyrene can be obtained[244] by coordinative 2,1-polyinsertion.[246,253]

More recent studies aimed at quantifying the relationship of syndiospecific styrene polymerization activity and the concentration of Ti(III) species under polymerization conditions by Chien et al.[254] show that both the tetravalent and trivalent Ti cationic species are active for syndiospecific styrene polymerization, with the former actually having the greater activity than the latter (~10−20×). Therefore, the single-ring Cp^{x}TiX$_3$ catalysts when activated with borane/borate activators as well as with MAO are capable of being multisite catalysts depending on the specific precursor used (ease of reduction), aging time (ratios of species with different oxidation states), and the duration of the polymerization (degree of reductive decomposition).

IV. Catalyst–Cocatalyst Structure–Activity Relationships

Besides the intense research activity in synthesizing new activators and catalyst precursors, as well as in studying activation processes for metallocene- and CGC-mediated polymerization, the Northwestern group has been particularly interested in the characterization of isolable, crystallographically characterizable metallocenium cation−anion pairs for studying the molecular basis of the polymerization catalysis. A significant effort has been devoted to understanding the nature of the metallocenium cation−anion interaction(s) and their consequences for polymerization characteristics. This section of the review focuses on the thermodynamic and kinetic aspects of
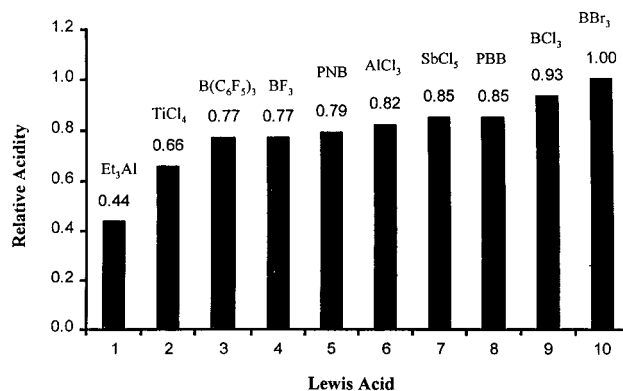

Figure 15. Relative acidity ordering of perfluoroarylboranes and other Lewis acids based on crotonaldehyde H$_3$ NMR parameters.

metallocenium ion-pair formation, dissociation, and structural reorganization, as represented in Figure 14, as well as on the effects of these phenomena on olefin polymerization activity and stereospecificity.

## A. Lewis Acidity of Fluoroaryl Boranes

The emergence of a number of new perfluoroarylboranes offers a diverse array of abstractor structures for metallocene activation. With the diversity of the activation chemistry and polymerization performance, it is of great interest to calibrate the acidities of these organo-Lewis acids on a common scale with respect to more commonly used Lewis acids. Using NMR spectroscopic methods developed by Childs et al.[255] which assesses the relative Lewis acidity in a semiquantitative fashion by measuring chemical shift changes of H$_3$ in crotonaldehyde upon binding a Lewis acid, the three perfluoroarylboranes, FAB, PBB, and PNB, can be compared with other strong Lewis acids (Figure 15).[256]

It can be seen from the above figure that the present fluoroarylboranes are highly Lewis acidic, however, not as acidic as the most acidic boron or aluminum halides. With respect to crotonaldehyde, the NMR-derived perfluoroarylborane acidities decrease in the order PBB > PNB > FAB, which also reflects the ethylene polymerization activity ordering of this series (vide supra). This acidity measurement is thought to be relatively insensitive to steric effects.[257] However, this ordering of acidity is altered somewhat from results provided by solution reaction calorimetry

data and the resultant heats of reaction.[256,258] For instance, using CH_3CN as the reference base, the relative calorimetric borane acidity is PNB ≈ FAB > PBB. Sterics appear to play an important role here as the reaction enthalpies of perfluoroarylboranes respond differently with respect to change of Lewis base substrates. This result emphasizes the importance of *structural match* for metallocene activation (section IV.E). By the selection of different activators with respect to a precatalyst structure, the difference in polymerization results can be dramatic (vide infra).

To further examine the effects of varying triarylborane Lewis acidity on the metallocene catalyst activation process, a series of triarylbones in which two of the aryl groups are $C_6F_5^-$ and the third is varied has been synthesized.[259] The triarylborane $ArB(C_6F_5)_2$ (**76**) substituents (at 3,5-positions substituted with F, H, and Me, respectively) were chosen in order to incrementally modulate the Lewis acidity of the triarylboranes as compared to FAB. The metallocene dimethyl $1,2\text{-}Me_2Cp)_2ZrMe_2$ was chosen as a model metallocene. The substantially less Lewis acidic BPh_3 exhibits no detectable reaction with this metallocene dimethyl at room temperature.[67a] In contrast to the metallocene dimethyl behavior with FAB, analogous ^1H NMR studies using these less acidic boranes reveal incomplete methide abstraction from metallocenes. Rather, the spectra are consistent with a dynamic equilibrium between the neutral metallocene, borane, and the corresponding metallocenium salt (**77**, Scheme 18). These observations present a unique

Scheme 18
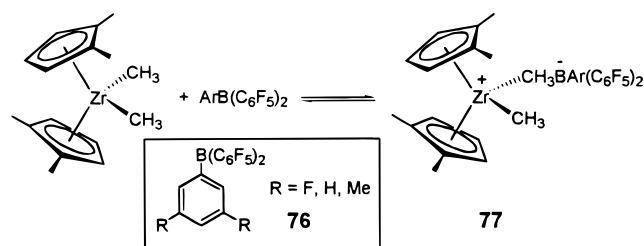
opportunity to measure the thermodynamic aspects of the above equilibrium as a quantitative assessment of the effectiveness of differently substituted organo-Lewis acids in creating "cationlike" metallocene species. Ethylene polymerization activities of the metallocene catalysts derived from these less Lewis acidic boranes are noticeably lower than those activated with FAB and correlate roughly with the Lewis acid strength within the borane series. The activity also approximately correlates with the mole percent of the ion pair structure present in the equilibrium, reflecting the importance of the Lewis acidity for efficient activation. However, in addition to having high native Lewis acidity, good activators must also lack labile nucleophilic substituents that might serve as catalyst poisons. For example, simple trihaloboranes (BF_3, BCl_3) irreversibly transfer F^- or Cl^- to the metal center affording inactive metallocene halides,[260] while alkylaluminum halides lead to $M(\mu\text{-}Cl)Al$ structures, which have proven challenging to characterize and exhibit only modest catalytic activity.[261–263]
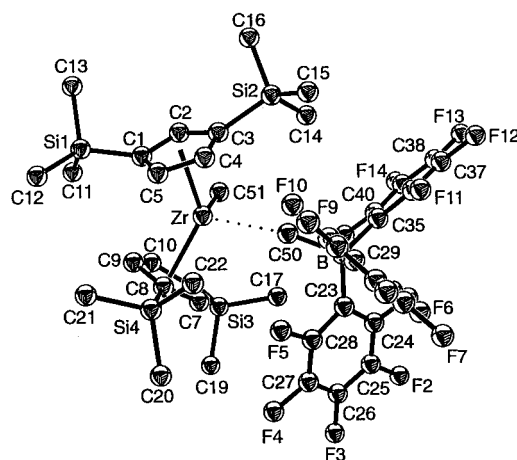
Figure 16. ORTEP drawing of the structure of the complex $(1,3\text{-}TMS_2Cp)_2ZrCH_3^+CH_3B(C_6F_5)_3^-$ (**78**). From ref 67a.
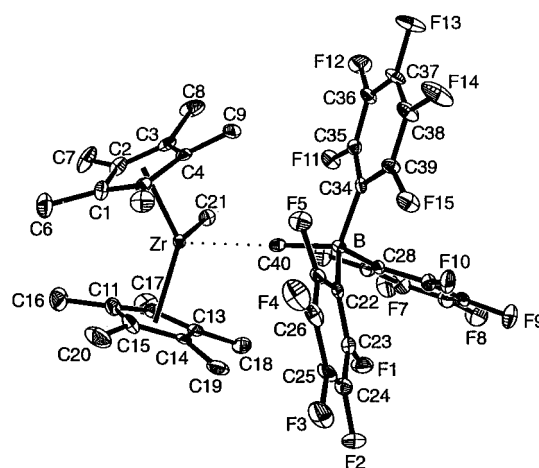
Figure 17. ORTEP drawing of the structure of the complex $Cp'_2ZrCH_3^+CH_3B(C_6F_5)_3^-$ (**79**). From ref 67a.

B. Solid-State Structural Features of the Cation–Anion Ion Pairs

1. MeB(C₆F₅)₃⁻ Anion Coordination via Agostic Interactions

The general solid-state structural features of the cationic complexes derived from the reaction of FAB with metallocene and CGC dimethyls consist of ion pairs in which the cation is weakly associated with the $MeB(C_6F_5)_3^-$ anion through a highly unsymmetrical Zr- - -CH_3−B bridge. The solid-state structures of $(1,2\text{-}Me_2Cp)_2ZrCH_3^+CH_3B(C_6F_5)_3^-$ (**34**),[67] (1,3-$TMS_2Cp)_2ZrCH_3^+CH_3B(C_6F_5)_3^-$ (**78**),[67,169] and $Cp'_2\text{-}ZrCH_3^+CH_3B(C_6F_5)_3^-$ (**79**)[67] are depicted in Figures 11, 16, and 17, respectively. The charge-separated character of these complexes is unambiguously established by the much longer Zr- - -CH_3(bridging) distance than the Zr−CH_3(terminal) distance in each complex and the relatively normal B−CH_3 distances. These Zr−C bridging and terminal distance differences are 0.297, 0.377, and 0.407 Å, respectively, for complexes **34**, **78**, and **79**, reflecting the influence of ancillary ligand steric bulk on the cation−anion separation. The steady decrease in Zr−CH_3(terminal) distance on going from **34** to **78** to **79** (2.252(4), 2.248-(5), and 2.223(6) Å, respectively) can be interpreted

as reflecting greater electron-deficiency/coordinative unsaturation, hence stronger $Zr-CH_3$ bonding as the anion coordination weakened.

Another interesting feature of these metallocenium complexes is that two of the bridging methyl hydrogens in **34** and **78** exhibit relatively close contacts to Zr, with Zr−H distances of 2.25(3) and 2.30(3) Å and acute Zr−C−H angles of 61(2) and 64(2)° in **34**, versus 2.47(3) and 2.44(3) Å in **78**, indicative of α-agostic interactions[264,265] (with a relatively weaker interaction in **78**), compared to nonbonding distances of 2.71(3) in **34** and 2.73(3) Å in **78** for the third

34
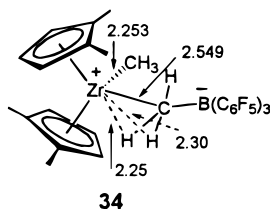
methyl hydrogen atom. Therefore, these structures are more accurately described in the sketch for **34**. Solution NMR spectroscopic data confirm the similarity of the solution and solid state structures and are consistent with the conclusion that the weak cation−anion coordinative interaction is principally through the hydrogen atoms of the bridging group. The aforementioned zwitterionic complex $Cp'_2Zr^+C_6H_4$-BPh_3^- stabilized via an *ortho* $C_{phenyl}-H$ agostic interaction has also been reported in the literature.[133]

2. Weak Anion Contacts via Fluorine Atoms

The crystal structure of $Cp'_2ZrH^+HB(C_6F_5)_3^-$ (**35**) (Figure 18)[67a,168] is similar to those of the cationic complexes discussed above in that it also consists of discrete ion pairs. However, there is major difference that instead of a Zr- - -H−B bridge to connect the cation and anion, as might be expected by analogy to the aforementioned unsymmetrical Zr- - -H_3C−B bridges, the anion is weakly coordinated to the cation through two Zr- - -F bridges. The relatively long Zr- - -F distances (Zr−F1 = 2.416(3) Å, Zr−F2 = 2.534(3) Å) indicate that these interactions are very weak, as does the rapid interconversion of C_6F_5 groups observed in the room-temperature ^{19}F NMR. These
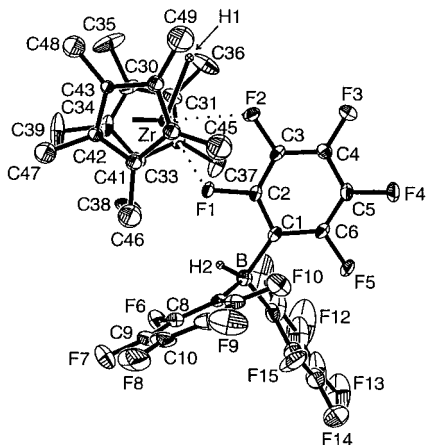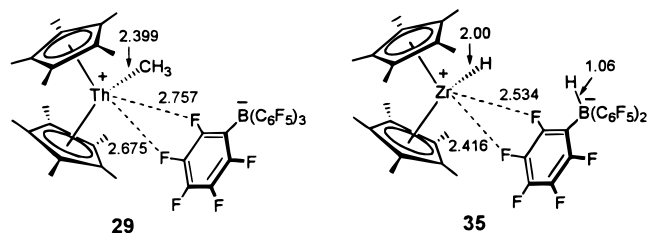

Figure 18. ORTEP drawing of the structure of the complex $Cp'_2ZrH^+HB(C_6F_5)_3^-$ (**35**). From ref 67a.

weak fluorine contacts with the electrophilic metal center are comparable in magnitude to analogous distances in **29** (Figure 10) after correcting for differences in Th/ Zr ionic radii.

3. Coordination by Neutral Alkyl Metal Complexes

The crystal structure of **43** (Figure 19)[77] features a discrete dinuclear cation $[(1,2-Me_2Cp)_2ZrMe(\mu-Me)$-$MeZr(1,2-Me_2Cp)_2]^+$ and a separated $MePBB^-$ anion.
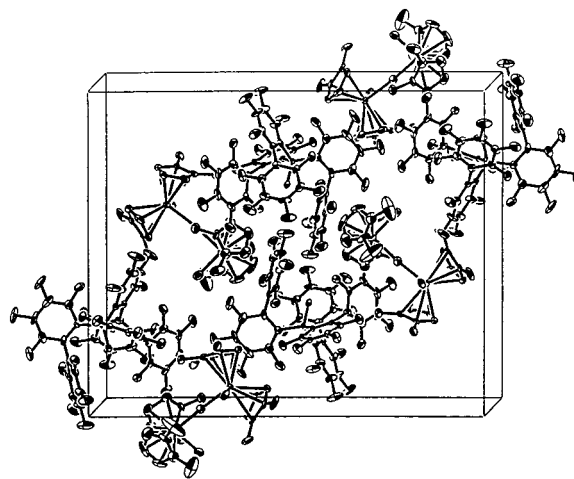

Figure 19. Packing diagram of a unit cell of complex **43**. From ref 77.

The two $1,2-Me_2CpZr$ fragments are crystallographically nearly identical and they are linked by a nearly linear Zr1−Me−Zr2 vector of 170.9(4)°. The two Zr−CH_3 (terminal) groups are arranged in a staggered geometry, and the metal−methyl distances are significantly shorter than the Zr−CH_3(bridging) distances. The shortened Zr−CH_3(terminal) distance as compared to that in **34** argues for a more electron-deficient/coordinatively unsaturated metal center in **43**. This observation supports and elaborates upon

43
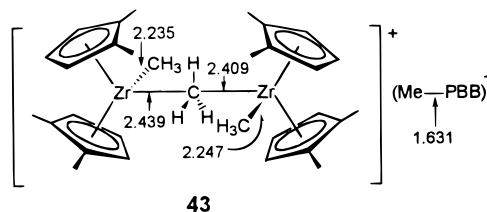
solution chemical results showing that neutral metallocene dimethyls are *less* coordinating/electron-donating than the $CH_3B(C_6F_5)_3^-$ counteranion and is also consistent with olefin polymerization activity differences.[77] The bridging methyl is essentially sp² in character, in agreement with the large $^1J_{C-H} =$ 134.3 Hz value observed in solution NMR measurements.
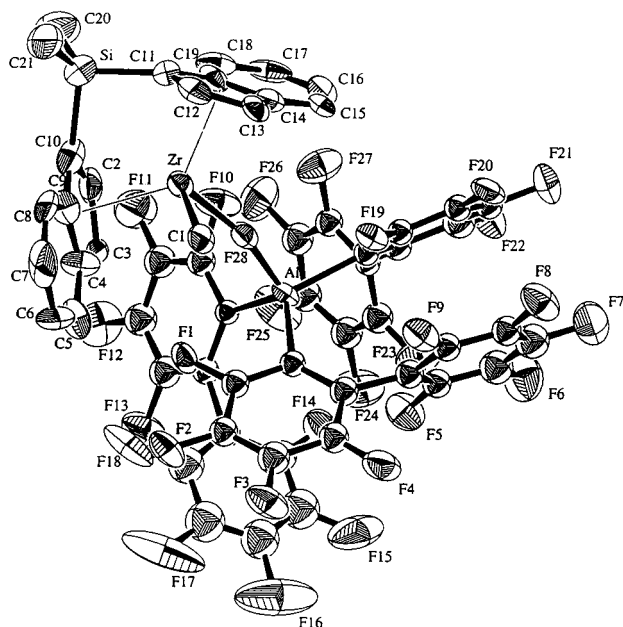
Figure 20. ORTEP drawing of the structure of the complex rac-Me$_2$Si(Ind)$_2$ZrCH$_3^+$PBA$^-$ (**28**). From ref 77.
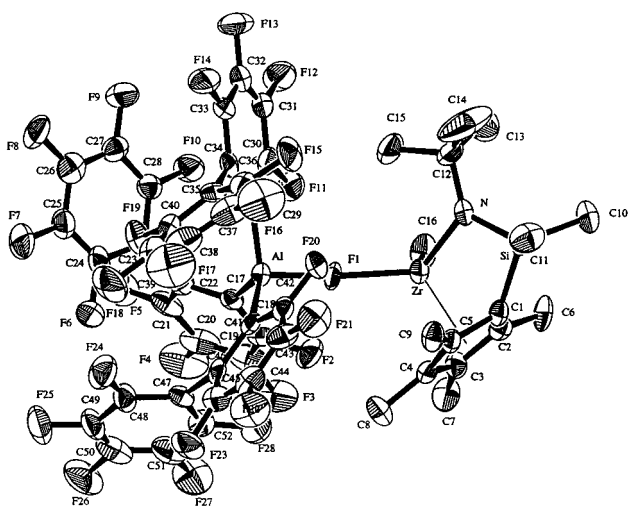

Figure 21. ORTEP drawing of the structure of the complex CGCZrCH$_3^+$PBA$^-$ (**80**). From ref 77.

4. Strong Anion Coordination via Fluoride or Hydride Bridges

The solid-state structures of PBA$^-$ cation−anion pairs **28** and CGCZrCH$_3^+$PBA$^-$ (**80**)[77] are shown in Figures 20 and 21, respectively. They both reveal PBA$^-$ anion coordination to the metal cation via nearly linear Zr- - -F−Al bridges, with respective Zr−F and Al−F distances of 2.123(6) and 1.780(6) Å for **80** and 2.10(1) and 1.81(1) Å for **28**. The Zr−CH$_3$-(terminal) distances are comparable to those in other metallocene L$_2$ZrCH$_3^+$ species which have been characterized structurally, reflecting the cationic character of both complexes.

A few Zr−F−Zr cation structures paired with various anions, including [(1,2-Me$_2$Cp)$_2$ZrMe(μ-F)MeZr-(1,2-Me$_2$Cp)$_2$]$^+$CH$_3$B(C$_6$F$_5$)$_3^-$ (**81**, Figure 22),[67] [(1,2-Me$_2$Cp)$_2$ZrF(μ-F)FZr(1,2-Me$_2$Cp)$_2$]$^+$B(C$_6$F$_4$TBS)$_4^-$ (**82**),[90]
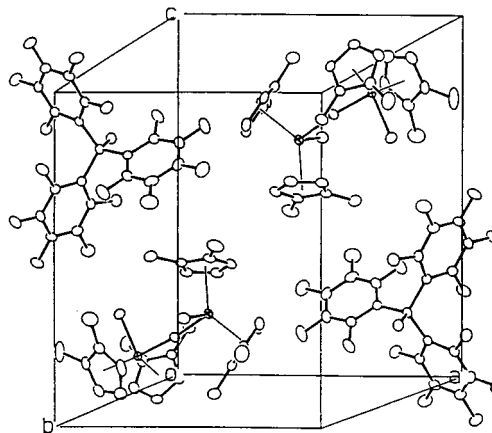
Figure 22. Packing diagram of a unit cell of the complex [(1,2-Me$_2$Cp)$_2$ZrMe(μ-F)MeZr(1,2-Me$_2$Cp)$_2$]$^+$CH$_3$B(C$_6$F$_5$)$_3^-$ (**81**). From ref 77.

and [Me$_2$C(Flu)(Cp)Zr(C$_6$F$_5$)(μ-F)(C$_6$F$_5$)Zr(Cp)(Flu)-CMe$_2$]$^+$CH$_3$B(C$_6$F$_5$)$_3^-$ (**83**),[77] have been crystallographically characterized. They all consist of well-separated cations and unassociated anions. The Zr−F−Zr bridges range from nearly linear configurations for **81** and **83** (173.3(1) and 174.4(4)°) to a slightly bent linear geometry for **82** (159.0(6)°).

Very tight ion pairs coordinated via hydride bridges (M−H−B) are common in cations paired with carboranyl and related anions.[133,148−150] This coordination, especially in the case of multihydrido linkages between the cation and anion, suppresses the catalytic activity drastically.[149,150] For instance, the tight ion-pairing in Cp′$_2$ThMe$^+$X$^-$ complexes [metal bis(dicarbollides), where X$^-$ = M(B$_9$C$_2$H$_{11}$)$_2$ and M = Co, Fe] having three close Th- - -H−B bridging interactions (2.42(3), 2.50(3), 2.67(4) Å) greatly diminishes the chemical reactivity.[149]

5. η^n-π Arene Coordination

Pellecchia et al.[191−192,202] have reported several structurally characterized Zr(IV) cations coordinated by the π system of the anion. As discussed in section III.C, reaction of CpZr(CH$_2$Ph)$_3$ with 1 equiv of FAB in toluene at room temperature results in the precipitation of CpZr(CH$_2$Ph)$_2^+$PhCH$_2$B(C$_6$F$_5$)$_3^-$ (**47**) as
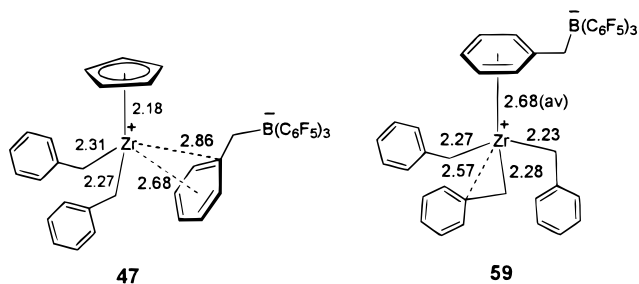
a red crystalline solid. The crystal structure[191] of **47** consists of a CpZr(CH$_2$Ph)$_2^+$ cation π-coordinated to a PhCH$_2$B(C$_6$F$_5$)$_3^-$ anion through Zr−arene bonding of the *Ph*CH$_2$B moiety. The two benzyl groups of the cation behave as normal, undistorted η^1 ligands without significant Zr- - -C$_{ipso}$ interations, while the phenyl ring of the anion is coordinated to Zr unsymmetrically and best described as η^5-arene coordina-

tion (2.86(2) Å for Zr–C6 and 2.68 (average) Å for the remaining Zr–C distances). On the other hand, an η^6-arene anion coordination is found in a similar cationic complex, $Zr(CH_2Ph)_3{}^+PhCH_2B(C_6F_5)_3{}^-$ (**59**; Zr–C = 2.68 (average) Å), although the third benzyl group is bound to Zr in an η^2 fashion with both close methylene and the *ipso*-phenyl carbon contacts.[202]

Very interestingly, with the sterically more bulky and more electron-donating pentamethyl Cp ligand, the crystal structure of $(Me_5Cp)Zr(CH_2Ph)_2{}^+PhCH_2B(C_6F_5)_3{}^-$ (**48**) reveals discrete ion pairs and negligible cation–anion association.[192] Presumably as a consequence of the more "naked" cation, stabilization occurs by a remarkable η^7-benzyl coordination. The structure of a single propylene insertion product of **48** has also been determined, revealing an unusual "back-biting" η^6-arene coordination to the d^0 metal center.[266]

48
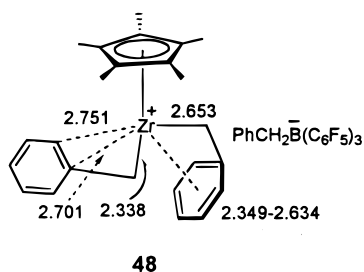
Arene coordination to displace a weakly coordinating anion from the metal coordination sphere has also been observed in the half-sandwich cationic complexes $Cp^xMMe_2(arene)^+CH_3B(C_6F_5)_3{}^-$ (**45**: M = Zr,

45
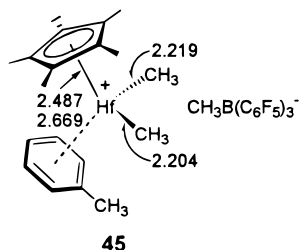
Hf; Cp^x = Me_5Cp, 1,3-TMS$_2$Cp), prepared from the reaction of Cp^xMMe_3 with FAB.[187,188] The crystal structure of $(Me_5Cp)HfMe_2(toluene)^+CH_3B(C_6F_5)_3{}^-$ (**45**)[187] reveals separated, discrete ion pairs in which the bent-sandwich cation is coordinated to an η^6-toluene ligand.

6. Multicenter M–Si–C Interactions

The solid-state structure of $M\{N(SiMe_3)_2\}_3{}^+MeB(C_6F_5)_3{}^-$ (M = Zr, Hf),[206] the synthesis of which was discussed in Section III.C, reveals charge-separated cations and anions, with the coordination sphere about the metal center exhibiting local C_3 pseudo-symmetry. The cation is pyramidally coordinated by three amide ligands (NSi–CH$_3$ moieties), and the Zr lies 0.688(2) Å above the plane of three Ns, while Hf is 0.707(2) Å above the analogous plane. Each amide ligand has one of six SiCH$_3$ units located in close proximity to the metal atom, and distances for the Zr complex are depicted in the sketch (**63**). The three

Si–C bonds close to the metal center are significantly longer than the noncoordinating Si–C bonds.

63
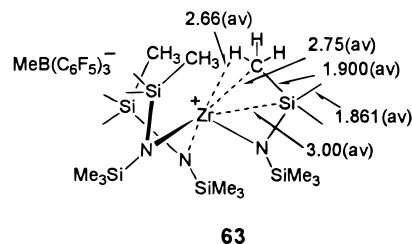
7. Alkenyl/Dienyl Coordination

A rather weak Zr–olefin bond has been identified in the model cationic alkoxy complex $Cp_2Zr(OCMe_2$-$CH_2CH_2CH{=}CH_2)^+MeB(C_6F_5)_3{}^-$ (**84**), studied by Jor-

84   **85**
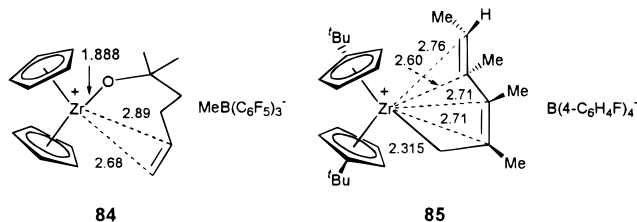
dan et al.[267] The weak interaction between the d^0 Zr-(IV) cation and double bond in the solid state is primarily through the terminal carbon atom (Zr–C = 2.68(2) Å). The presence of significant O → Zr π-donation could possibly strengthen the Zr-olefin binding by increased d → π^* back-bonding. In a closely related structure, $({}^tBuCp)_2Zr(\eta^5\text{-}CH_2C(Me){=}C(Me)C(Me){=}CHMe)^+B(4\text{-}C_6H_4F)_4{}^-$ (**85**), reported by Horton et al.,[268] pentadienyl coordination to Zr is via σ,π^2,π^2-interactions. Therefore, with a proper design, d^0 olefin complexes may be stable enough to allow isolation and characterization in the pure state.

C. Kinetics of Ion-Pair Dissociation/Reorganization

The static arrangements arrested in the solid-state structures of these cationic complexes depict only one facet of the structural features. In solution, two distinguishable dynamic processes for cationic species derived from borane abstraction have been established.[67,269,270] The first is cation–anion dissociation and reassociation (ion-pair separation/reorganization, k_{ips}). The second process involves M–CH$_3$/B–CH$_3$ exchange (B–CH$_3$ dissociation and subsequent recombination, k_{dr}) (Scheme 19). The symmetry probes inherent in the $(1,2\text{-}Me_2Cp)_2ZrMe^+$ cation structure[67] offer unique NMR spectroscopic approaches to quantifying these rates. Cation–anion separation–reorganization processes (k_{ips}) which invert the symmetry of the dissymmetric ion-pair structure permute diastereotopic Cp–Me and ring C–H groups. Processes which involve B–CH$_3$ dissociation and subsequent recombination (k_{dr}) also permute Cp–Me and ring C–H groups but additionally permute both B–CH$_3$ and M–CH$_3$ sites at identical rates. Similar analyses can be applied to systems that contain diagnostic diastereotopic groups on the Cp ring or bridge, such as CGC complexes.[73] In regard to the mechanism of
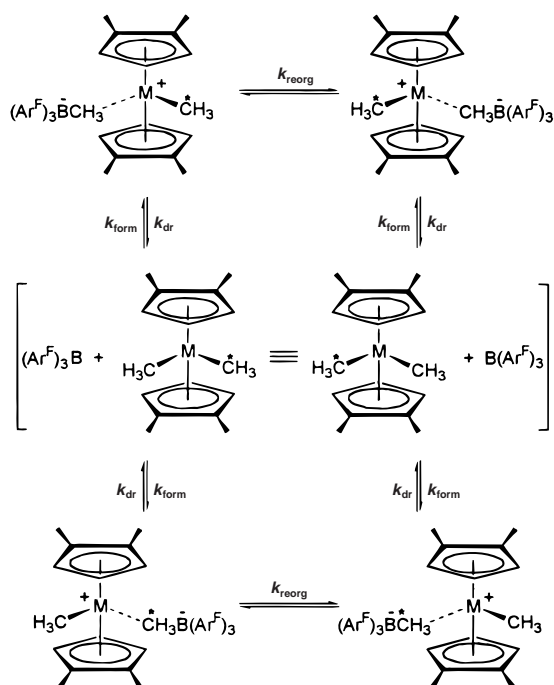
Scheme 19

Table 1. Kinetic Data for Metallocenium Ion-Pair Formation/Dissociation and Symmetrization Processes in Toluene-d_8[a]

entry	M	Ar	$\Delta H^\ddagger_{reorg}$ (kcal/mol)	$\Delta H^\ddagger_{reorg}$ (eu)	$\Delta H^\ddagger_{dr}$ (kcal/mol)	$\Delta S^\ddagger_{dr}$ (eu)
			$(1,2\text{-}Me_2Cp)_2MCH_3^+CH_3BAr(C_6F_5)_2^-$			
1	Zr	C_6F_5	24(1)	17(2)	27(2)	22(3)
2	Zr	$3,5\text{-}C_6H_3F_2$	b	b	23(2)	20(5)
3	Zr	C_6H_5	b	b	19(2)	14(2)
4	Zr	$3,5\text{-}C_6F_5Me_2$	b	b	17(2)	9(4)
5	Hf	C_6F_5	b	b	22(1)	6(1)
6	Hf	$3,5\text{-}C_6H_3F_2$	b	b	16(1)	4(4)
7	Hf	C_6H_5	b	b	15(1)	10(3)
8	Hf	$3,5\text{-}C_6F_5Me_2$	b	b	15(1)	10(3)
			$(CGC)MCH_3^+CH_3B(C_6F_5)_3^-$			
9	Ti	C_6F_5	16.2(3)	7(1)	c	c
10	Zr	C_6F_5	19.3(7)	2(1)	c	c
			$(CGC)MCH_3^+CH_3PBB^-$			
11	Zr	PBB	16.7(3)[d]		c	c

[a] Abbreviations reorg and dr defined in Figure 14 and Scheme 19. [b] Rate too slow to determine; $k_{reorg} \ll k_{dr}$. [c] Thermal decomposition prevents accurate determination. [d] $\Delta G^\ddagger$ at 40 °C.

the process associated with k_{dr}, several lines of evidence have been established to argue that it is dissociative in character.[269]

The rates of the various solution dynamic processes for a series of borane abstraction-derived cationic complexes have been determined by standard dynamic NMR techniques using modified Bloch equation line-shape analyses.[271] Results are summarized in Tables 1 and 2. Table 1 compiles kinetic data[73,259,269] for ion-pair symmetrization (k_{reorg}) and borane dissociation (k_{dr}) in toluene-d_8. It can be seen from the table that for the $(1,2\text{-}Me_2Cp)_2ZrMe^+CH_3BAr(C_6F_5)_2^-$ ion pairs, except for M = Zr and Ar = C_6F_5, the rate of ion-pair symmetrization in toluene is undetectably small in comparison to borane dissociation–recombination ($k_{dr} \gg k_{reorg}$). In the case of $B(C_6F_5)_3$, the methide ion is bound most strongly to the B so that ion-pair symmetrization is more rapid than borane dissociation and recombination at all temperatures. This situation also obtains for the $CGCMCH_3^+$-CH_3X^- complexes where X is a perfluoroarylborane which has large binding energy and high methide affinity.

Solvent polarity is known to have an impact on cationic metallocene-mediated olefin polymerization activity and stereoregulation.[272–276] As the polarity of the solvent increases, Fink et al.[275] found that the rate of syndiospecific propylene polymerization catalyzed by isopropylidene(fluorenyl)cyclopentadienyl-zirconium dichloride–MAO increases but the syndiotactic index decreases. Oliva et al.[276] observed earlier that the propylene polymerization rate catalyzed by the three-component catalytic system Cp_2-$Ti(C_6H_5)_2/Me_2AlF/Me_3Al$ increases noticeably when using CH_2Cl_2 instead of toluene as solvent. Eisch[25] suggested that solvent-separated ion pairs are more active sites but are less syndioselective than contact ion pairs. In light of these important effects of solvent polarity on olefin polymerization, the dynamics of ion-pair reorganization have been examined as a function of solvent polarity/coordinating ability using NMR line-shape analysis techniques. Data are summarized in Table 2.[259,269] For M = Zr, the ion-pair symmetrization rate (k_{reorg}) is dramatically enhanced on going from toluene to more polar solvents; however, the borane dissociation/recombination rate (k_{dr}) experiences only a modest increase, reflecting more facile separation of charged species in higher dielec-

Table 2. Kinetic Data for Ion-Pair Reorganization Processes in $(1,2\text{-}Me_2Cp)_2MCH_3^+CH_3B(C_6F_5)_3^-$ Complexes as a Function of Solvent and Solvent Dielectric Constant

entry	M	solvent (ϵ)[a]	k_{reorg}[b] (10^{-3}/s)	k_{dr}[b] (10^{-3}/s)	$\Delta H^\ddagger_{reorg}$[c] (kcal/mol)	$\Delta S^\ddagger_{reorg}$[c] (eu)	$\Delta H^\ddagger_{dr}$[c] (kcal/mol)	$\Delta S^\ddagger_{dr}$[c] (eu)
1	Zr	toluene-d_8 (2.37)	30(10)	3(2)	24(1)	17(2)	27(2)	22(3)
2	Zr	C_6D_5Cl (5.71)	60 000(20 000)	20(8)	11(2)	−15(8)	19(1)	0(2)
3	Zr	$1,2\text{-}C_6D_4Cl_2$ (9.93)	70 000(20 000)	<1	12(2)	−10(4)		
4	Hf	toluene-d_8 (2.37)	d	1300(400)			22(1)	16(1)
5	Hf	C_6F_6 (2.03)	d	5600(200)			16(1)	−2(4)
6	Hf	CCl_2FCF_2Cl (2.41)	d	8000(4000)			15(2)	−2(4)
7	Hf	C_6D_5Cl (5.71)	15 000(9000)	600(300)	13(4)	−9(1)	20(1)	9(3)
8	Hf	$1,2\text{-}C_6D_4Cl_2$ (9.93)	9000(4000)	5(2)	12(3)	−5(8)	23(1)	7(1)
9	Hf	CD_2Cl_2 (9.08)	20 000(10 000)	<1	11(1)	−16(2)		

[a] Dielectric constant from: *CRC Handbook of Chemistry and Physics*, 77th ed.; CRC Press: New York, 1996; p G-161. [b] Rate constant at 298 K derived from least-squares fitting of Eyring plot. [c] Eyring parameters derived from line shape analysis. [d] Rate too slow to determine; $k_{reorg} \ll k_{dr}$.

Table 3. Thermodynamics of Methide Abstraction from Group 4 Metallocenes and Related Complexes by Fluoroarylborane Lewis Acids and MAO[a]

entry	complex	Lewis acid	$-\Delta H_{form}$[b] (kcal/mol)	ΔS_{form} (eu)
1	CGCTiMe$_2$	B(C$_6$F$_5$)$_3$	22.6(2)	
2	CGCZrMe$_2$	B(C$_6$F$_5$)$_3$	23.9(4)	
3	CGCHfMe$_2$	B(C$_6$F$_5$)$_3$	20.8(5)	
4	CGCZrMe$_2$	PNB	>44.2[c]	
5	CGCZrMe$_2$	PBB	44.2(6)	
6	Cp$_2$ZrMe$_2$	B(C$_6$F$_5$)$_3$	23.1(3)	
7	(1,2-Me$_2$Cp)$_2$ZrMe$_2$	B(C$_6$F$_5$)$_3$	24.3(4)	
8	(Me$_5$Cp)$_2$ZrMe$_2$	B(C$_6$F$_5$)$_3$	36.7(5)	
9	(1,2-Me$_2$Cp)$_2$HfMe$_2$	B(C$_6$F$_5$)$_3$	20.8(5)	
10	(1,2-Me$_2$Cp)$_2$ZrMe$_2$	B(C$_6$F$_5$)$_2$(3,5-C$_6$H$_3$F$_2$)	18.7(7)	−42(2)
11	(1,2-Me$_2$Cp)$_2$ZrMe$_2$	B(C$_6$F$_5$)$_2$(C$_6$H$_5$)	14.8(8)	−31(2)
12	(1,2-Me$_2$Cp)$_2$ZrMe$_2$	B(C$_6$F$_5$)$_2$(3,5-C$_6$H$_3$Me$_2$)	10.8(6)	−19(2)
13	(1,2-Me$_2$Cp)$_2$HfMe$_2$	B(C$_6$F$_5$)$_2$(3,5-C$_6$H$_3$F$_2$)	15.2(8)	−35(3)
14	(1,2-Me$_2$Cp)$_2$HfMe$_2$	B(C$_6$F$_5$)$_2$(C$_6$H$_5$)	13.3(6)	−39(2)
15	(1,2-Me$_2$Cp)$_2$HfMe$_2$	B(C$_6$F$_5$)$_2$(3,5-C$_6$H$_3$Me$_2$)	12.7(5)	−36(4)
16	(1,2-Me$_2$Cp)$_2$ZrMe$_2$	MAO	10.9(3)	
17	(1,2-Me$_2$Cp)$_2$HfMe$_2$	MAO	8.9(4)	
18	CGCZrMe$_2$	MAO	8.8(2)	
19	CGCZrCl$_2$	MAO	4.2(2)	

[a] All data from refs 67, 73, 256, 258, and 259. [b] As defined in Figure 14. [c] From NMR equilibration vs PBB.

tric media. Interestingly, for M = Hf, borane dissociation/recombination is the predominant process in toluene, where k_{reorg} is not detectable. This may, to some degree, reflect the relatively greater Hf−C bond dissociation enthalpy (D(Hf−CH$_3$) is ca. 10 kcal/mol greater than D(Zr−CH$_3$)). Upon dissolution in polar solvents such as C$_6$D$_5$Cl, 1,2-C$_6$D$_4$Cl$_2$, and CD$_2$-Cl$_2$, however, k_{reorg} for Hf becomes nearly as large as in the case of M = Zr. Another interesting observation is that there is a depression in the rates of borane dissociation/recombination (entries 7−9), which could then be ascribed to stabilization of the charge-separated ground-state vs the neutral dissociation products (cf. Figure 14). The $\Delta S^{\ddagger}$ parameters in Table 2 suggest that the transition states for both borane dissociation and ion-pair reorganization are more highly organized in the higher dielectric solvents, possibly reflecting solvation sphere reorganization.

D. Thermodynamics of Catalyst Activation

The results of thermodynamic measurements[67,73,256,258,259] of catalyst activation processes, investigated by solution calorimetry and NMR equilibration for a variety of metal complexes having differing ancillary ligation and metal identity, and using a variety of organo-Lewis acids are summarized in Table 3. The broad range of exothermicities observed illustrates the marked sensitivity of the measured methide abstraction enthalpies (ΔH_{form}) to the M−CH$_3$ homolytic bond dissociation enthalpies, the L$_2$MCH$_3$ ionization potentials, the borane methide affinity, and the ion-pair binding energetics as illustrated in Figure 23. This approximate thermodynamic cycle depicts the interplay of these parameters in determining the enthapy for metallocenium ion-pair formation from neutral precursors.[256,259]

From the data presented in Table 3, several noteworthy trends may readily be inferred from the enthalpies of reaction and can be related to variation in ancillaryl ligation (L$_2$), metal (M), and organo-Lewis acid (A). First, for a fixed ligand framework, the methide abstraction enthalpy is a function of the
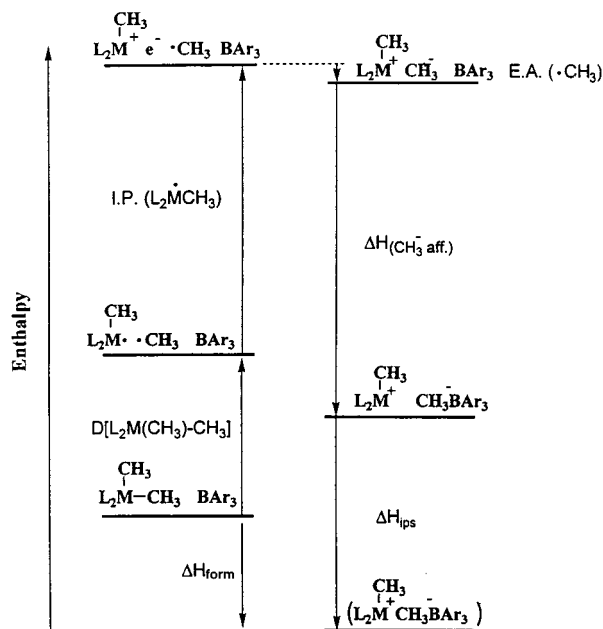

Figure 23. Approximate thermodynamic cycle for metallocenium ion pair formation from neutral dimethyl precursors in a nonpolar medium. From refs 256 and 259.

metal. Methide abstraction from Hf is generally less exothermic than from Zr by ca. 2−4 kcal/mol, and the Ti methide abstraction exothermicity is approximately intermediate between that of Zr and Hf. Second, for fixed M, increased Cp$_2$ ring methyl functionalization effects consistent but nonlinear increases in ΔH_{form}. Third, for constant metallocene, it can be seen that reaction exothermicity in the B(C$_6$F$_5$)$_2$Ar series falls with decreasing Ar electron-withdrawing tendency C$_6$F$_5$ > 3,5-C$_6$H$_3$F$_2$ > C$_6$H$_5$ > 3,5-C$_6$H$_3$Me$_2$. Also, the reaction of CGCZrMe$_2$ with PBB and PNB is considerably more exothermic than with B(C$_6$F$_5$)$_3$. This latter trend is not immediately obvious from the ordering of Lewis acidity and suggests that the overall thermodynamics of catalyst activation reflects not only the borane Lewis acidity/methide affinity but also the nature of ion pair structure and cation−anion interactions. The rather

negative entropies of ion-pair formation are consistent with substantially reduced degrees of freedom.

It can also be seen in the table that the interaction of a typical MAO with both conventional metallocenes and "constrained geometry" complexes is significantly less exothermic than for the perfluoroarylboranes, with $\Delta H_{form}(\text{MAO}) \approx \Delta H_{form}[\text{B}(\text{C}_6\text{F}_5)_2(3,5\text{-}\text{C}_6\text{H}_3\text{Me}_2)]$. Assuming ΔS_{dr} for $(1,2\text{-}\text{Me}_2\text{Cp})_2\text{ZrMe}_2$ + MAO is approximately the same as for the aforementioned boranes, then, at 298 K, the equilibrium constant for MAO abstraction (1.0 MAO "formula units") is on the order of 2×10^3. Thus, at submillimolar catalytic concentrations, the equilibrium lies to the left and abstraction/activation reaction proceeds only ~20% to completion. This may be one of the reasons large stoichiometric excesses of MAO are generally necessary in typical polymerization reactions, above and beyond functions such as alkylation and scavenging of impurities. Furthermore, thermometric titraton experiments[258] in which a CGCZrMe₂ solution is titrated into an MAO solution in toluene do not exhibit "breaks" in the titration curve corresponding to discrete stoichiometric "end points". Instead, the evolved heat per equiv of added zirconium complex is essentially constant until Zr/Al ≈ 0.67, at which point a gradual drop in the evolved heat is observed. In view of the current MAO structural models (see section II.B), these results appear to be in best accord with either a predominance of nondissociating MAO clusters in which most methide binding sites are essentially noninteracting and have comparable binding enthalpies or with a rapidly equilibrating mixture of presumably associated structures in which successive methide binding is accompanied by extensive dissociation.

From more detailed considerations,[256,259] the results in Table 3 can be straightforwardly understood. For the types of group 4 metallocenes and quasi-metallocenes studied here, ancillary ligation as expressed in cation stabilizing ability (e.g., the IP in Figure 23) appears to have the greatest influence on ΔH_{form} for constant borane, while $D(\text{M--CH}_3)$ and ΔH_{ips} are in all probability less variable. It is likely that differences between Zr and Hf metallocene enthalpies reside in a combination of ΔIP and $\Delta D(\text{M--CH}_3)$ effects. For constant metallocene, it is likely that the borane methide affinity is the greatest determinant of ΔH_{form}, while ΔH_{ips} is probably more constant, except in cases of highly directed anion coordination (e.g. **28**).[77]

The present thermodynamic and kinetic data allow construction of quantitative experimental enthalpic reaction coordinates describing the energetics of the above processes. Figure 24 shows that, in toluene solution, $(1,2\text{-}\text{Me}_2\text{Cp})_2\text{ZrCH}_3{}^+\text{CH}_3\text{B}(\text{C}_6\text{F}_5)_3{}^-$ undergoes ion-pair symmetrization more rapidly than borane dissociation/recombination while the opposite scenario holds for the Hf analogue. Both reaction coordinates indicate that the enthalpic barrier to ion-pair formation from the neutral reactants is very small; i.e., $\Delta H^{\ddagger}_{dr} - \Delta H_{dr}$ = a few kcal/mol at most. The small, nearly constant magnitude of $\Delta H^{\ddagger}_{dr} - \Delta H_{dr}$ with $\text{B}(\text{C}_6\text{F}_5)_2\text{Ar}$ variation in Table 1 indicates that the barrier for metallocene + borane recombina-
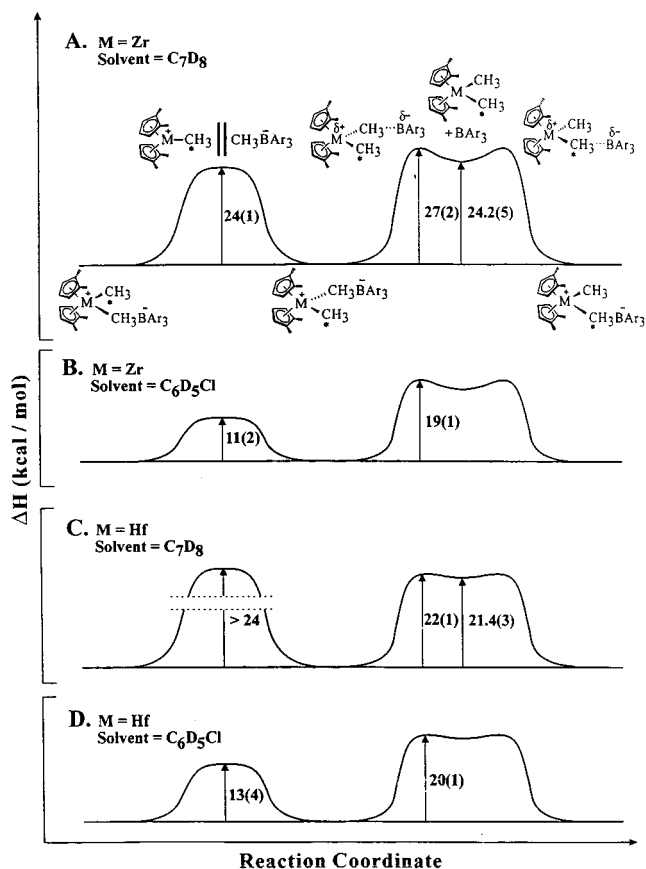

Figure 24. Experimental enthalpic profiles for $(1,2\text{-}\text{Me}_2\text{-}\text{Cp})_2\text{MCH}_3{}^+\text{CH}_3\text{B}(\text{C}_6\text{F}_5)_3{}^-$ ion-pair formation and reorganization for M = Zr or Hf in toluene-d_8 and chlorobenzene-d_5 solution. From ref 259.

tion is uniformly small. This type of Brønsted/Hammett-like correlation[277] indicates classical and well-behaved transmission of substituent effects in the methide abstraction process. Figure 24 also depicts the effects of solvent polarity on the $(1,2\text{-}\text{Me}_2\text{-}\text{Cp})_2\text{MCH}_3{}^+\text{CH}_3\text{B}(\text{C}_6\text{F}_5)_3{}^-$ ion-pair symmetrizaton, formation, and dissociation profiles. For both Zr and Hf cases, polar solvents substantially reduce the kinetic barrier to ion-pair separation, with rate enhancements reminiscent of more classical systems.[278]

E. Activity and Stereoselectivity Aspects

1. Catalyst-Cocatalyst Structure Match

With sterically open and more accessible catalyst precursors, such as "constrained geometry" complexes, both PBB and FAB activate the dialkyls effectively to generate the corresponding cationic complexes. However, while the activated CGCMCH₃⁺MeB-$(\text{C}_6\text{F}_5)_3{}^-$ species is essentially inactive (M = Zr) or marginally active (M = Ti) for ethylene polymerization at 25 °C, the MePBB⁻ analogues are highly active with *rate enhancements of 10^5 and ~70×* for the Zr and Ti catalysts, respectively.[73,77] This trend holds for the ethylene–1-hexene and ethylene–styrene copolymerizations as well, with both PBB-derived catalysts exhibiting comparable comonomer incorporation selectivities and narrower polydispersities at higher polymerization rates. These MeB-

$(C_6F_5)_3^-$ vs MePBB$^-$ activity differences again reflect the relative coordinative tendencies of the anions and tightness of the ion pairing as well as their important role in the olefin polymerization process. As indicated by dynamic NMR studies of ion-pair symmetrization,[73] the free energy of activation differences ($\Delta G^{\ddagger}$ = 16.7(3) kcal/mol for MePBB$^-$ vs 19.3(4) kcal/mol for MeB$(C_6F_5)_3^-$ at 40 °C) suggest looser MePBB$^-$ ion pairing with respect to CGCMMe$^+$. This significantly amplified activity difference for the CGC catalysts with the Me anions suggests that anion dimensions will have the greatest effects on polymerization activity for sterically more accessible (coordinatively more open) catalysts, such as the CGC system. For other sterically more open complexes such as single-ring (mono-Cp) catalysts, the Cp*TiMe$_3$/PBB catalytic system also exhibits considerably higher activity with respect to ethylene−1-hexene copolymerization.

In contrast, for metallocene (nonbridged or *ansa*) dialkyls, PBB preferentially affords cationic dinuclear complexes having the general formula [L$_2$ZrMe(μ-Me)Me ZrL$_2$]$^+$MePBB$^-$ at room temperature, even with a stoichiometric excess of PBB and extended reaction times. Although olefin polymerization activities of these dinuclear catalysts are comparable to those monomeric species generated with FAB, the activation of metallocene dialkyls with PBB is usually sluggish and requires extended reaction times (0.5−1 h) to complete the activation at room temperature in toluene. One extreme example of this aspect of PBB activation chemistry is when the very bulky metallocene [1,3-(TMS)$_2$-Cp]$_2$ZrMe$_2$ is used. Rather than abstracting a methide anion as FAB, PBB catalyzes C−H bond activation to form a ring-metalated C−H activation product (Scheme 20).[279]

Scheme 20
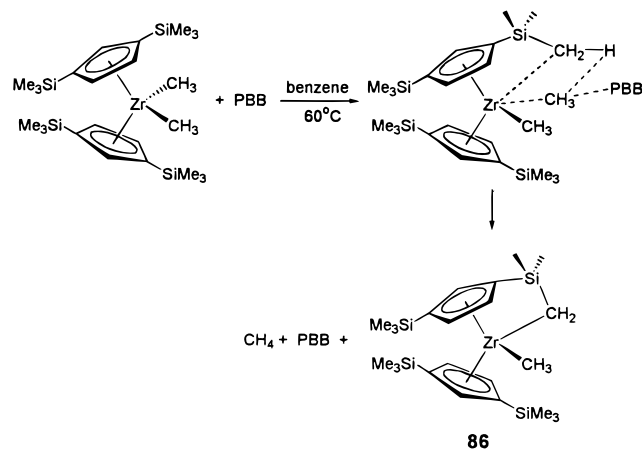
Under identical conditions and in absence of a catalytic amount of PBB, no such product is formed.

A totally different activity trend with respect to catalyst ligation is observed when the sterically encumbered aluminate-based activator Ph$_3$C$^+$PBA$^-$ (**17**) is used to activate metallocene and CGC complexes.[77] In this case, activation is via irreversible heterolysis of the M−R bond by Ph$_3$C$^+$, which is relatively insensitive to the steric bulk of metal−ligand framework. On the other hand, the relative strength of PBA$^-$ coordination via an F-bridge to the
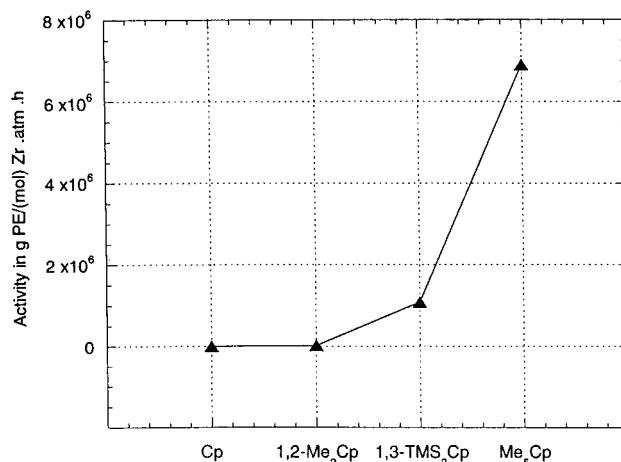

Figure 25. Ethylene polymerization activity dependence on ancillary ligand bulk in the Cp$^x_2$ZrCH$_3^+$PBA$^-$ catalytic system.

resulting metallocenium cation is very sensitive to the nature of ancillary ligand bulk. Therefore, there is a remarkable sensitivity of ethylene polymerization characteristics to ion pairing as inferred from ancillary ligand bulk, diffraction structural data, and NMR δ(^{19}F−Al) values. For example, while Cp$_2$Zr-CH$_3^+$PBA$^-$ exhibits negligible ethylene polymerization activity at 25 °C/1.0 atm monomer pressure, increasing the ancillary ligand bulk effects dramatic increases in polymerization activity as the anion PBA$^-$ coordination is weakened (Figure 25). As the ion-pair separation increases, complexes such as Cp′$_2$ZrCH$_3^+$PBA$^-$ become too thermally unstable to isolate, reminiscent of findings by Siedle et al.[280] in gas-phase reactivity studies of L$_2$ZrCH$_3^+$ cations with alkenes. Furthermore, CGCMCH$_3^+$ polymerization characteristics are markedly temperature-dependent. With negligible activities for Zr and Ti catalysts at 25 °C/1.0 atm, good yields of ultrahigh molecular weight polyethylene ($M_w = 2.05 \times 10^6$) are produced with CGCTiCH$_3^+$PBA$^-$ at 110 °C.

2. Correlations of Ion-Pair Energetics, Dynamics, and Polymerization Activity

Detailed studies[77,87,90,281] of counteranion modulation of polymerization activity have yielded a general activity trend for bis-Cp metallocene and CGC catalysts. It is found that the weaker the coordinating characteristics of the anion, the higher the reactivity for a fixed cation, e.g., B$(C_6F_5)_4^- >$ CH$_3$B$(C_6F_5)_3^- >$ X-MAO$^- \gg$ BF$_4^-$, B$(C_6H_5)_4^-$. Of the latter two anions, facile F$^-$ abstraction by electrophilic metals may be operative for the former and Ph-transfer to the metal or C−H activation/strong anion coordination may be operative for the latter. Either process is expected to diminish catalytic activity. Therefore, some of the ideal properties of weakly coordinating anions[260] which are applicable to metallocenium catalysis should include a high degree of charge delocalization, large size, and absence of basic sites (i.e., resistance to electrophilic attact).

For catalysts based on mono-Cp ligation, the same activity trend has been observed. For example, syndiospecific polymerization of styrene by Cp′TiR$_3$ activated with Ph$_3$C$^+$B$(C_6F_5)_4^-$ exhibits increased polym-

Table 4. Effects of Borate Anion on Syndiospecific Styrene Polymerzation Activity[155]

conditions	borate anions	activity (kg/g of Ti)
Cp'TiMe$_3$: 5 × 10^{-7} mol	[B(C$_6$H$_5$)$_4$]$^-$	0
cocatalyst: 5 × 10^{-7} mol	[B(C$_6$H$_4$F)$_4$]$^-$	0
TIBA: 3 × 10^{-6} mol	[B(2,4-F$_2$C$_6$H$_3$)$_4$]$^-$	5
temp: 70 °C	[B(3,4,5-F$_3$C$_6$H$_2$)$_4$]$^-$	10
time: 4 h	[B(3-CF$_3$C$_6$F$_4$)$_4$]$^-$	20
	[B(C$_6$F$_5$)$_4$]$^-$	250

erization activity by a factor of 2 over B(C$_6$F$_5$)$_3$ and by a factor of 10 over MAO.[282] This activity trend and the importance of anion properties were recently demonstrated by Ishihara et al.[155] in the syndiospecific polymerization of styrene catalyzed by Cp'TiMe$_3$/TIBA/HNMe$_2$Ph$^+$borate$^-$. The effect of borate anion on polymerization activity is summarized in Table 4. Similar studies carried out earlier by Zambelli et al. demonstrated anion modulation of activity and molecular weight of the resulting syndiotactic polystyrene produced by Cp'TiR$_3$, activated with Ph$_3$C$^+$B-(C$_6$F$_5$)$_4$$^-$, B(C$_6F_5$)$_3$, and MAO, respectively.[283] Another recent example reported by Pellecchia et al.[284] revealed a significant influence of cocatalyst variation on the polymerization performance of the nickel α-diimine catalyst, (ArN=CH−CH=NAr)NiMe$_2$ (Ar = 2,6-^{i}Pr$_2$C$_6$H$_3$), especially as concerns the degree of polymer branching.

On the other hand, for a given counterion, the polymerization activity of electrophilic Zr catalysts does not necessarily correlate with the intrinsic electrophilicity of [L$_2$ZrCH$_3$]$^+$ as L is varied.[280] The ion-pairing tendency of L$_2$ZrCH$_3$$^+$ cations in solution is a key contributor to the overall propagation rate, and the stability of the ion pair for a given counterion is expected to decrease as L becomes more electron donating and sterically encumbered and, thus, more reactive despite the reduced electrophilicity of the metallocenium ion.[77]

For a constant cation, a roughly linear relationship between the enthalpy of ion pair formation and the ^{13}C NMR downfield shift of the M−CH$_3$$^+$ groups in the (1,2-Me$_2$Cp)$_2$MCH$_3$$^+CH_3$B(C$_6F_5$)$_3$$^-$/CH$_3$BAr(C$_6F_5$)$_2$$^-$ series has been established (Figure 26).[259] These results argue that fluoroarylborane Lewis acidity considerably influences the electrophilicity/electron deficiency of the resulting metallocenium cation. Correlations of metallocenium physical observables with olefin polymerization activities are complicated by several factors. First, catalysts such as some (1,2-Me$_2$Cp)$_2$MCH$_3$$^+CH_3$BAr(C$_6F_5$)$_2$$^-$ complexes are not completely in the cationic form for sub-mM solutions in toluene at 25 °C.[259] Second, the active forms of the catalysts in ethylene polymerization are generally not methyl complexes but either polyalkyl [(L$_2$M(CH$_2$-CH$_2$)$_n$H)$^+$X$^-$] or hydrido [(L$_2$MH)$^+$X$^-$] cations. These metallocenium steric and electronic environments are not expected to be identical to those of the L$_2$MCH$_3$$^+X^-$ precursors, with differing alkyl steric encumberance and agostic interactions expected in the former as well as differing cation−anion interactions likely in the latter. Indeed, a recent study[285] indicates that in (1,2-Me$_2$Cp)$_2$ZrR$^+$CH$_3$B(C$_6$F$_5$)$_3$$^-$ series there are substantial Zr−R alkyl group effects on ion-pair thermodynamic stability as well as on ion-pair solution
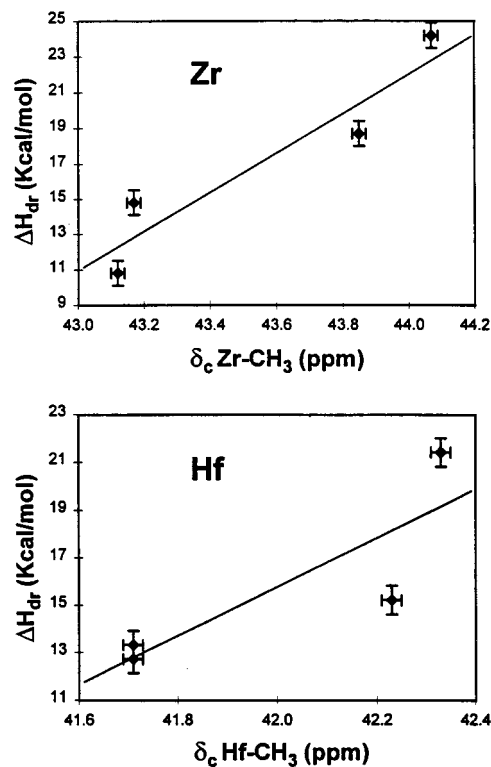

Figure 26. Relationship between the enthalpy of ion-pair formation from the neutral precursors and the M−^{13}CH$_3$ chemical shift for a series of (1,2-Me$_2$Cp)$_2$MCH$_3$$^+CH_3$B-(C$_6F_5$)$_3$$^-$/CH$_3$BAr(C$_6F_5$)$_2$$^-$ complexes. From ref 259.
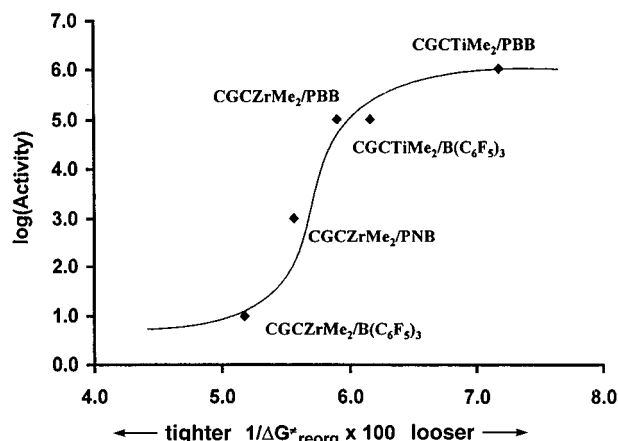

Figure 27. Relationship between $\Delta G^{\ddagger}_{reorg}$ values for a series of CGS catalyst ion pairs and ethylene polymerization activity. Looser and tighter refer to the qualitative strength of the ion pairing.

structure and structural dynamics. Nevertheless, plots of ethylene polymerization activity vs either ΔH_{dr} or δ(M−CH$_3$) for the (1,2-Me$_2$Cp)$_2$MCH$_3$$^+CH_3$B-(C$_6F_5$)$_3$$^-$/CH$_3$BAr(C$_6F_5$)$_2$$^-$ series evidence a rough correlation.[259] It is also interesting to note that, for a series of constrained geometry complexes, there is a roughly inverse correlation between the $\Delta G^{\ddagger}_{reorg}$ activation parameters, derived from dynamic NMR studies assaying the "tightness" of the metallocenium−methylborate ion pairing, and ethylene polymerization activity (Figure 27).

3. Polymerization Stereospecificity

There are several conflicting reports regarding the stereospecificity of propylene polymerization for a

given catalyst with variation of the cocatalyst. *Atactic polypropylene* is produced by the catalyst [(Me$_3$Si)$_2$N]$_2$Zr(CH$_2$Ph)$_2$ when activated with HNMe$_2$Ph$^+$B(C$_6$F$_5$)$_4$$^-$,[204] which is in sharp contrast to patent claims of *isotactic* polypropylene formation using the catalyst [(Me$_3$Si)$_2$N]$_2$ZrCl$_2$ activated with MAO.[286] The general features of mono-Cp–amido complexes [η:$^5\eta^1$-Me$_2$SiCp^x(RN)]MCl$_2$ (M = Ti, Zr) when activated with MAO are described as including catalysts for producing high molecular weight *atactic* to *slightly syndiotactic* polyolefins.[287,288] On the contrary, *isotactic* polypropylene[289] is claimed to be produced by [Me$_2$Si(fluorenyl)^{t}BuN]ZrCl$_2$/MAO whereas *syndiotactic* polypropylene[290] is claimed to be produced by [Me$_2$Si(fluorenyl)^{t}BuN]ZrMe$_2$/HNMe$_2$Ph$^+$B(C$_6$F$_5$)$_4$$^-$. Furthermore, inversion of stereoselectivity for propylene polymerization with the same catalyst, [Me$_2$Si(Flu)^{t}BuN]ZrCl$_2$, is claimed when activated with MAO (*syndiospecific*) versus when activated with Ph$_3$C$^+$B(C$_6$F$_5$)$_4$$^-$/TIBA (*isospecific*).[291a] However, in a later communication, it was revealed that a major portion of the polymeric product is toluene-soluble and syndiotactic while only a small amount is toluene-insoluble and isotactic.[291b] A careful study by Shiono et al.[292] confirmed that the catalyst [Me$_2$Si(Flu)^{t}BuN]TiMe$_2$, when activated with MAO, Ph$_3$C$^+$(BC$_6$F$_5$)$_4$$^-$, or B(C$_6F_5$)$_3$, produces syndiotactic-enriched polypropylene (*rrrr* ~ 0.3) in all cases at 40 °C. Living polymerization of propylene and 1-hexene at −50 °C mediated by [Me$_2$Si(Flu)^{t}BuN]TiMe$_2$ with the activator B(C$_6$F$_5$)$_3$ has also been observed to produce syndiotactic-enriched polymers (*rrrr* ~ 0.24).[293] Because of these differences reported in the literature, it is important to understand the role of the activator as well as the resulting anion on the stereospecificity of polymerization. Unfortunately, little is well-understood.

The influence of anion on propylene polymerization rate, chain transfer, and isospecificity catalyzed by the chiral, non-C_2-symmetric zirconium complexes (*R*)- and (*S*)-Me$_2$Si(Me$_4$C$_5$)(C$_5$H$_3$R*)ZrMe$_2$ (R* denotes chiral menthyl or neomenthyl substituent) combined with the cocatalysts MAO, B(C$_6$F$_5$)$_3$, HNR$_3$$^+$B(C$_6F_5$)$_4$$^-$, and Ph$_3C^+$B(C$_6F_5$)$_4$$^-$ has been investigated.[294] The cocatalysts introducing the B(C$_6$F$_5$)$_4$$^-$ counteranion exhibit the highest activities and stereoregularities, yielding the highest molecular weights for a given precatalyst and polymerization temperature. It appears that the presence of coproduct amine base derived from HNR$_3$$^+$B(C$_6F_5$)$_4$$^-$ activation significantly depresses the molecular weight of the polymer produced under the polymerization conditions reported in the paper. Similar anion modulation of propylene polymerization stereospecificity for Et(Ind)$_2$ZrMe$_2$-based catalytic systems has been reported by Chien et al.[281] These results further demonstrate the influence of the cation–anion ion pairing on polymerization characteristics, including chain transfer and the stereospecificity of enchainment.

Ewen[295] reported that isospecific Et(Ind)$_2$Zr(R)$^+$ and syndiospecific Me$_2$C(Flu)CpZr(R)$^+$ cations paired with Al(C$_6$F$_5$)$_4$$^-$ are significantly more stereospecific in propylene polymerization than the corresponding systems with B(C$_6$F$_5$)$_4$$^-$ and Me-MAO$^-$ counteranions under certain polymerization conditions. However,

the Al(C$_6$F$_5$)$_4$$^-$-containing catalysts are less active than the B(C$_6$F$_5$)$_4$$^-$-containing catalysts under the same reaction conditions.

An appealing thought is whether chirality inherent in the anionic portion of the catalyst might influence propylene insertion stereochemistry in the coordination sphere of an anchiral metallocene.[77,97] The chiral PBA$^-$ anion, when coordinated to a metallocenium cation, is a good candidate for this study. This sterically demanding C_3-symmetric, propeller-like anion strongly interacts with the cation stereochemistry, converting C_{2v}-symmetric bis-Cp, C_s-symmetric CGC, C_2-symmetric *ansa*-bis(Ind), and C_s-symmetric bridged Cp-Flu metallocene dimethyls into cationic complexes existing as a pair of enantiomers (**87**) or unequally populated diastereomers (**88**–**90**, enantiomers not shown; Scheme 21).
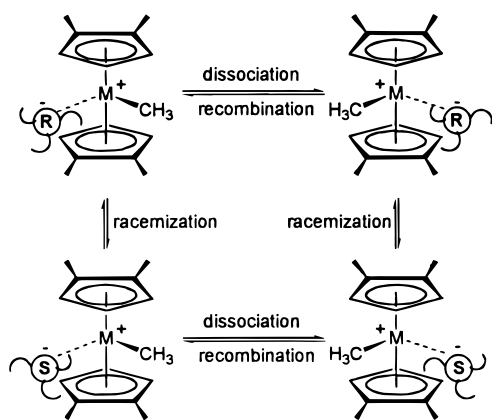
Scheme 21
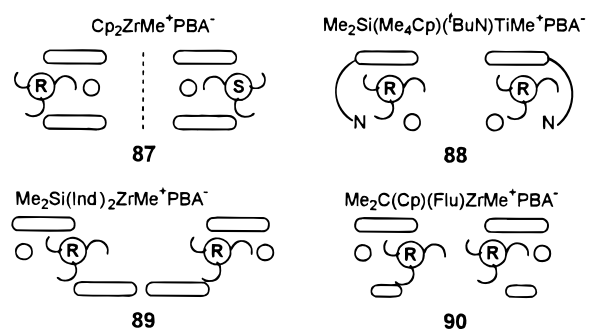
With regard to anion effects on chiral cation stereoregulation, propylene polymerization at 60 °C mediated by *rac*-Me$_2$Si(Ind)$_2$ZrMe$_2$/Ph$_3$C$^+$B(C$_6$F$_5$)$_4$$^-$ yields isotactic polypropylene with [*mmmm*] = 84%, while, under similar polymerization conditions, the strongly ion-paired PBA$^-$ analogue produces highly isotactic polypropylene with [*mmmm*] as high as 98%, albeit with reduced polymerization activity.[97] As revealed by the crystal structure of *rac*-Me$_2$Si-(Ind)$_2$ZrMe$^+$PBA$^-$ (Figure 20), the strongly ion-paired PBA$^-$ anion coordinatively "intrudes" into the cation coordination sphere, which may account for the decrease of polymerization activity and the enhancement in stereoselectivity. In addition to introduction of steric perturbations in the monomer activation/insertion zone, such strong cation–anion interactions may prevent (or minimize) growing polymer chain isomerization (epimerization of the last-inserted polymer unit)[296] and thereby increase stereoselectivity. The significantly more rapid rate of anion racemization (k(60 °C) = 86.7 s^{-1}) (Scheme 22) over the polymerization propagation rate (k(60 °C) ~ 0.2 s^{-1}) for this catalyst under the present conditions argues that the chirality of the coordinated chiral C_3-symmetric PBA$^-$ anion does not directly contribute (in a chirality transfer sense) to the observed enhancement in stereoselection.

These results complement and support observations of Fink et al.[275] that stereospecificity is influenced with increasing separation of cation–anion ion pairs. Weakening of ion pairing in more polar solvents enhances propylene polymerization activity at the expense of stereoselectivity for the isopropyl-
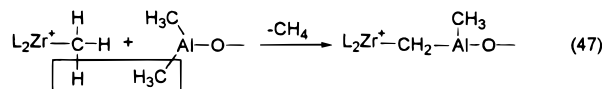
Scheme 22

idene(fluorenyl)cyclopentadienylzirconium dichloride–MAO catalyst system in CH$_2$Cl$_2$–toluene mixtures studied in the paper.

It should be noted that many factors such as monomer concentration, catalyst loading, solvent, polymerization temperature, and polymerization exothermicity (temperature control during the polymerization) complicate propylene polymerization results, especially regarding stereospecificity data, and thus reproducibility may suffer from small variations in these conditions.
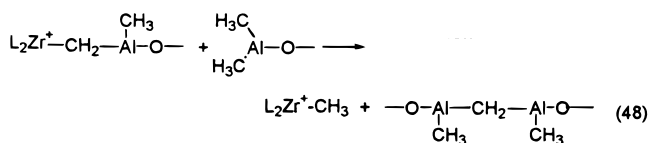
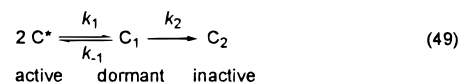## F. Deactivation and Stabilization in Solution

1. Deactivation Processes

An important deactivation process for MAO-activated catalytic systems is α-hydrogen transfer which leads to the production of methane.[50,223] The condensation reaction of the metallocenium alkyl + MAO forms Zr–CH$_2$–Al or Zr–CH$_2$–Zr structures (eq 47), and these species are considered to be

catalytically inactive. The condensation rate depends on the zirconocene structure, temperature, Al/Zr ratio, and concentration. The methane production is much more rapid with MAO than with less Lewis acidic TMA. It was observed in ^{1}H NMR studies that the inactive Zr–CH$_2$–Al structures can be reactivated with excess of MAO, forming L$_2$Zr(CH$_3$)$^+$ and Al–CH$_2$–Al structures. That is, these deactivated species are reactivated according to eq 48.
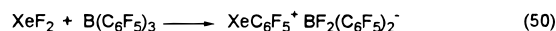

Mülhaupt et al.[297] studied the kinetics of propylene oligomerization catalyzed by Cp$_2$ZrCl$_2$/MAO in toluene and subsequently proposed a reversible + irreversible deactivation process kinetic scheme to fit the decay of the polymerization rate as a function of time (eq 49). The reversible deactivation is second-order relative to the zirconium active site concentra-

$$2\ C^* \underset{k_{-1}}{\overset{k_1}{\rightleftharpoons}} \underset{\text{dormant}}{C_1} \overset{k_2}{\longrightarrow} \underset{\text{inactive}}{C_2} \qquad (49)$$

active　dormant　inactive

tion, which may involve interactions between active as well as inactive Zr sites (binuclear processes), for example dimerization and disproportionation. At low temperatures deactivation is predominantly reversible.

Reduction of the group 4 M(IV) center by MAO or trialkylaluminum to lower-valent species is a common phenomenon, especially for titanium complexes and sometimes for zirconium complexes as well.[18,249–251,298–300] These reductive processes are not considered to be deactivation but rather part of generating the true catalytically active species in the case of mono-Cp titanium complexes for syndiospecific styrene polymerization (vide supra). Addition of a monomer to an active catalytic system often surprisingly increases the quantity of Ti(III)[301] or Zr(III)[298] present, leading to the hypothesis that either the M–R insertion product is more easily reduced than the initial M–CH$_3$ species and/or that most of M(III) species initially existed as bimetallic or polynuclear structures before addition of monomers or Lewis bases.

A number of deactivation and irreversible decomposition processes have been documented for the catalytic systems involved in borane/borate/aluminate activation. The most commonly observed decomposition mode is *C$_6$F$_5$-group transfer* to the electron-deficient transition metal. An early example actually utilized C$_6$F$_5$-group transfer in the synthesis of (pentafluorophenyl)xenon compounds (eq 50).[302]

$$XeF_2 + B(C_6F_5)_3 \longrightarrow XeC_6F_5^+ BF_2(C_6F_5)_2^- \qquad (50)$$

L$_2$ZrMe$^+$MeB(C$_6$F$_5$)$_3^-$ complexes are usually stable in hydrocarbon solution for days at room temperature under an inert atmosphere with the exception of complexes having bulky L groups.[67] For example, the moderately stable complex (1,3-TMS$_2$Cp)$_2$ZrMe$^+$MeB(C$_6$F$_5$)$_3^-$ slowly undergoes decomposition via C$_6$F$_5$ transfer (eq 51). Similar aryl abstraction processes

$$(TMS_2Cp)_2ZrMe^+ B(C_6F_5)_3^- \longrightarrow (TMS_2Cp)_2ZrMe(C_6F_5) + Me\,B(C_6F_5)_2 \qquad (51)$$
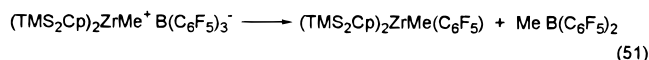
from non-perfluorophenyl-based borate anions, such as BPh$_4^-$ by cationic Zr species, are more facile and have been reported by several groups.[135–136,303] Unlike relatively stable L$_2$ZrMe$^+$MeB(C$_6$F$_5$)$_3^-$ complexes, the Al analogue Cp$_2$ZrMe$^+$MeAl(C$_6$F$_5$)$_3^-$, undergoes very facile C$_6$F$_5$ transfer to Zr above 0 °C to form two neutral species, Cp$_2$ZrMe(C$_6$F$_5$) and MeAl(C$_6$F$_5$)$_2$,[184] suggesting that these bis-Cp type cationic metallocene aluminate ion pairs are much less stable than the borate analogues.

Similar transfer to Ti/Zr involving non-group 13 anions has been observed in the case of group 4 metallocene or CGC cations paired with M(OC$_6$F$_5$)$_6^-$ (M = Ta, Nb) anions.[99] At room temperature, facile C$_6$F$_5$O$^-$ transfer from Nb and Ta to Zr and Ti is observed for coordinatively more open precursor complexes such as CGCTiMe$_2$, Me$_2$Si(Ind)$_2$ZrMe$_2$, and

A

B

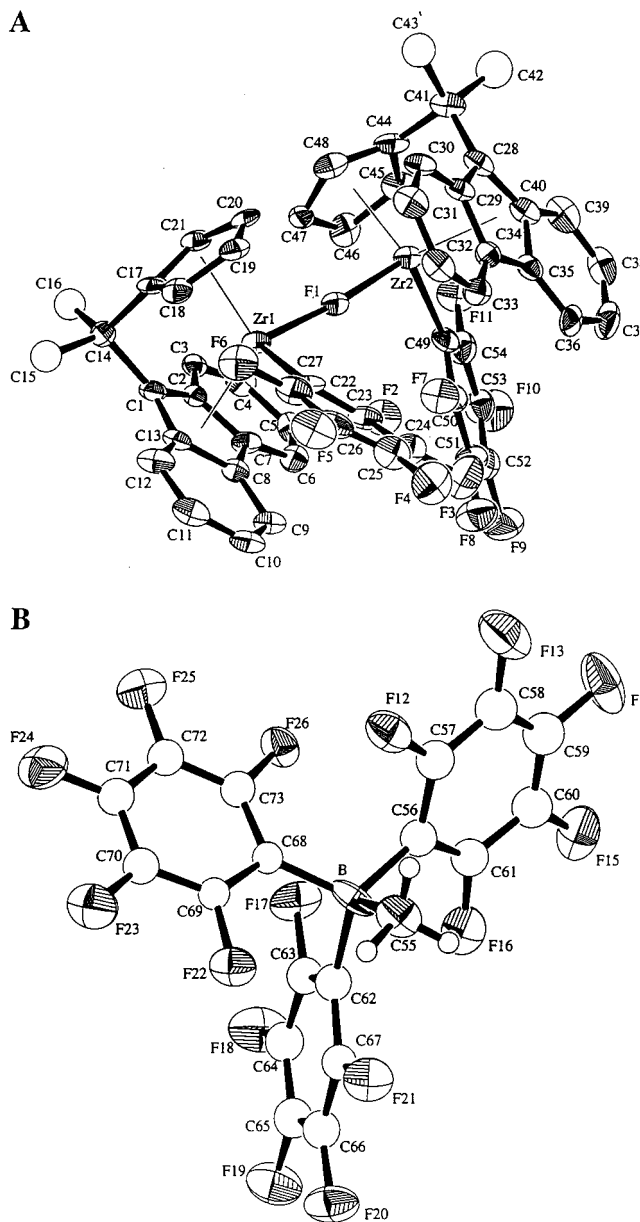**Figure 28.** ORTEP drawing of the structure of the complex $[Me_2C(Flu)(Cp)Zr(C_6F_5)]_2(\mu\text{-F})^+MeB(C_6F_5)_3^-$ (**83**): (A) cation; (B) Anion. From ref 77.

Cp_2ZrMe_2, upon reaction with $Ph_3C^+M(OC_6F_5)_6^-$ activators. The products are the corresponding L_2Zr-$(Ti)Me(OC_6F_5)$ species.

Decomposition products arising from *fluoride abstraction* often result from prolonged standing of $L_2ZrMe^+MeB(C_6F_5)_3^-$ solutions at room temperature over the course of weeks. Both crystallographically characterized F^- abstraction products $[(1,2\text{-}Me_2\text{-}Cp)_2ZrMe]_2(\mu\text{-F})^+MeB(C_6F_5)_3^-$ (**81**)[67] and $[(1,2\text{-}Me_2\text{-}Cp)_2ZrF]_2(\mu\text{-F})^+B(C_6F_4TBS)_4^-$ (**82**)[90] are formed during attempts to grow single crystals of the parent compounds. In other cases, such as the activation reaction of metallocene dimethyls and the borane PNB, F^- abstraction derivatives are inseparable and inevitable byproducts in quantities up to $\sim$20%.[75] The unusual decomposition product, $[Me_2C(Flu)\text{-}(Cp)Zr(C_6F_5)]_2(\mu\text{-F})^+MeB(C_6F_5)_3^-$ (**83**), a result of a combination of *C_6F_5-group transfer* and *fluoride abstraction*, has also been identified and character-

ized by X-ray diffraction (Figure 28).[77]

Another commonly observed decomposition pathway involves C−H bond activation. Unlike the reaction of FAB with most metallocene dialkyls, reaction of bulky $(1,3\text{-}^tBu_2Cp)_2ZrMe_2$ with FAB yields a C−H activated η^5,η^1 "tuck-in" cation (**91**) (eq 52), which is

(52)
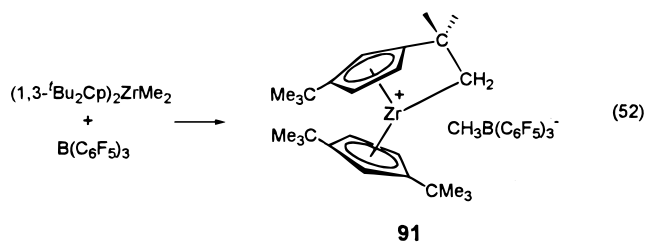
inert with respect to ethylene polymerization or oligomerization.[67] Facile intramolecular C−H activation at Cp−(dimethylamino)alkyl substituents by a methylzirconocene cation has also been observed by Erker et al.[304] to form cyclometalated zirconocenium products (**92**; Scheme 23).

Scheme 23
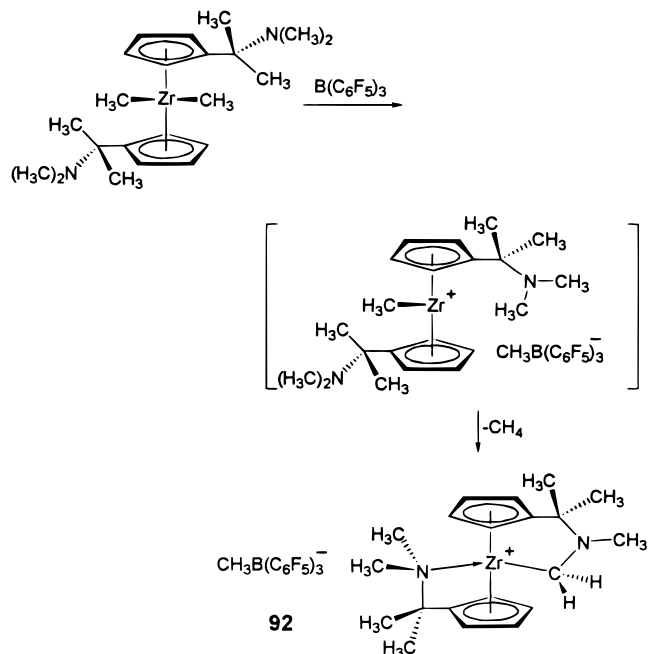
A dinuclear Zr fulvalene complex is reported to react with $Ph_3C^+B(C_6F_5)_4^-$ or FAB, even at −60 °C, with immediate elimination of methane to afford relatively inert $\mu\text{-}CH_2$ complex **93** (eq 53).[305]

(53)
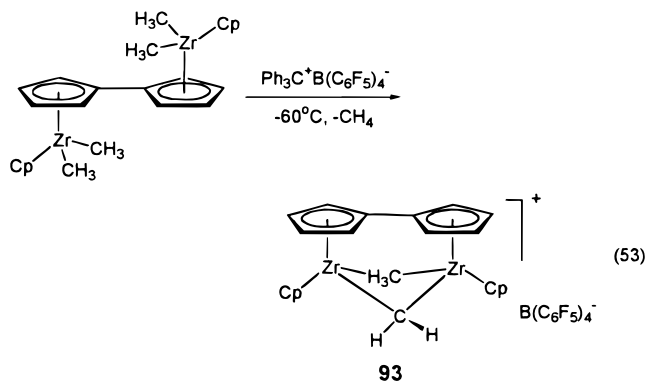
Isolation of the reaction product of CGCTi(CH$_2$Ph)$_2$ with FAB (or Ph$_3$C$^+$B(C$_6$F$_5$)$_4^-$) at ambient temperature affords C–H activation (elimination of toluene) products, i.e., intramolecularly metalated η,$^5\eta^1$ "tuck-in"-type complexes (**94**) (eq 54).[143] The resulting

(54)

94
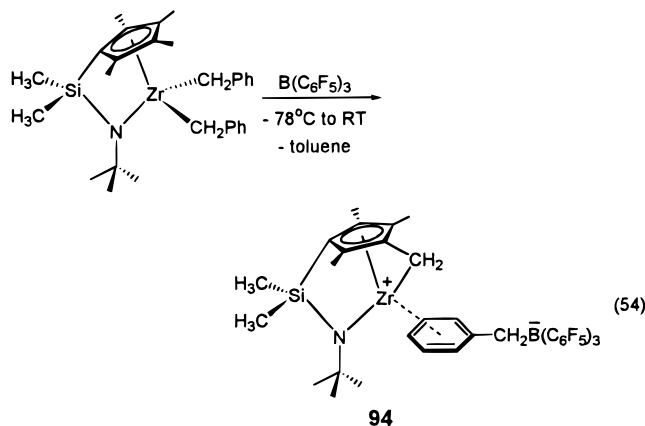
PhCH$_2$B(C$_6$F$_5$)$_3^-$ anion is associated with the cation via η^6-arene coordination of the abstracted benzyl group (or toluene coordination in the case of the B(C$_6$F$_5$)$_4^-$ anion). Although complex **94** is still quite active in olefin polymerization, formation of such "tuck-in" structures induces broadening of the polydispersity and lower α-olefin comonomer incorporation in the resulting polymers, presumably for steric reasons. A similar ring-metalated fulvene-type structure has been proposed on the basis of spectroscopic data from the NMR-scale reaction of Cp′TiMe$_3$ and PBB.[77] Besides the initially formed Cp′TiMe$_2^+$MePBB$^-$ complex and C–H activated ring-metalated species, other low-valent Ti species may be produced in dimeric or polymeric forms.
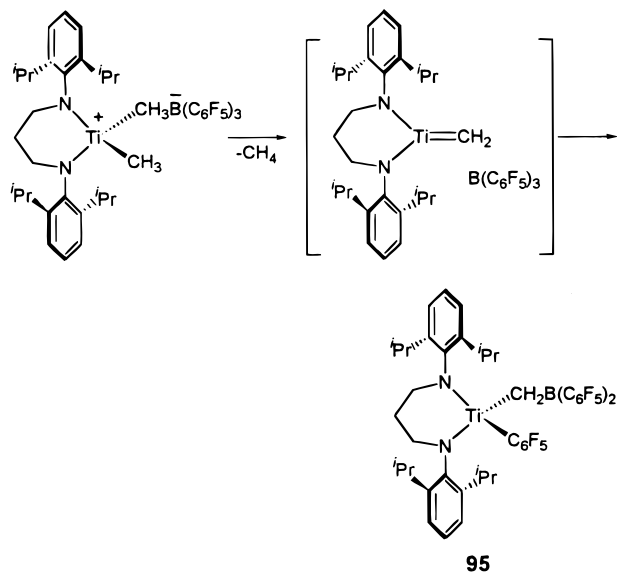
The living α-olefin polymerization catalyst, [RN-(CH$_2$)$_3$NR]TiMe$_2$ (R = 2,6-^{i}Pr$_2$C$_6$H$_3$), forms an unstable, catalytically-active species after reaction with FAB in the absence of monomer. This intermediate gradually evolves methane over course of several hours to form inactive species **95**. Formation of **95**

Scheme 24

95

was proposed to involve loss of CH$_4$, followed by addition of the B–C$_6$F$_5$ group across the Ti=C bond of a transitory the 12-electron titanium methylidene complex (e.g., [RN(CH$_2$)$_3$NR]Ti=CH$_2$]) (Scheme 24).[306] Similar decomposition products have been identified and one crystallographically characterized, from the reaction of FAB with dimethyltitanium complexes containing Cp and o-arylphenoxide ligation.[307]

As discussed above, aluminum trialkyls are often used as in-situ alkylating reagents and as scavengers. In the presence of TMA, group 4 metallocene cations form heterodinuclear complexes (**96**; eq 55).[137] Alkyl-

(55)

96
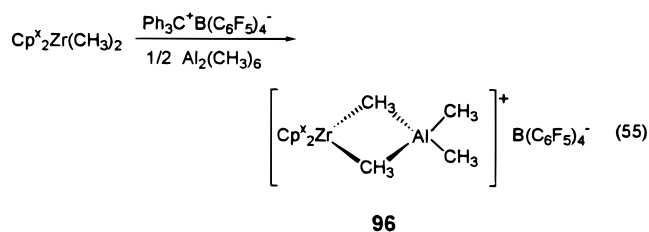
aluminum adducts such as **96** are coordinatively saturated, and initiation of polyolefin chain growth requires dissociation of the bound trialkylaluminum. Therefore, the presence of excess trialkylaluminum may inhibit or lower the catalytic efficiency.

The majority of activation processes have been studied in hydrocarbon solvents. Deactivation may readily occur if the reaction is carried out in polar solvents. Reaction of Ph$_3$C$^+$B(C$_6$F$_5$)$_4^-$ with dialkyl mono-Cp benzamidinato group 4 complexes in halogenated solvents such as CH$_2$Cl$_2$ often results in formation of Cl$^-$ abstraction products. In the example shown (eq 56), the dicationic bis(μ-Cl) product **97** has been crystallographically characterized.[308]

(56)

97
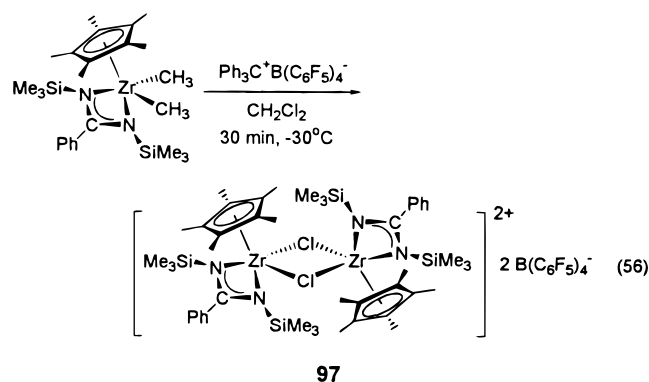
2. Stabilization of Ion Pairs in Solution

As discussed in Section IV.B, a general structural feature of single-site polymerization catalyst ion pairs is the presence of weak donor–acceptor interactions involving the cation and anion moieties or a solvent molecule. Many of these weak interactions still persist in solution and thus likely stabilize the chemically very reactive ion pairs. These stabilization forces, along with complexation with functional monomers in the presence of polymerizable monomers, doubtless play a key role in determining catalyst high-temperature stability, lifetime, and overall kinetic profile, as well as polymerization characteristics.

Anion coordination is the chief interaction involved in solution stabilization. An associated anion can coordinate to a cation through C−H agostic interactions, close halogen or fluorine-to-cation contacts, and η^n-arene coordination. There is a rough correlation between the degree of anion coordination and olefin polymerization activity in hydrocarbon solvents (vide supra). However, efforts to discover and implement "ultimate" noncoordinating anions[260] must take into account activity−stability tradeoffs. For efficient catalytic processes, the ideal situation would be that the catalyst be both highly active or tunable in activity and thermally stable under the conditions of polymerization. It is important to realize how these two properties are to some degree related. For example, although $B(C_6F_5)_4^-$ comes close to the ideal "noncoordinating anion", there are still detectable metal−fluorine interactions in the crystal structure of $Cp'_2ThCH_3+B(C_6F_5)_4^-$.[87] On the other hand, such complexes of sterically less accessible zirconocene analogues are thermally unstable despite the excellent catalytic efficiency they usually display. Exceptions are those CGC-type complexes where aromatic solvent coordination appears to enhance thermal stability.[90,143] Also, for anions such as $B(C_6F_4SiR_3)_4^-$, although they are slightly more coordinating than $B(C_6F_5)_4^-$, they have proven to be more efficient in bis-Cp type zirconocene-catalyzed olefin polymerization.[90]

In the case of MAO-based counteranions, coordination of an MAO oxygen atom to the metal center has been suggested, as in **98** or **99**.[309] Erker et al.[310] were


98

99   **100**
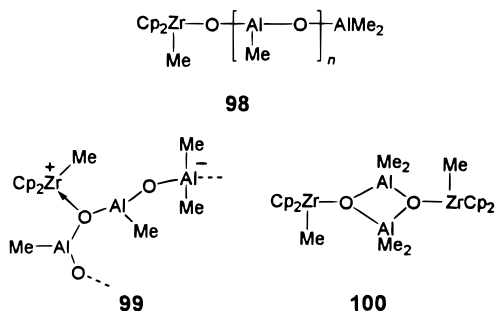
able to isolate complex **100**, formally an adduct between $[Cp_2ZrMe]^+$ and $[Al_2O_2Me_4]^{2-}$, which may be regarded as a model for such an interation. However, complex **100** does not possess any readily accessible coordination sites and is not catalytically active for olefin polymerization in the absence of excess MAO.

If the anion is well-separated from the cation, other types of interactions may be involved in cation stabilization. Coordination modes often observed include solvent (aromatic) (cf., **26**, **45**),[91,143,187,188] neutral metallocene alkyl (cf., **24**, **43**, **53**),[77,90,137,138,143] and multihapto benzyl interactions (cf., **25**, **27**, **36**, **48**, **55**, **61**).[143−144,192,202,311] Benzylmetallocene precursors often form more stable cationic complexes after activation, especially with noncoordinating anion-based activators such as $Ph_3C^+B(C_6F_5)_4^-$, as a result of η^n-benzyl stabilization of the cation (cf., **25**, **27**, **36**, **48**, **55**, **61**).[143,144] Evidence for intramolecular phenyl coordination of cationic monobenzyl-substituted zirconocene complexes (**101**) has also been established by low-

101   **102**
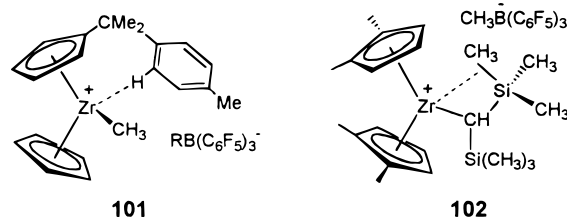
temperature NMR studies.[312] Finally, the β-cation stabilizing effects of the silyl functionalities has been suggested in ion pair $[(1,2\text{-}Me_2Cp)_2ZrCHTMS_2]^+CH_3B(C_6F_5)_3^-$ (**102**) to explain the nonassociation of anion $CH_3B(C_6F_5)_3^-$ to the cation.[285] Such silyl functionalities are known to stabilize α-carbanions and β-carbocations,[313] and there is ample precedent in neutral lanthanocene analogues[314] as well as in complex **63**[206] discussed in section IV.B.

Preference for neutral metallocene dimethyl coordination over anion coordination to form μ-Me dinuclear cationic complexes (e.g., **43**) is observed for those truly weakly coordinating anions such as $B(C_6F_5)_4^-$ [137] and MePBB$^-$.[77,143] Stabilization of highly reactive and unstable metallocenium cations by μ-Me coordination allows isolation and characterization of such species in the pure state, yet affords excellent polymerization activity in solution, presumably via dissociation to a more reactive monomeric form, as indicated by NMR studies.[77] For more coordinating anions such as $CH_3B(C_6F_5)_3^-$, μ-Me bimetallic cationic complexes are not detected, except when an excess of neutral metallocene dimethyl is employed (Scheme 25).[143,315] This equilibrium can be utilized to stabilize

Scheme 25
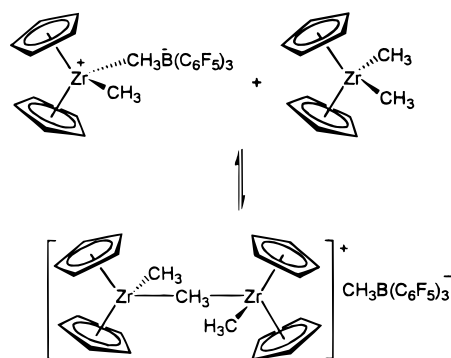
the highly active form of the monomeric cations and to prevent deactivation. Thus, using an excess of the neutral metallocene dimethyl vs activator often results in enhanced polymerization activity by virtue of the binuclear species formation, especially for those systems with $B(C_6F_5)_4^-$-based activators.[315,316]

V. Concluding Remarks

The combination of synthetic, structural, and polymerization studies of ion pairs derived from activation reactions employing the structurally and compositionally diverse families of newly synthesized cocatalysts and metal complexes has provided much insight into activation processes and the nature of cation−anion interactions in these highly active polymerization catalysts. Such studies have also pro-

vided a far better understanding of how the coordinative and dynamic features of the ion pairs are related to polymerization characteristics and product polymer properties.

A series of triarylboranes and MAO have been used to abstract the methide anion from group 4 metallocene and related dimethyl complexes and to form highly electrophilic cations paired with various anions having differing coordinating propensities. As can be seen from selected examples, the versatility of boranes for activating a variety of metal complexes is truly remarkable. The thermodynamic driving force and the kinetic facility of these abstraction reactions has been quantified by titration calorimetry as well as by static and dynamic NMR spectroscopy. The energetics and kinetics of cation formation, dissociation, and structural reorganization are a sensitive function of quantifiable borane acidity, metal ancillary ligation, metal identity, and solvent polarity. Many of the trends can be interpreted in terms of the electron-withdrawing and steric characteristics of the borane substituents, the capacity of the metallocene ancillary ligands to stabilize positive charge, and the homolytic $M-CH_3$ bond dissociation enthalpies. Within a relatively broad metallocenium−methylborate series, qualitative correlations exist between the enthalpies of methide abstraction, the ^{13}C chemical shifts of the resulting $M-CH_3^+$ groups, the free energies of activation for ion pair separation, and the ethylene polymerization activities.

Reversible deactivation or irreversible decomposition processes are more likely if the cation is extremely electron-deficient and highly coordinatively unsaturated. In this regard, a certain degree of weak coordination by anion, solvent, weak intramolecular contacts, or other coordinating sources is required to prevent the cation from undergoing decomposition. However, Lewis base coordination also suppresses catalytic activity and influences other aspects of polymerization characteristics as well. Therefore, the anion Lewis basicity properties must be balanced sterically and electronically with cation Lewis acidity properties to obtain ion-paired catalysts with optimal stability and activity. As exemplified by catalyst−cocatalyst matches such as in $CGCMCH_3^+MePBB^-$ and $(C_5Me_5)_2ZrMe^+PBA^-$, near-optimal efficiency is achieved in such series. The general strategy for selecting the best ion-pair match appears to be that the weakest coordinating anions studied so far such as $B(C_6F_5)_4^-$, $MePBB^-$, $B(C_6F_4TBS)_4^-$ are best matched for sterically more accessible and coordinatively more unsaturated metal cations such as those having CGC, single-ring, and some bridged ligation as well as the large Th(IV) cation. On the other hand, cations having sterically bulky ligands such as nonbridged and some *ansa*-metallocenes, as well as nonmetallocene metal complexes having bulky protecting ligand substituents, can tolerate more coordinating anions such as $CH_3B(C_6F_5)_3^-$ and $X-MAO^-$, which provide good stability without compromising polymerization activity. This "fine-tuning" of ion pair stabilization and activity is in someways analogous to other aspects of homogeneous catalyst ligand

engineering and should allow fine-tuning of many aspects of olefin polymerization catalysis.

Finally, besides the well-recognized influence of cocatalyst on catalyst activity and stability, anion modulation of polymer properties such as molecular weight and stereoregularity is emerging as an important aspect of this catalysis. These important observations have further expanded our view of cocatalyst function and suggest great potential for anion engineering in this rapidly growing field. It is hoped that the rich chemistry exhibited by this field and the knowledge accrued in its exploration can benefit many other polymerization processes.

VI. Acknowledgment

VII. References and Notes

(1) For recent reviews, see: (a) Marks, T. J., Stevens, J. C., Eds. *Topics in Catalysis*; Baltzer: Amsterdam, 1999; Vol. 7, pp 1−208 (special volume on Advances in Polymerization Catalysis. Catalysts and Processes). (b) Kaminsky, W., Ed. *Metalorganic Catalysts for Synthesis and Polymerization: Recent Results by Ziegler-Natta and Metallocene Investigations*; Springer-Verlag: Berlin, 1999. (c) Britovsek, G. J. P.; Gibson, V. C.; Wass, D. F. *Angew. Chem., Int. Ed. Engl.* **1999**, *38*, 428−447 (nonmetallocene olefin polymerization catalysts). (d) Jordan, R. F. Ed. *J. Mol. Catal.* **1998**, *128*, 1−337 (special issue on metallocene and single-site olefin catalysts). (e) McKnight, A. L.; Waymouth, R. M. *Chem. Rev.* **1998**, *98*, 2587−2598 (constrained geometry polymerization catalysts). (f) Kaminsky, W.; Arndt, M. *Adv. Polym. Sci.* **1997**, *127*, 144−187 (metallocenes for polymer catalysis). (g) Bochmann, M. *J. Chem. Soc., Dalton Trans.* **1996**, 255−270 (cationic group 4 metallocene complexes and their role in polymerization catalysis). (h) Brintzinger, H.-H.; Fischer, D.; Mülhaupt, R.; Rieger, B.; Waymouth, R. M. *Angew. Chem., Int. Ed. Engl.* **1995**, *34*, 1143−1170 (stereospecific olefin polymerization with chiral metallocene catalysts). (i) Fink, G.; Mülhaupt, R., Brintzinger, H.-H., Eds. *Ziegler Catalysts*; Springer-Verlag: Berlin, 1995. (j) Huang, J.; Rempel, G. L. *Prog. Polym. Sci.* **1995**, *20*, 459−526 (mechanistic insights from metallocene systems). (k) Soga, K., Terano, M., Eds. *Catalyst Design for Tailor-Made Polyolefins*; Elsevier: Tokyo, 1994. (l) Möhring, P. C.; Coville, N. J. *J. Organomet. Chem.* **1994**, *479*, 1−29 (influence of Cp-ring substituents on polymerization). (m) Marks, T. J. *Acc. Chem. Res.* **1992**, *25*, 57−65 (organometallic connections between heterogeneous and homogeneous catalysis). (n) Jordan, R. F. *Adv. Organomet. Chem.* **1991**, *32*, 325−387 (chemistry of cationic bis-Cp group 4 complexes).
(2) Morse, P. M. *Chem. Eng. News* **1998**, *51* (July 6), 11−16.
(3) Thayer, A. M. *Chem. Eng. News* **1995**, *48* (Sept 11), 15−19.
(4) Chowdhury, J.; Fouhy, K.; Shanley, A. *Chem. Eng. (N.Y.)* **1996**, *103* (Feb), 35−41.
(5) Boor, J., Jr. *Ziegler-Natta Catalysts and Polymerizations*; Academic Press: New York, 1979.
(6) Chien, J. C. W., Ed. *Coordination Polymerization*; Academic Press: New York, 1975.
(7) Natta, G.; Pasquon, I.; Zambelli, A. *J. Am. Chem. Soc.* **1962**, *84*, 1488−1490.
(8) Doi, Y.; Ueki, S.; Keii, T. *Macromolecules* **1979**, *12*, 814−819.
(9) Bier, G. *Angew. Chem.* **1961**, *73*, 186−197.
(10) Boor, J., Jr.; Youngman, E. A. *J. Polym. Sci., Part A* **1966**, *4*, 1861−1884.
(11) Muthukumaru Pillari, S.; Ravindranathan, M.; Sivaram, S. *Chem. Rev.* **1986**, *86*, 353−399.
(12) Keim, W.; Kowaldt, F. H.; Goddard, R.; Krüger, C. *Angew. Chem., Int. Ed. Engl.* **1978**, *17*, 466−467.
(13) (a) Breslow, D. S.; Newburg, N. R. *J. Am. Chem. Soc.* **1957**, *79*, 5072−5073. (b) Breslow, D. S. U.S. Pat. Appl. 537039, 1955.
(14) (a) Natta, G.; Pino, P.; Mazzanti, G.; Lanzo, R. *Chim. Ind. (Milan)* **1957**, *39*, 1032−1033. (b) Natta, G.; Pino, P.; Mazzanti, G.; Giannini, U.; Mantica, E. *J. Polym. Sci.* **1957**, *26*, 120−123. (c) Natta, G.; Pino, P.; Mazzanti, G.; Giannini, U. *J. Am. Chem. Soc.* **1957**, *79*, 2975−2976.

(15) (a) Long, W. P.; Breslow, D. S. *J. Am. Chem. Soc.* **1960**, *82*, 1953−1957. (b) Breslow, D. S.; Newburg, N. R. *J. Am. Chem. Soc.* **1959**, *81*, 81−86. (c) Long, W. P. *J. Am. Chem. Soc.* **1959**, *81*, 5312−5316.

(16) Chien, J. C. W. *J. Am. Chem. Soc.* **1959**, *81*, 86−92.

(17) Skupinska, J. *Chem. Rev.* **1991**, *91*, 613−648.

(18) Sinn, H.; Kaminsky, W. *Adv. Organomet. Chem.* **1980**, *18*, 99−149.

(19) (a) Arlman, E. J.; Cossee, P. *J. Catal.* **1964**, *3*, 99−104. (b) Cossee, P. *J. Catal.* **1964**, *3*, 80−88. (c) Cossee, P. *Tetrahedron Lett.* **1960**, *12*, 12−16, 17−21.

(20) (a) Dyachkovskii, F. S.; Shilova, A. K.; Shilov, A. E. *J. Polym. Sci., Part C* **1967**, *16*, 2333−2339. (b) Zefirova, A. K.; Shilov, A. E. *Dokl. Akad. Nauk. SSSR* **1961**, *136*, 599−602.

(21) Eisch, J. J.; Piotrowski, A. M.; Brownstein, S. K.; Gabe, E. J.; Lee, F. L. *J. Am. Chem. Soc.* **1985**, *107*, 7219−7221.

(22) Reichert, K. H. In *Transition Metal Catalyzed Polymerizations*; Quirk, R. P., Ed.; Academic Press: New York, 1981; p 465.

(23) (a) Mynott, R.; Fink, G.; Fenzl, W. *Angew. Makromol. Chem.* **1987**, *154*, 1−21. (b) Fink, G.; Rottler, R. *Angew. Makromol. Chem.* **1981**, *94*, 25−47. (c) Fink, G.; Rottler, R.; Kreiter, C. G. *Angew. Makromol. Chem.* **1981**, *96*, 1−20.

(24) (a) Eisch, J. J.; Pombrik, S. I.; Zheng, G.-X. *Organometallics* **1993**, *12*, 3856−3863. (b) Eisch, J. J.; Pombrik, S. I.; Zheng, G.-X. *Macromol. Symp.* **1993**, *66*, 109−120.

(25) Eisch, J. J.; Pombrik, S. I.; Gurtzgen, S.; Rieger, R.; Uzick, W. In ref 1k, pp 221−235.

(26) Eisch, J. J.; Mackenzie, K.; Windisch, H.; Kruger, C. *Eur. J. Inorg. Chem.* **1999**, 153−162.

(27) Reichert, K. H.; Meyer, K. R. *Makromol. Chem.* **1973**, *169*, 163−176.

(28) Long, W. P.; Breslow, D. S. *Liebigs Ann. Chem.* **1975**, 463−469.

(29) (a) Andresen, A.; Cordes, H. G.; Herwig, H.; Kaminsky, W.; Merk, A.; Mottweiler, R.; Pein, J.; Sinn, H.; Vollmer, H. J. *Angew. Chem., Int. Ed. Engl.* **1976**, *15*, 630−632.

(30) Sinn, H.; Kaminsky, W.; Vollmer, H.-J.; Woldt, R. *Angew. Chem., Int. Ed. Engl.* **1980**, *19*, 390−392.

(31) Isotactic polypropylene: (a) Spaleck, W.; Küber, F.; Winter, A.; Rohrmann, J.; Bachmann, B.; Antberg, M.; Dolle, V.; Paulus, E. P. *Organometallics* **1994**, *13*, 954−963. (b) Stehling, U.; Diebold, J.; Kirsten, R.; Röll, W.; Brintzinger, H.-H. *Organometallics* **1994**, *13*, 964−970. (c) Kaminsky, W.; Kulper, K.; Brintzinger, H.-H.; Wild, F. R. W. P. *Angew. Chem., Int. Ed. Engl.* **1985**, *24*, 507−508. (d) Ewen, J. A. *J. Am. Chem. Soc.* **1984**, *106*, 6355−6364.

(32) Syndiotactic polypropylene: Ewen, J. A.; Jones, R. L.; Razavi, A.; Ferrara, J. D. *J. Am. Chem. Soc.* **1988**, *110*, 6255−6256.

(33) Stereoblock polypropylene: (a) Coates, G. W.; Waymouth, R. M. *Science* **1995**, *267*, 217−219. (b) Gauthier, W. J.; Cornigan, J. F.; Taylor, N. J.; Collins, S. *Macromolecules* **1995**, *28*, 3771−3778. (c) Gauthier, W. J.; Collins, S. *Macromolecules* **1995**, *28*, 3779−3786. (d) Chien, J. C. W.; Llinas, G. L.; Rausch, M. D.; Lin, G.-Y.; Winter, H. H. *J. Am. Chem. Soc.* **1991**, *113*, 8569−8570. (e) Mallin, D. T.; Rausch, M. D.; Lin, G.-Y.; Dong, S.; Chien, J. C. W. *J. Am. Chem. Soc.* **1990**, *112*, 2030−2031.

(34) Long-chain branching polyethylene: (a) Lai, S. Y.; Wilson, J. R.; Knight, G. W.; Stevens, J. C.; Chum, P. W. S. U.S. Patent 5,272,236, 1993 (Dow Chemical Co.). (b) Swogger, K. W.; Kao, C. I. Polyolefins VIII. *Technol. Pap., Reg. Technol. Conf.-Soc. Plast. Eng.* **1993**, 14.

(35) Vandenberg, E. J. *J. Polym. Sci.* **1960**, *47*, 486-489.

(36) Sinn, H., Kaminsky, W., Hoker, H., Eds. *Alumoxanes*; Macromolecular Symposia 97; Huthig & Wepf: Heidelberg, Germany, 1995.

(37) Srinivasa Reddy, S.; Sivaram, S. *Prog. Polym. Sci.* **1995**, *20*, 309−367.

(38) (a) Sinn, H. *Macromol. Symp.* **1995**, *97*, 27−52. (b) Sinn, H.; Schimmel, I.; Ott, M.; von Thienen, N.; Harder, A.; Hagendorf, W.; Heitmann, B.; Haupt, E. In ref 1b, pp 105−122.

(39) Mason, M. R.; Smith, J. M.; Bott, S. G.; Barron, A. R. *J. Am. Chem. Soc.* **1993**, *115*, 4971−4984.

(40) Imhoff, D. W.; Simeral, L. S.; Sangokoya, S. S.; Peel, J. H. *Organometallics* **1998**, *17*, 1941−1845.

(41) Babushkin, D. E.; Semikolenova, N. V.; Panchenko, V. N.; Sobolev, A. P.; Zakharov, V. A.; Talsi, E. P. *Macromol. Chem. Phys.* **1997**, *198*, 3845−3854.

(42) Sugano, T.; Matsubara, K.; Fujita, T.; Takahashi, T. *J. Mol. Catal.* **1993**, *82*, 93−101.

(43) Siedle, A. R.; Lamanna, W. M.; Newmark, R. A.; Stevens, J.; Richardson, D. E.; Ryan, M. *Macromol. Symp.* **1993**, *66*, 215−224.

(44) Siedle, A. R.; Newmark, R. A.; Lamanna, W. M.; Schroepfer, J. N. *Polyhedron* **1990**, *9*, 301−308.

(45) Resconi, L.; Bossi, S.; Abis, L. *Macromolecules* **1990**, *23*, 4489−4491.

(46) Pasynkiewicz, S. *Polyhedron* **1990**, *9*, 429−453.

(47) Giannetti, E.; Nicoletti, G.; Mazzochi, R. *J. Polym. Sci., Polym. Chem. Ed.* **1985**, *23*, 2117−2133.

(48) (a) Tritto, I.; Mealares, C.; Carmela Sacchi, M.; Locatelli, P. *Macromol. Chem. Phys.* **1997**, *198*, 3963−3977. (b) Tritto, I.; Sacchi, M. C.; Locatelli, P.; Li, S. X. *Macromol. Chem. Phys.* **1996**, *197*, 1537−1544.

(49) Eilertsen, J. L.; Rytter, E.; Ystenes, M. In ref 1b, pp 136−141.

(50) Kaminsky, W.; Steiger, R. *Polyhedron* **1988**, *7*, 2375−2381.

(51) Dall'Occo, T.; Galimberti, M.; Resconi, L.; Albizzati, E.; Pennini, G. PCT Int. Appl. WO 96/02580, 1996 (Montell).

(52) (a) Dall'Occo, T.; Galimberti, M.; Camurati, I.; Destro, M.; Fusco, O.; Brita, D. In ref 1b, pp 142−149. (b) Galimberti, M.; Destro, M.; Fusco, O.; Piemontesi, F.; Camurati, I. *Macromolecules* **1999**, *32*, 258−263.

(53) Chien, J. C. W.; Wang, B. *J. Polym. Sci., Part A* **1988**, *26*, 3089−3102.

(54) Srinivasa Reddy, S.; Shashidhar, G.; Sivaram, S. *Macromolecules* **1993**, *26*, 1180−1182.

(55) Tomotsu, N.; Ishihara, N.; Newman, T. H.; Malanga, M. T. *J. Mol. Catal.* **1998**, *128*, 167−190.

(56) Tritto, I.; Donnetti, R.; Sacchi, M. C.; Locatelli, P.; Zannoni, G. *Macromolecules* **1997**, *30*, 1247−1252.

(57) Michiels, W.; Munoz-Escalona, A. *Macromol. Symp.* **1995**, *97*, 171−183.

(58) Smith, G. M.; Palmaka, S. W.; Roger, J. S.; Malpass, D. B.; Monfiston, D. J. PCT Int. Appl. WO 9723288, 1997 (Akzo-Nobel).

(59) Jin, J.; Uozumi, T.; Soga, K. *Macromol. Chem. Phys.* **1996**, *197*, 849−854.

(60) Massey, A. G.; Park, A. J. *J. Organomet. Chem.* **1964**, *2*, 245−250.

(61) Biagini, P.; Lugli, G.; Abis, L.; Andreussi, P. U.S. Pat. 5,602,-269, 1997 (Enichem).

(62) Lee, C. H.; Lee, S. J.; Park, J. W.; Kim, K. H.; Lee, B. Y.; Oh, J. S. *J. Mol. Catal., A: Chem.* **1998**, *132*, 231−239.

(63) Carnahan, E. M.; Chen, E. Y.-X.; Jacobsen, G. B.; Stevens, J. C. PCT Int. Appl. WO 99/15534; U.S. Pat. Appl. 59572, 1997 (Dow Chemical Co.).

(64) Massey, A. G.; Park, A. J. *J. Organomet. Chem.* **1966**, *5*, 218−225.

(65) For reviews on polyfluoroaromatic derivatives of metals and metalloids, see: (a) Brooke, G. M. *J. Fluorine Chem.* **1997**, *86*, 1−76. (b) Cohen, S. C.; Massey, A. G. *Adv. Fluorine Chem.* **1970**, *6*, 83−285.

(66) For a recent review on pentafluorophenylborane chemistry, see: Piers, W. E.; Chivers, T. *Chem. Soc. Rev.* **1997**, *26*, 345−354.

(67) (a) Yang, X.; Stern, C. L.; Marks, T. J. *J. Am. Chem. Soc.* **1994**, *116*, 10015−10031. (b) Yang, X.; Stern, C. L.; Marks, T. J. *J. Am. Chem. Soc.* **1991**, *113*, 3623−3625.

(68) Ewen, J. A.; Elder, M. J., Eur. Patent Appl. 0,427,697, 1991; U.S. Pat. 5,561,092, 1996.

(69) Jacobsen, H.; Berke, H.; Döring, S.; Kehr, G.; Erker, G.; Fröhlich, R.; Meyer, O. *Organometallics* **1999**, *18*, 1724−1735.

(70) Danopoulos, A. A.; Galsworthy, J. R.; Green, M. L. H.; Cafferkey, S.; Doerrer, L.; Hursthouse, M. B. *Chem. Commun.* **1998**, 2529−2530.

(71) (a) Parks, D. J.; Piers, W. E.; Parvez, M.; Atencio, R.; Zaworotko, M. J. *Organometallics* **1998**, *17*, 1369−1377. (b) Parks, D. J.; Piers, W. E. *J. Am. Chem. Soc.* **1996**, *118*, 9440−9441.

(72) Parks, D. J.; Spence, R. E. v H.; Piers, W. E. *Angew. Chem., Int. Ed. Engl.* **1995**, *34*, 809−811.

(73) Chen, Y.-X.; Yang, S.; Stern, C. L.; Marks, T. J. *J. Am. Chem. Soc.* **1996**, *118*, 12451−12452.

(74) Li, L.; Marks, T. J. Submitted for publication.

(75) (a) Li, L.; Marks, T. J. *Organometallics* **1998**, *17*, 3996−4003. (b) Marks, T. J.; Li, L.; Chen, Y.-X.; McAdon, M. H.; Nickias, P. N. PCT Int. Appl. WO 99/06412, 1999.

(76) Penton, D. E.; Park, A. J.; Shaw, D.; Massey, A. G. *J. Organomet. Chem.* **1964**, *2*, 437−446.

(77) Chen, Y.-X.; Metz, M. V.; Li, L.; Stern, C. L.; Marks, T. J. *J. Am. Chem. Soc.* **1998**, *120*, 6287−6305.

(78) (a) Schwartz, D. J.; Marks, T. J. Manuscript in preparation. (b) Fritze, C.; Küber, F.; Bohmen, H. Eur. Pat. Appl. 811,627, 1997 (Hoechst AG).

(79) Williams, V. C.; Piers, W. E.; Clegg, W.; Elsegood, M. R. J.; Collins, S.; Marder, T. B. *J. Am. Chem. Soc.* **1999**, *121*, 3244−3245.

(80) (a) Metz, M. V.; Schwartz, D. J.; Beswick, C. L.; Stern, C. L.; Marks, T. J. *Abstracts of Papers*, 217th National Meeting of the American Chemical Society, Anaheim, CA, March, 1999; American Chemical Society: Washington, DC, 1999; INOR 015. (b) McAdon, M. H.; Nickias, P. N.; Marks, T. J.; Schwartz, D. J. PCT Int. Appl. WO 99/06413, 1999. (c) Williams, V. C.; Dai, C.; Li, Z.; Collins, S.; Piers, W. E.; Clegg, W.; Elsegood, M. R. J.; Marder, T. B. *Angew. Chem., Int. Ed. Engl.* **1999**, *38*, 3695−3698. (d) Metz, M. V.; Schwartz, D. J.; Stern, C. L.; Marks, T. J.; Nickias, P. N. *Angew. Chem., Int. Ed. Engl.*, in press.

(81) Pohlmann, J. L. W.; Brinckman, F. E. *Z. Naturforsch. B: Anorg. Chem. Org. Chem.* **1965**, *20B*, 5−11.

(82) Belgardt, T.; Storre, J.; Roesky, H. W.; Noltemeyer, M.; Schmidt, H.-G. *Inorg. Chem.* **1995**, *34*, 3821−3822.

(83) Hair, G. S.; Cowley, A. H.; Jones, R. A.; Mcburnett, B. G.; Voigt, A. *J. Am. Chem. Soc.* **1999**, *121*, 4922–4923.

(84) Chien, J. C. W.; Tsai, W.-M.; Rausch, M. D. *J. Am. Chem. Soc.* **1991**, *113*, 8570–8571.

(85) Ewen, J. A.; Elder, M. J. Eur. Pat. Appl. 0,426,637, 1991.

(86) (a) Hlatky, G. G.; Upton, D. J.; Turner, H. W. PCT Int. Appl. WO 91/09882 1991. (Exxon Chemical Co.). (b) Turner, H. W. Eur Pat. Appl. EP 0 277 004 A1, 1988 (Exxon Chemical Co.).

(87) Yang, X.; Stern, C. L.; Marks, T. J. *Organometallics* **1991**, *10*, 840–842.

(88) Elder, M. J.; Ewen, J. A. Eur. Pat. Appl. 0,573,403, 1993.

(89) Jia, L.; Yang, X.; Ishihara, A.; Marks, T. J. *Organometallics* **1995**, *14*, 3135–3137.

(90) Jia, L.; Yang, X.; Stern, C. L.; Marks, T. J. *Organometallics* **1997**, *16*, 842–857.

(91) Chen, Y.-X.; Marks, T. J. Unpublished results.

(92) Ishihara, A.; Stern, C. L.; Marks, T. J. Manuscript in preparation.

(93) Jia, L.; Yang, X.; Stern, C. L.; Marks, T. J. *Organometallics* **1994**, *13*, 3755–3757.

(94) Kohler, K.; Piers, W. E.; Jarvis, A. P.; Xin, S.; Feng, Y.; Bravakis, A. M.; Collins, S.; Clegg, W.; Yap, G. P. A.; Marder, T. B. *Organometallics* **1998**, *17*, 3557–3566.

(95) Lancaster, S. L.; Walker, D. A.; Thornton-Pett, M.; Bochmann, M. *Chem. Commun.* **1999**, 1533–1534.

(96) LaPointe, R. E. PCT Int. Appl. WO 99/42467, 1999 (Dow Chemical Co.); U.S. Pat. Appl. 75329, 1998.

(97) Chen, Y.-X.; Stern, C. L.; Marks, T. J. *J. Am. Chem. Soc.* **1997**, *119*, 2582–2583.

(98) For synthesis of the related fluoroalkoxide complex, Li⁺{Al[OC(R)-(CF₃)₂]₄}⁻ (R = H, CH₃, Ph), see: Barbarich, T. J.; Miller, S. M.; Anderson, O. P.; Strauss, S. H. *J. Mol. Catal.* **1998**, *128*, 289–331.

(99) (a) Sun, Y.; Stern, C. L.; Marks, T. J. *Abstracts of Papers*, 217th National Meeting of the American Chemical Society, Anaheim, CA, March, 1999; American Chemical Society: Washington, DC, 1999; INOR 014. (b) Sun, Y.; Metz, M. V.; Stern, C. L.; Marks, T. J. *Organometallics*, in press.

(100) Chen, Y.-X.; Marks, T. J. Unpublished results.

(101) Chien, J. C. W. in ref 1a, pp 23–36.

(102) Kaminsky, W.; Winkelbach, H. In ref 1a, pp 61–67.

(103) Jenny, C.; Maddox, P. *Curr. Opin. Solid State Chem. Mater. Sci.* **1998**, *3*, 94–103.

(104) Ribeiro, M. R.; Deffieux, A.; Portela, M. F. *Ind. Eng. Chem. Res.* **1997**, *36*, 1224–1237.

(105) Olabisi, O.; Atiqullah, M.; Kaminsky, W. *J. Macromol. Sci., Rev. Macromol. Chem. Phys.* **1997**, *C37*, 519–554.

(106) Soares, J. B. P.; Hamielec, A. E. *Polym. React. Eng.* **1995**, *3*, 131–200.

(107) Soga, K.; Aria, T.; Nozawa, H.; Uozumi, T. *Macromol. Symp.* **1995**, *97*, 53–62.

(108) Chien, J. C. W.; He, D. *J. Polym. Sci., Part A: Polym. Chem.* **1991**, *29*, 1603–1607.

(109) Collins, S.; Kelly, W. M.; Holden, D. A. *Macromolecules* **1992**, *25*, 1780–1785.

(110) Soga, K.; Kaminaka, M. *Makromol. Chem.* **1993**, *194*, 1745–1755.

(111) Kaminsky, W.; Renner, F. *Makromol. Chem., Rapid Commun.* **1993**, *14*, 239–243.

(112) Chen, Y.-X.; Rausch, M. D.; Chien, J. C. W. *J. Polym. Sci., Part A: Polym. Chem.* **1995**, *33*, 2093-2108.

(113) Chang, M. U.S. Pat. 5,008,228, 1991; 4,935,397, 4,914,253, 4,912,075, 1990 (Exxon Chemicals Co.).

(114) Herrmann, H.-F.; Bachmann, B.; Spaleck, W. U.S. Pat. 5,578,-537, 1996 (Hoechst, AG).

(115) Woo, S. I.; Ko, Y. S.; Han, T. K. *Macromol. Rapid Commun.* **1995**, *16*, 489–494.

(116) (a) Kresge, C. T.; Leonowicz, M. E.; Roth, W. J.; Vartuli, J. C.; Beck, J. S. *Nature* **1992**, *359*, 710–712. (b) Beck, J. S.; Vartuli, J. C.; Toth, W. J.; Leonowicz, M. E.; Kresge, C. T.; Schmitt, K. D.; Chu, C. T.-W.; Olson, D. H.; Sheppard, E. W.; McCullen, S. B.; Higgins, J. B.; Schlenker, J. L. *J. Am. Chem. Soc.* **1992**, *114*, 10834–10843.

(117) Van Looveren, L. K.; Geysen, D. F.; Vercruysse, K. A.; Wouters, B. H.; Grobet, P. J.; Jacobs, P. A. *Angew. Chem., Int. Ed. Engl.* **1998**, *37*, 517–520.

(118) Ernst, E.; Reussner, J.; Denifl. In ref 1b, pp 407–412.

(119) (a) Walzer, J. F.; White, J. L. *Abstracts of Papers*, 215th National Meeting of the American Chemical Society, Dallas, TX, March, 1998; American Chemical Society: Washington, DC, 1998; INOR 051. (b) Walzer, J. F., Jr. U.S. Patent 5,643,847, 1997 (Exxon Chemical Co.).

(120) Lancaster, S. J.; O'Hara, S. M.; Bochmann, M. In ref 1b, pp 413–425.

(121) (a) Siedle, A. R.; Miller, J. A.; Lamanna, W. M. PCT Int. Appl. WO 96/26967, 1996 (3M Co.). (b) Siedle, A. R.; Lamanna, W. M. U.S. Pat. 5,296,433, 1994. (c) Siedle, A. R.; Lamanna, W. M.; Newmark, R. A.; Stevens, J.; Richardson, D. E.; Ryan, M. Makromol. Chem. Macromol. Symp. **1993**, *66*, 215–224.

(122) Ward, D. G.; Carnahan, E. M. PCT Int. Appl. WO 96/23005, 1996 (W.R. Grace).

(123) Hlatky, G. G.; Upton, D. J. *Macromolecules* **1996**, *29*, 8019–8020.

(124) Roscoe, S. B.; Frechet, J. M. J.; Walzer, J. F.; Dias, A. J. *Science* **1998**, *280*, 270–273.

(125) Hinokuma, S.; Miyake, S.; Ono, M.; Inazawa, S., U. S. Pat. 5,-869,723, 1999 (Showa Denko K.K.).

(126) (a) Jacobsen, G. B.; Wijkens, P.; Jastrzebski, J. T. B. H.; Van Koten, G. U.S. Pat. 5,834,393, 1998 (Dow Chemical). (b) Jacobsen, G. B.; Stevens, T. J. P.; Loxis, P. H. H. U.S. Pat. 5,783,-512,1998, (Dow Chemical). (c) Carnahan, E. M., Carney, M. J.; Neithamer, D. R.; Nickias, P. N.; Shin, K.-Y.; Spencer, L. PLT Int. Appl. WO 97/19959, 1997 (Dow Chemical/W.R. Grace).

(127) Ono, M.; Hinokuma, S.; Miyake, S.; Inazawa, S. Eur. Pat. Appl. EP0710663A1, 1996 (Japan Polyolefins Co.).

(128) (a) Eisen, M. S.; Marks, T. J. *J. Mol. Catal.* **1994**, *86*, 23–50. (b) Eisen, M. S.; Marks, T. J. *J. Am. Chem. Soc.* **1992**, *114*, 10358–10368. (c) Gillespie, R. D.; Burwell, R. L., Jr.; Marks, T. J. *Langmuir* **1990**, *6*, 1465–1477. (d) Dahmen, K. H.; Hedden, D.; Burwell, R. L., Jr.; Marks, T. J. *Langmuir* **1988**, *4*, 1212–1214.

(129) Ahn, H.; Marks, T. J. *J. Am. Chem. Soc.* **1998**, *120*, 13533–13534.

(130) Jordan, R. F.; Dasher, W. E.; Echols, S. F. *J. Am. Chem. Soc.* **1986**, *108*, 1718–1719.

(131) Jordan, R. F.; Bajgur, C. S.; Willett, R.; Scott, B. *J. Am. Chem. Soc.* **1986**, *108*, 7410–7411.

(132) Jordan, R. F.; Lapointe, R. E.; Bajgur, C. S.; Willett, R. *J. Am. Chem. Soc.* **1987**, *109*, 4111–4113.

(133) Hlatky, G. G.; Turner, H. W.; Eckman, R. R. *J. Am. Chem. Soc.* **1989**, *111*, 2728–2729.

(134) Hlatky, G. G.; Eckman, R. R.; Turner, H. W. *Organometallics* **1992**, *11*, 1413–1416.

(135) (a) Horton, A. D.; Orpen, A. G. *Organometallics* **1991**, *10*, 3910–3918. (b) Horton, A. D.; Frijins, J. H. G. *Angew. Chem., Int. Ed. Engl.* **1991**, *30*, 1152–1154.

(136) Bochmann, M.; Jagger, A. J.; Nicholls, J. C. *Angew. Chem., Int. Ed. Engl.* **1990**, *29*, 780–782.

(137) Bochmann, M.; Lancaster, S. J. *Angew. Chem., Int. Ed. Engl.* **1994**, *33*, 1634–1637.

(138) Coles, M. P.; Jordan, R. F. *J. Am. Chem. Soc.* **1997**, *119*, 8125–8126.

(139) (a) Stevens, J. C. In *Studies in Surface Science and Catalysis*; Hightower, J. W., Delglass, W. N., Iglesia, E., Bell, A. T., Eds.; Elsevier: Amsterdam, 1996; Vol. 101, pp 11–20 and references therein. (b) Stevens, J. C.; Timmers, F. J.; Wilson, D. R.; Schmidt, G. F.; Nickias, P. N.; Rosen, R. K.; Knight, G. W.; Lai, S. Eur. Pat. Appl. EP 416 815-A2, 1991 (Dow Chemical Co.).

(140) (a) Canich, J. M.; Hlatky, G. G.; Turner, H. W. PCT Appl. WO 92/00333, 1992. (b) Canich, J. M. Eur. Patent Appl. EP 420 436-A1, 1991 (Exxon Chemical Co.).

(141) Okuda, J. *Comments Inorg. Chem.* **1994**, *16*, 185–205.

(142) (a) Shapiro, P. J.; Cotter, W. D.; Schaefer, W. P.; Labinger, J. A.; Bercaw, J. E. *J. Am. Chem. Soc.* **1994**, *116*, 4623–4640. (b) Piers, W. E.; Shapiro, P. J.; Bunnel, E. E.; Bercaw, J. E. *Synlett* **1990**, *2*, 74–84.

(143) Chen, Y.-X.; Marks, T. J. *Organometallics* **1997**, *16*, 3649–3657.

(144) Bochmann, M.; Lancaster, S. J. *Organometallics* **1993**, *12*, 633–640.

(145) Chen, Y.-X.; Fu, P.-F.; Stern, C. L.; Marks, T. J. *Organometallics* **1997**, *16*, 5958–5963.

(146) (a) Bochmann, M.; Wilson, L. M.; Hursthouse, M. B.; Short, R. L. *Organometallics* **1987**, *6*, 2556–2563. (b) Bochmann, M.; Wilson, L. M. *J. Chem. Soc., Chem. Commun.* **1986**, 1610–1611.

(147) Lin, Z.; Le Marechal, J.-F.; Sabat, M.; Marks, T. J. *J. Am. Chem. Soc.* **1987**, *109*, 4127–4129.

(148) Hlatky, G. G.; Eckman, R. R.; Turner, H. W. *Organometallics* **1992**, *11*, 1413–1416.

(149) Yang, X.; King, W. A.; Sabat, M.; Marks, T. J. *Organometallics* **1993**, *12*, 4254–4258.

(150) Crowther, D. J.; Borkowsky, S. L.; Swenson, D.; Meyer, T. Y.; Jordan, R. F. *Organometallics* **1993**, *12*, 2897–2903.

(151) Stevens, J. C.; Neithamer, D. R. U.S. Patent 5,064,802, 1991; 5,132,380, 1992 (Dow Chemical Co.).

(152) Campbell, R. E., Jr. U.S. Pat. 5,066,741, 1991 (Dow Chemical Co.).

(153) (a) Horton, A. D.; de With, J. *Organometallics* **1997**, *16*, 5424–5436. (b) Horton, A. D.; de With J.; van der Linden, A. J.; van de Weg, H. *Organometallics* **1996**, *15*, 2672–2674.

(154) Bei, X.; Swenson, D. C.; Jordan, R. F. *Organometallics* **1997**, *16*, 3282–3302.

(155) Yokota, Y.; Inoue, T.; Naganuma, S.; Shozaki, H.; Tomotsu, N.; Kuramoto, M.; Ishihara, N. In ref 1b, pp 435–445.

(156) Bochmann, M.; Lancaster, S. J. *J. Organomet. Chem.* **1992**, *434*, C1–C5.

(157) Ewen, J. A.; Elder, M. J. *Makromol. Chem. Macromol. Symp.* **1993**, *66*, 179–190.

(158) Brookhart, M.; Grant, B.; Volpe, A. F., Jr. *Organometallics* **1992**, *11*, 3920–3922.

(159) Nishida, H.; Takada, N.; Yoshimura, M.; Sonoda, T.; Kobayashi, H. *Bull. Chem. Soc, Jpn.* **1984**, *57*, 2600−2604.
(160) Johnson, L, K.; Killian, C. M.; Brookhart, M. *J. Am. Chem. Soc.* **1995**, *117*, 6414−6415.
(161) (a) Mecking, S.; Johnson, L. K.; Wang, L.; Brookhart, M. *J. Am. Chem. Soc.* **1998**, *120*, 888−899. (b) Johnson, L. K.; Mecking, S.; Brookhart, M. *J. Am. Chem. Soc.* **1996**, *118*, 267−268.
(162) He, M.-Y.; Xiong, G.; Toscano, P. J.; Burwell, R. L., Jr.; Marks, T. J. *J. Am. Chem. Soc.* **1985**, *107*, 641−652.
(163) Toscano, P. J.; Marks, T. J. *J. Am. Chem. Soc.* **1985**, *107*, 653−659.
(164) Toscano, P. J.; Marks, T. J. *Langmuir* **1986**, *2*, 820−823.
(165) Hedden, D.; Marks, T. J. *J. Am. Chem. Soc.* **1988**, *110*, 1647−1649.
(166) Finch, W. C.; Gillespie, R. D.; Hedden, D.; Marks, T. J. *J. Am. Chem. Soc.* **1990**, *112*, 6221−6232.
(167) Green, M. L. H.; Sassmannshausen, J. *Chem. Commun.* **1999**, 115−116.
(168) Yang, X.; Stern, C. L.; Marks, T. J. *Angew. Chem., Int. Ed. Engl.* **1992**, *31*, 1375−1377.
(169) Bochmann, M.; Lancaster, S. J. *Organometallics* **1994**, *13*, 2235−2243.
(170) Horton, A. D. *Organometallics* **1996**, *15*, 2675−2677.
(171) Resconi, L.; Piemontesi, F.; Fraciscono, G.; Abis, L.; Fiorani, T. *J. Am. Chem. Soc.* **1992**, *114*, 1025−1032.
(172) Sun, Y.; Spence, R. E. v. H.; Piers, W. E.; Parvez, M.; Yap, G. P. A. *J. Am. Chem. Soc.* **1997**, *119*, 5132−5143.
(173) van der Heijden, H.; Hessen, B.; Orpen, A. G. *J. Am. Chem. Soc.* **1998**, *120*, 1112−1113.
(174) Song, X.; Bochmann, M. *J. Organomet. Chem.* **1997**, *545−546*, 597−600.
(175) For recent review on zwitterionic metallocenes, see: Piers, W. E. *Chem. Eur. J.* **1998**, *4*, 13−18.
(176) (a) Temme, B.; Erker, G.; Karl, J.; Luftmann, H.; Frohlich, R.; Kotila, S. *Angew. Chem., Int. Ed. Engl.* **1995**, *34*, 1755−1757. (b) Temme, B.; Karl, J.; Erker, G. *Chem. Eur. J.* **1996**, *2*, 919−924.
(177) Karl, J.; Erker, G.; Frohlich, R. *J. Am. Chen. Soc.* **1997**, *119*, 11165−11173.
(178) Spence, R. E. v. H.; Piers, W. E.; Sun, Y.; Parvez, M.; MacGillivray, L. R.; Zaworotko, M. J. *Organometallics* **1998**, *17*, 2459−2469.
(179) Spence, R. E. v. H.; Parks, D. J.; Piers, W. E.; MacDonald, M.-A.; Zaworotko, M. J.; Rettig, S. J. *Angew. Chem., Int. Ed. Engl.* **1995**, *34*, 1230−1233.
(180) Bochmann, M.; Green, M. L. H.; Powell, A. K.; Sassmann-shausen, J.; Triller, M. U.; Wocadlo, S. *J. Chem. Soc., Dalton Trans.* **1999**, 43−49.
(181) Deng, H.; Shiono, T.; Soga, K. *Macromolecules* **1995**, *28*, 3067−3073.
(182) Soga, K.; Deng, H.; Yano, T.; Shiono, T. *Macromolecules* **1994**, *27*, 7938−7940.
(183) (a) Li, Y.; Ward, D. G.; Reddy, S. S.; Collins, S. *Macromolecules* **1997**, *30*, 1875−1883. (b) Collins, S.; Ward, D. G. *J. Am. Chem. Soc.* **1992**, *114*, 5460−5462.
(184) Bochmann, M.; Sarsfield, M. J. *Organometallics* **1998**, *17*, 5908−5912.
(185) Cowley, A. H.; Hair, G. S.; McBurnett, B. G.; Jones, R. A. *J. Chem. Soc. Chem. Commun.* **1999**, 437−438.
(186) Gillis, D. J.; Tudoret, M.-J.; Baird, M. C. *J. Am. Chem. Soc.* **1993**, *115*, 2543−2544.
(187) Gillis, D. J.; Quyoum, R.; Tudoret, M.-J.; Wang, Q.; Jeremic, D.; Roszak, A. W.; Baird, M. C. *Organometallics* **1996**, *15*, 3600−3605.
(188) Lancaster, S. J.; Robinson, O. B.; Bochmann, M. *Organometallics* **1995**, *14*, 2456−2462.
(189) Wang, Q.; Gillis, D.; Quyoum, R.; Jeremic, D.; Tudoret, M.-J.; Baird, M. C. *J. Organomet. Chem.* **1997**, *527*, 7−14.
(190) Ewart, S. W.; Baird, M. C. In ref 1a, pp 1−8.
(191) Pellecchia, C.; Immirzi, A.; Grassi, A.; Zambelli, A. *Organometallics* **1993**, *12*, 4473−4478.
(192) Pellecchia, C.; Immirzi, A.; Pappalardo, D.; Peluso, A. *Organometallics* **1994**, *13*, 3773−3775.
(193) (a) Pindado, G. J.; Thornton-Pett, M.; Bouwkamp, M.; Meetsma, A.; Hessen, B.; Bochmann, M. *Angew. Chem., Int. Ed. Engl.* **1997**, *36*, 2358−2361. (b) Pindado, G. J.; Thornton-Pett, M.; Bochmann, M. *J. Chem. Soc., Dalton Trans.* **1997**, 3115−3127.
(194) Pindado, G. J.; Thornton-Pett, M.; Hursthouse, M. B.; Coles, S. J.; Bochmann, M. *J. Chem. Soc., Dalton Trans.* **1999**, 1663−1668.
(195) Pindado, G. J.; Lancaster, S. J.; Thornton-Pett, M.; Bochmann, M. *J. Am. Chem. Soc.* **1998**, *120*, 6816−1817.
(196) Lapointe, R. E.; Stevens, J. C.; Nickias, P. N.; Mark, M. H. Eur. Pat. Appl. 520,732 A1, 1992 (Dow Chemical Co.).
(197) (a) Lanza, G.; Fragala, I. L.; Marks, T. J. *J. Am. Chem. Soc.* **1998**, *120*, 8257−8258. (b) Lanza, G.; Fragala, I. L. In ref 1a, pp 45−60.
(198) Woo, T. K.; Margl, P. M.; Lohrenz, J. C. W.; Blochl, P. E.; Ziegler, T. *J. Am. Chem. Soc.* **1996**, *118*, 13021−13030.
(199) Fu, P.-F.; Luo, L.; Lanza, D. J.; Wilson, D. J.; Rudolph, P. R.; Fragala, I. L.; Stern, C. L.; Marks, T. J. Submitted for publication.
(200) Sinnema, P.-J.; Liekelema, K.; Staal, O. K. B.; Hessen, B.; Teuben, J. H. *J. Mol. Catal.* **1998**, *128*, 143−153.
(201) Amor, F.; Butt, A.; du Plooy, K. E.; Spaniol, T. P.; Okuda, J. *Organometallics* **1998**, *17*, 5836−5849.
(202) (a) Pellecchia, C.; Grassi, A.; Immirzi, A. *J. Am. Chem. Soc.* **1993**, *115*, 1160−1162. (b) Pellecchia, C.; Proto, A.; Zambelli, A. *Makromol. Chem. Rapid Commun.* **1992**, *13*, 277−281.
(203) Scollard, J. D.; McConville, D. H. *J. Am. Chem. Soc.* **1996**, *118*, 10008−10009.
(204) Horton, A. D.; de With, J. *Chem. Commun.* **1996**, 1375−1376.
(205) Wright, J. M.; Landis, C. R.; Ros, M. A. M. P.; Horton, A. D. *Organometallics* **1998**, *17*, 5031−5040.
(206) Galsworthy, J. R.; Green, M. L. H.; Maxted, N.; Muller, M. *J. Chem. Soc., Dalton Trans.* **1998**, 387−392.
(207) Van der Linden, A.; Schaverien, C. J.; Meijboom, N.; Ganter, C.; Orpen, A. G. *J. Am. Chem. Soc.* **1995**, *117*, 3008−3021.
(208) Thorn, M. G.; Etheridge, Z. C.; Fanwick, P. E.; Rothwell, I. P. *Organometallics* **1998**, *17*, 3636−3638.
(209) Baumann, R.; David, W. M.; Schrock, R. R. *J. Am. Chem. Soc.* **1997**, *119*, 3830−3831.
(210) Baumann, R.; Schrock, R. R. *J. Organomet. Chem.* **1998**, *557*, 69−75.
(211) Hill, G. S.; Rendina, L. M.; Puddephatt, R. J. *J. Chem. Soc., Dalton Trans.* **1996**, 1809−1813.
(212) Wang, C.; Friedrich, S.; Younkin, T. R.; Li, R. T.; Grubbs, R. H.; Bansleben, D. A.; Day, M. W. *Organometallics* **1998**, *17*, 3149−3151.
(213) Song, X.; Thornton-Pett, M.; Bochmann, M. *Organometallics* **1998**, *17*, 1004−1006.
(214) Lee, L. W. M.; Piers, W. E.; Elsegood, M. R. J.; Clegg, W.; Parvez, M. *Organometallics* **1999**, *18*, 2947−2949.
(215) Green, M. L. H.; Haggitt, J.; Mehnert, C. P.. *J. Chem. Soc., Chem. Commun.* **1995**, 1853−1854.
(216) Bochmann, M.; Dawson, D. M. *Angew. Chem., Int. Ed. Engl.* **1996**, *35*, 2226−2228.
(217) Coles, M. P.; Swenson, D. C.; Jordan, R. F. *Organometallics* **1997**, *16*, 5183−5194.
(218) Cam, D.; Giannini, U. *Makromol. Chem.* **1992**, *193*, 1049.
(219) Gassman, P. G.; Callstrom, M. R. *J. Am. Chem. Soc.* **1987**, *109*, 7875−7876.
(220) Sishta, C.; Hathorn, R. M.; Marks, T. J. *J. Am. Chem. Soc.* **1992**, *114*, 1112−1114.
(221) Siedle, A. R.; Lamanna, W. M.; Newmark, R. A.; Schroepfer, J. N. *J. Mol. Catal.* **1998**, *128*, 257−271.
(222) (a) Tritto, I.; Li, S. X.; Sacchi, M. C.; Locatelli, P.; Zannoni, G. *Macromolecules* **1995**, *28*, 5358−5362. (b) Tritto, I.; Li, S.; Sacchi, M. C.; Zannoni, G. *Macromolecules* **1993**, *26*, 7111−7115.
(223) Kaminsky, W. *Makromol. Chem. Phys.* **1996**, *197*, 3907−3945.
(224) Kaminsky, W.; Strubel, C. *J. Mol. Catal.* **1998**, *128*, 191−200.
(225) Tritto, I.; Donetti, R.; Sacchi, M. C.; Locatelli, P.; Zannoni, G. *Macromolecules* **1999**, *32*, 264−269.
(226) Harlan, C. J.; Bott, S. G.; Barron, A. R. *J. Am. Chem. Soc.* **1995**, *117*, 6465−6474.
(227) Killian, C. M.; Tempel, D. J.; Johnson, L. K.; Brookhart, M. *J. Am. Chem. Soc.* **1996**, *118*, 11664−11665.
(228) (a) Svejda, S. A.; Brookhart, M. *Organometallics* **1999**, *18*, 65−74. (b) Killian, C. M.; Johnson, L. K.; Brookhart, M. *Organometallics* **1997**, *16*, 2005−2007.
(229) Small, B. L.; Brookhart, M.; Bennett, A. M. A. *J. Am. Chem. Soc.* **1998**, *120*, 4049−4050.
(230) Britovsek, G. J. P.; Gibson, V. C.; Kimberley, B.; Maddox, P. J.; McTavish, S. J.; Solan, G. A.; White, A. J. P.; Williams, D. J. *Chem. Commun.* **1998**, 849−850.
(231) Small, B. L.; Brookhart, M. *Macromolecules* **1999**, *32*, 2120−2130.
(232) Pellecchia, C.; Mazzeo, M.; Pappalardo, D. *Macromol. Rapid Commun.* **1998**, *19*, 651−655.
(233) Chien, J. C. W.; Tsai, W.-M. *Makromol. Chem., Macromol. Symp.* **1993**, *66*, 141−156.
(234) Tsai, W.-M.; Rausch, M. D.; Chien, J. C. W. *Appl. Organomet. Chem.* **1993**, *7*, 71−74.
(235) Chen, Y.-X.; Rausch, M. D.; Chien, J. C. W. *Macromolecues* **1995**, *28*, 5399−5404.
(236) (a) Chen, Y.-X.; Rausch, M. D.; Chien, J. C. W. *Organometallics* **1994**, *13*, 748−749. (b) Chen, Y.-X.; Rausch, M. D.; Chien J. C. W. *J. Organomet. Chem.* **1995**, *487*, 29−34.
(237) Jin, J.; Tsubaki, S.; Uozumi, T.; Sano, T.; Soga, K. *Macromol. Rapid Commun.* **1998**, *19*, 597−600.
(238) Naga, N.; Mizunuma, K. *Polymer* **1998**, *39*, 5059−5067.
(239) Bochmann, M.; Jagger, A. J.; Wilson, L. M.; Hursthouse, M. B.; Motevalli, M. *Polyhedron* **1989**, *8*, 1838−1843.
(240) Cuenca, T.; Royo, P. *J. Organomet. Chem.* **1985**, *295*, 159−165.
(241) Lapointe, R. E.; Rosen, R. K.; Nickias, P. N. Eur. Pat. Appl. 0495375A2, 1992 (Dow Chemical Co.).

(242) Devore, D. D.; Mussell, R. D.; Stevens, J. C., U.S. Pat. 5,372,682, 1994 (Dow Chemical Co.).
(243) For a review, see: Po, R.; Cardi, N. *Prog. Polym. Sci.* **1996**, *21*, 47−88.
(244) Wang, Q.; Quyoum, R.; Gillis, D. J.; Tudoret, M.-J.; Jeremic, D.; Hunter, B. K.; Baird, M. C. *Organometallics* **1996**, *15*, 693−703.
(245) (a) Ready, T. E.; Day, R. O.; Chien, J. C. W.; Rausch, M. D. *Macromolecules* **1993**, *26*, 5822−5823. (b) Kucht, A.; Kucht, H.; Barry, S.; Chien, J. C. W.; Rausch, M. D. *Organometallics* **1993**, *12*, 3075−3078. (c) Chien, J. C. W.; Salajka, Z. *J. Polym. Sci., Part A: Polym. Chem.* **1991**, *29*, 1253−1263.
(246) Pellecchia, C.; Pappalardo, D.; Oliva, L.; Zambelli, A. *J. Am. Chem. Soc.* **1995**, *117*, 6593−6594. (b) Pellecchia, C.; Longo, P.; Proto, A.; Zambelli, A. *Makromol. Chem. Rapid Commun.* **1992**, *13*, 265−268.
(247) (a) Campbell, R. E., Jr. PCT, WO 93/03067; Eur. Pat. Appl. 502683, 1992; Eur. Pat. Appl. 421659, 1991. (b) Campbell, R. E., Jr.; Hefner. U.S. Pat. 5,045,517, 1991 (Dow Chemical Co.).
(248) (a) Ishihara, N.; Seimiya, T.; Kuramoto, M.; Uoi, M. *Macromolecules* **1988**, *21*, 3356−3360. (b) Ishihara, N.; Seimiya, T.; Kuramoto, M.; Uoi, M. *Macromolecules* **1986**, *19*, 2465−2466.
(249) (a) Grassi, A.; Zambelli, A.; Laschi, F. *Organometallics* **1996**, *15*, 480−482. (b) Grassi, A.; Pellecchia, C.; Oliva, L.; Laschi, F. *Macromol. Chem. Phys.* **1995**, *196*, 1093−1100.
(250) (a) Chien, J. C. W.; Salajka, Z.; Dong, S. *Macromolecules* **1992**, *25*, 3199−3203. (b) Bueschges, U.; Chien, J. C. W. *J. Polym. Sci., Polym. Chem.* **1989**, *27*, 1525−1538.
(251) Campbell, R. E., Jr.; Newman, T. H.; Malanga, M. T. *Macromol. Symp.* **1995**, *97*, 151−160.
(252) Newman, T. H.; Malanga, M. T. *J. Macromol. Sci., Pure Appl. Chem.* **1997**, *A34*, 1921−1927.
(253) Pellecchia, C.; Grassi, A. In ref 1a, pp 125−132.
(254) (a) Chien, J. C. W.; Rausch, M. D. In ref 1b, pp 446−464. (b) Ready, T. E.; Gurge, R.; Chien, J. C. W.; Rausch, M. D. *Organometallics* **1998**, *17*, 5236−5239.
(255) Childs, R. F.; Mulholland, D. L.; Nixon, A. *Can. J. Chem.* **1982**, *60*, 801−808.
(256) Luo, L.; Marks, T. J. In ref 1a, pp 97−106.
(257) Childs, R. F.; Mulholland, D. L.; Nixon, A. *Can. J. Chem.* **1982**, *60*, 809−812.
(258) Luo, L.; Marks, T. J. Manuscript in preparation.
(259) Deck, P. A.; Beswick, C. L.; Marks, T. J. *J. Am. Chem. Soc.* **1998**, *120*, 1772−1784.
(260) Strauss, S. H. *Chem. Rev.* **1993**, *93*, 929−942.
(261) Eisch, J. J.; Pombrik, S. I.; Zheng, G.-X. *Organometallics* **1993**, *12*, 3856−3863.
(262) Kaminsky, W.; Engehausen, R.; Zounis, K.; Spaleck, W.; Rohrmann, J. *Makromol. Chem.* **1992**, *193*, 1643−1651.
(263) Möhring, P.; Coville, N. J. *J. Mol. Catal.* **1992**, *77*, 41−50.
(264) For a recent review, see: Grubbs, R.; Coates, G. W. *Acc. Chem. Res.* **1996**, *29*, 85−93.
(265) (a) Brookhart, M.; Green, M. L. H. *J. Organomet. Chem.* **1983**, *250*, 395−408. (b) Brookhart, M.; Green, M. L. H.; Wang, L. *Prog. Inorg. Chem.* **1988**, *36*, 1−124. (c) Crabtree, R. H.; Hamilton, D. G. *Adv. Organomet. Chem.* **1988**, *28*, 299−338.
(266) Pellecchia, C.; Immirzi, A.; Zambelli, A. *J. Organomet. Chem.* **1994**, *479*, C9−C11.
(267) Wu, Z.; Jordan, R. F.; Petersen, J. L. *J. Am. Chem. Soc.* **1995**, *117*, 5867−5868.
(268) Horton, A. D.; Orpen, A. G. *Organometallics* **1992**, *11*, 8−10.
(269) Deck, P. A.; Marks, T. J. *J. Am. Chem. Soc.* **1995**, *117*, 6128−6129.
(270) Siedle, A. R.; Newark, R. A. *J. Organomet. Chem.* **1995**, *497*, 119−125.
(271) (a) Sandstrøm, J. *Dynamic NMR Spectroscopy*; Academic Press: New York, 1982; pp 77−92. (b) Kaplan, J. I..; Franenkel, G. *NMR of Chemically Exchanging Systems*; Academic Press: New York, 1980; pp 71−128.
(272) Chien, J. C. W.; Song, W.; Rausch, M. D. *Macromolecules* **1993**, *26*, 3239−3240.
(273) Vizzini, J. C.; Chien, J. C. W.; Babu, G. N.; Newmark, R. A. *J. Polym. Sci., Part A: Polym. Chem.* **1994**, *32*, 2049−2056.
(274) Forlini, F.; Fan, Z.-Q.; Tritto, I.; Locatelli, P.; Sacchi, M. C. *Macromol. Chem. Phys.* **1997**, *198*, 2397−2408.
(275) Herfert, N.; Fink, G. *Makromol. Chem.* **1992**, *193*, 773−778.
(276) Longo, P.; Oliva, L.; Grassi, A.; Pellecchia, C. *Makromol. Chem.* **1989**, *190*, 2357−2361.
(277) (a) Moore, J. W.; Pearson, R. G. *Kinetics and Mechanism*, 3rd ed.; John Wiley: New York, 1981; pp 353−363 and references therein. (b) Maskill, H. *The Physical Basis of Organic Chemistry*; Oxford University Press: Oxford, U.K., 1985: Chapter 10.3−10.5. (c) Isaacs, N. S. *Physical Organic Chemistry*, 2nd ed.; Longman: Essex, U.K., 1995; Chapter 5.
(278) Reference 277c, Chapter 5.
(279) Marks, T. J.; Chen, Y.-X. U.S. Pat. 5,856,256, 1999.
(280) Richardson, D. E.; Alameddin, N. G.; Ryan, M. F.; Hayes, T.; Eyler, J. R.; Siedle, A. R. *J. Am. Chem. Soc.* **1996**, *118*, 11244−11253.
(281) Chien, J. C. W.; Song, W.; Rausch, M. D. *J. Polym. Sci., Part A: Polym. Chem.* **1994**, *32*, 2387−2393.
(282) Kucht, H.; Kucht, A.; Chien, J. C. W.; Rausch, M. D. *Appl. Organomet. Chem.* **1994**, *8*, 393−396.
(283) Grassi, A.; Lamberti, C.; Zambelli, A.; Mingozzi, I. *Macromolecules* **1997**, *30*, 1884−1889.
(284) Pappalardo, D.; Mazzeo, M.; Pellecchia, C. *Macromol. Rapid Commun.* **1997**, *18*, 1017−1023.
(285) Beswick, C. L.; Marks, T. J. *Organometallics* **1999**, *18*, 2410−2412.
(286) Canich, J. M.; Turner, H. W. PCT Int. Appl. WO 92/12612, 1992 (Exxon Chemical Co.).
(287) Stevens, J. C. *Proceedings of MetCon'93*; Houston, TX, 1993, Catalyst Consultants, pp 157−170.
(288) McKnight, A. L.; Masood, M. A.; Waymouth, R. M.; Straus, D. A. *Organometallics* **1997**, *16*, 2879−2885.
(289) Canich, J. M., U.S. Pat. 5,026,798, 1991 (Exxon Chemical Co.).
(290) Turner, H. W.; Hlatky, G. G.; Canich, J. M. PCT Int. Appl. WO 93/19103, 1993 (Exxon Chemical Co.).
(291) (a) Shiomura, T.; Asanuma, T.; Inoue, N. *Macromol. Rapid Commun.* **1996**, *17*, 9−14. (b) Shiomura, T.; Asamura, T.; Sunaga, T. *Macromol. Rapid Commun.* **1997**, *18*, 169−173.
(292) Hagihara, H.; Shiono, T.; Ikeda, T. *Macromolecules* **1997**, *30*, 4783−4785.
(293) Hagihara, H.; Shiono, T.; Ikeda, T. *Macromolecules* **1998**, *31*, 3184−3188.
(294) (a) Giardello, M. A.; Eisen, M. S.; Stern, C. L.; Marks, T. J. *J. Am. Chem. Soc.* **1993**, *115*, 3326−3327 (b) Giardello, M. A.; Eisen, M. S.; Stern, C. L.; Marks, T. J. *J. Am. Chem. Soc.* **1995**, *117*, 12114−12129.
(295) Ewen, J. A. In ref 1k, pp 405−410.
(296) (a) Busico, V.; Caporaso, L.; Cipullo, R.; Landriani, L.; Angelini, G.; Margonelli, A.; Segre, A. C. *J. Am. Chem. Soc.* **1996**, *118*, 2105−2106. (b) Leclerc, M. K.; Brintzinger, H.-H. *J. Am. Chem. Soc.* **1996**, *118*, 9024−9032. (c) Busico, V.; Cipullo, R. *J. Am. Chem. Soc.* **1994**, *116*, 9329−9330.
(297) (a) Fisher, D.; Jüngling, S.; Mülhaupt, R. *Makromol. Chem. Macromol. Symp.* **1993**, *66*, 191−202. (b) Fisher, D.; Mülhaupt, R. *J. Organomet. Chem.* **1991**, *417*, C7−C11.
(298) Cam, D.; Sartori, F.; Maldotti, A. *Makromol. Chem. Phys.* **1994**, *195*, 2817−2826.
(299) Yu, P.; Muller, P.; Said, M. A.; Roesky, H. W.; Uson, I.; Bai, G.; Noltemeyer, M. *Organometallics* **1998**, *18*, 1669−1674.
(300) Huang, Y. H.; Yu, Q.; Zhu, S.; Remple, G. L.; Li. L. *J. Polym. Sci., Part A: Polym. Chem.* **1999**, *37*, 1465−1472.
(301) Grassi, A.; Saccheo, S.; Zambelli, A.; Laschi, F. *Macromolecules* **1998**, *31*, 5588−5591.
(302) (a) Naumann, D.; Tyrra, W. *J. Chem. Soc., Chem. Commun.* **1989**, 47−50. (b) Frohn, H. J.; Jakobs, S.. *J. Chem. Soc., Chem. Commun.* **1989**, 625−627.
(303) Lin, Z. Ph.D. Dissertation, Northwestern University, Evanston, IL, 1988.
(304) Bertuleit, A.; Fritze, C.; Erker, G.; Frohlich, R. *Organometallics* **1997**, *16*, 289−2899.
(305) Bochmann, M.; Cuenca, T.; Hardy, D. T. *J. Organomet. Chem.* **1994**, *484*, C10−C12.
(306) Scollard, J. D.; McConville, D. H.; Rettig, S. J. *Organometallics* **1997**, *16*, 1810−1812.
(307) Thorn, M. G.; Vilardo, J. S.; Fanwick, P. E.; Rothwell, I. P. *Chem. Commun.* **1998**, 2427−2428.
(308) Gomez, R.; Green, M. L. H.; Haggitt, J. L. *J. Chem. Soc., Dalton Trans.* **1996**, 939−946.
(309) Giannetti, E.; Nicoletti, G. M.; Mazzocchi, R. *J. Polym. Sci., Part A: Polym. Chem.* **1985**, *23*, 2117−2133.
(310) Erker, G.; Alberecht, M.; Werner, S.; Kruger, C. *Z. Naturforsch. B* **1990**, *45*, 1205−1209.
(311) Jordan, R. F.; LaPointe, R. E.; Baenziger, N. C.; Hinch, G. D. *Organometallics* **1990**, *9*, 1539−1545.
(312) Doerrer, L. H.; Green, M. L. H.; Haussinger, D.; Sassmannshausen, J. *J. Chem. Soc., Dalton Trans.* **1999**, 2111−2118.
(313) Bassindale, A. R.; Taylor, P. G. In *The Chemistry of Organic Silicon Compounds*; Patai, S., Rappaport, Z., Eds.; Wiley: Chichester, U.K., 1989; Chapter 14. (b) Fleming, I. In *Comprehensive Organic Chemistry*; Jones, N. D., Ed.; Pergamon Press: Oxford, U.K., 1979; Chapter 13.
(314) (a) Klooster, W. T.; Brammer, L.; Schaverien, C. J.; Budzelaar, P. H. M. *J. Am. Chem. Soc.* **1999**, *121*, 1381−1382. (b) Koga, N.; Morokuma, K. *J. Am. Chem. Soc.* **1988**, *110*, 108−112. (c) Di Bella, S.; Lanza, G.; Fragala, I. L.; Marks, T. J. *Organometallics* **1996**, *15*, 205−208. (d) Harr, C. M.; Stern, C. L.; Marks, T. J. *Organometallics* **1996**, *15*, 1765−1784. (e) Giardello, M. A.; Conticello, V. P.; Brard, L.; Sabat, M.; Rheingold, A. L.; Stern, C. L.; Marks, T. J. *J. Am. Chem. Soc.* **1994**, *116*, 10212−10240.
(315) Beck, S.; Prosenc, M.-H.; Brintzinger, H.-H.; Goretzki, R.; Herfert, N.; Fink, G. *J. Mol. Catal.* **1996**, *111*, 67−79.
(316) Hahn, S.; Fink, G. *Macromol. Rapid Commun.* **1997**, *18*, 117−124.